國立臺灣大學生命科學學院生化科學研究所

碩士論文

Institute of Biochemical Sciences
College of Life Science
National Taiwan University
Master Thesis

# CRISPR-Cas9 技術應用於粒線體基因編輯之優化設計

# Repurposing CRISPR-Cas9 Technology for Mitochondrial Genome Editing

馮聖富

Michael Sheng-Fu Feng

指導教授：凌嘉鴻 博士

Advisor: Steven Lin, Ph.D.

中華民國一〇八年六月

June 2019

doi:10.6342/NTU201902787

# 謝辭

感謝楊維元老師與張壯榮老師擔任我的口試委員，並提出客觀建議以及修改方向。感謝這兩年半以來指導教授凌嘉鴻老師的悉心指導，及實驗室同伴慧瑜學姊、婉君學姊、George 學長、信安學長、日昇、俞安、欣如、Bella、Max 及幸蓉的陪伴，還有實驗上的意見交流。雖然起初來到中研院生化所 503 實驗室時懷著忐忑不安的心情，經過一個多月的實驗室組會才終於下定決心加入，但在老師的帶領下，從剛開始實驗上經常出現問題，一直到後期慢慢學會從問題中自己找出解決辦法，真的在這段日子當中成長很多。尤其在許多個孤單一人進行實驗的夜晚，抑或面對不如預期的實驗結果而心情低落時，真心感謝過程當中基督教福音宣教會鄭明析牧師所傳講的寶貴箴言，若這一路上沒有信仰的支持，這一份碩班論文就不可能完成。最後感謝爸爸媽媽不僅在過程中不斷給予鼓勵，在經濟上也總是毫不保留地予以支持，讓我可以毫無後顧之憂。妹妹棋棋這段日子也同在台北努力打拼，雖然我們道路不同，但是看著彼此全力以赴的生活也間接地鼓舞著自己。

原本沒有預期要讀的碩士學位，回過頭卻發現是　神賜下最棒的禮物。這兩年半的過程中，我學會更謙遜地看待過去的成就，也更感謝每一天生活當下所得到的一切祝福。也因為這段時間的沉潛，讓我能戳破原本包覆在生活周圍的糖衣泡泡，更能夠看清生命中最重要的事物與關係，也認清到自己能力不足的事實，而更加鞭策自己不論在實驗上抑或想法上的層次。如果當初我直接前往美國攻讀博士班，恐怕會因為無法適應而跌入更深的谷底，為此我真心感謝在碩士班這段時間當中所有願意教導我、讓我了解自己哪裡還做得不好的人天使們。最後，感謝　神、聖靈、聖子與主透過福音生下了我，僅以此碩士論文作為一切靈肉祝福的致謝。



doi:10.6342/NTU201902787

# 中文摘要

粒線體對於維持細胞內的能量及動態恆定扮演極重要的角色，當粒線體基因受損時會造成粒線體功能部分失活，甚至導致嚴重的遺傳性疾病，例如萊氏症(Leigh syndrome)。目前雖然有許多團隊嘗試利用限制酶或人工合成的 DNA 內切酶，例如：ZFN 或 TALEN，來針對突變的粒線體基因進行剪切剔除，但這些方法往往會受到選擇位點不足、製作不易等缺點所限制。近年來迅速發展的基因編輯技術 CRISPR-Cas9 便可解決上述兩項問題，目前除了三篇仍具有爭議的研究發表外，尚未有其他人提出相關研究成果或重複其研究。因此，在此篇研究中，我們分別在 Cas9 蛋白及嚮導 RNA (guide RNA)上進行一系列不同粒線體標的序列(mitochondria-targeting sequence, MTS)的修飾。根據結果，我們發現帶有 MTHFD1L MTS 之 mito-Cas9 蛋白與僅帶有 5’端 10 個核苷酸延長序列之嚮導 RNA 51 號，這兩者可以最有效率地進入粒線體。我們的結果可望運用 CRISPR-Cas9 技術來建立一套更加完善的粒線體基因編輯工具，未來將可應用於生物學研究與罕見粒線體疾病之治療。

# 中文關鍵字

粒線體疾病、CRISPR-Cas9、基因治療、粒線體 RNA、PNPase



doi:10.6342/NTU201902787

# Abstract

The mitochondrial genome is responsible for the maintenance of the cellular energy source and homeostasis. Therefore, partial loss of mitochondrial functionality and even devastating diseases happen when the mitochondrial genome is damaged. Nowadays, several strategies like restriction enzymes, ZFNs and TALENs, have been developed to specifically eliminate mutated mitochondrial DNA. However, all methods aforementioned have their own limitations on either limited target site choice or laborious manufactural process. CRISPR-Cas9 is a soaring new DNA editing tool which has not been widely applied in mitochondrial genome engineering, except for three controversial papers published. Consequently, in this study, we aim to establish a more reliable and tractable platform by fusing both Cas9 protein and guide RNA with various mitochondria-targeting sequences (MTSs). Our data show that the mito-Cas9 with the MTS from mitochondrial monofunctional C1-tetrahydrofolate synthase (MTHFD1L) and the mito-guide RNA 51 with only 10-nucleotide extended form the 5' end both have the best import efficiency into mitochondria. Our study provides a potential technique to edit mitochondrial genome through CRISPR-Cas9 gene tool and may help generate gene therapy for mitochondrial diseases.



# Keywords

Mitochondrial genome editing, mitochondria-targeting Cas9, mitocondria RNA import, PNPase




doi:10.6342/NTU201902787

# 目　　錄


謝辭 ..... 2

中文摘要 ..... 3

Abstract ..... 4

Introduction ..... 8

1. Significance of mitochondria ..... 8
2. Diseases caused by pathogenic mtDNA mutations ..... 9
3. Current status in mitochondrial genome manipulation ..... 10
4. CRISPR-Cas9 gene editing technology and its application on mtDNA ..... 11
5. DNA double-strand break repair mechanism in mammalian mitochondria ..... 13
6. Mitochondrial protein import machinery ..... 14
7. Mitochondrial RNA import machinery ..... 15
8. Specific aim of this study ..... 16

Results ..... 17

1. Folded protein cannot be transported into mitochondria ..... 17
2. A novel MTS is able to import mito-Cas9 into mitochondria ..... 18
3. Putative RNA transporter and its counterpart RNAs exist in HeLa mitochondria ..... 20
4. Structures from nucleus-encoded mitochondrial RNAs maintain Cas9 cleavage ..... 21
5. Mito-sgRNA with only linker on 5' end performs the best import ..... 22
6. Cellular abnormality observed after sorting of mito-Cas9-GFP-positive cells ..... 23

Discussion ..... 25

1. Previous research on mtDNA editing by CRISPR-Cas9 system ..... 25
2. Cas9 can only enter mitochondria with the assistance of a novel MTS ..... 26
3. All modifications on guide RNA show no complete impediment on Cas9 cleavage ability ..... 27
4. Guide RNA with only linker shows unexpectedly high mitochondrial import rate ..... 28
5. Low expression level of mito-Cas9 may hinder downstream experiments ..... 29
6. Recommendation for future research ..... 29

Materials and Methods ..... 31

1. Bacterial strains, primers and plasmids ..... 31
2. Competent cell preparation ..... 31
3. Plasmid construction ..... 32
4. Cell culture ..... 35




doi:10.6342/NTU201902787

5. Nucleofection ..... 36
6. Immunofluorescence ..... 36
7. Synthesis of RNA by T7 in vitro transcription ..... 37
8. Calf intestinal alkaline phosphatase (CIP) treatment ..... 40
9. In vitro cleavage assay ..... 41
10. RNA transfection ..... 42
11. Dynabead mitochondrial extraction ..... 43
12. MACS mitochondrial extraction ..... 44
13. RNA extraction ..... 46
14. Reverse transcription-quantitative polymerase chain reaction (RT-qPCR) ..... 46
Reference ..... 98

## 圖 目 錄

Figure 1. Comparison between current methods for mtDNA manipulation ..... 48
Figure 2. Schematic design for mito-EGFP transfection ..... 49
Figure 3. The intracellular localization of mito-EGFP ..... 50
Figure 4. Co-translational mechanism for mitochondrial protein import ..... 51
Figure 5. Plasmid map for pSL127 series ..... 52
Figure 6. Schematic flow to determine localization of mito-Cas9s ..... 53
Figure 7. Common MTSs are not enough for mito-Cas9 to enter mitochondria ..... 54
Figure 8. Candidate MTSs from large nuclear-encoded mitochondrial proteins on UniProt ..... 55
Figure 9. Most candidate MTSs from UniProt are not suitable for mito-Cas9 ..... 56
Figure 10. MTHFD1L MTS is suitable for mito-Cas9 ..... 57
Figure 11. PNPase as a putative RNA transporter ..... 58
Figure 12. PNPase exists in HeLa mitochondria ..... 59
Figure 13. Schematic flow for mitochondrial RNA extraction ..... 60
Figure 14. Calculation for mitochondrial translocation rates of PNPase-related RNAs ..... 61
Figure 15. PNPase-related nuclear-encoded RNAs exist in HeLa mitochondria ..... 62
Figure 16. Reported hairpin-shaped motifs for mitochondrial RNA transportation ..... 63
Figure 17. Hypothesis for PNPase-mediated mitochondrial import of mito-sgRNA ..... 64
Figure 18. Cartoon illustration of predicted mito-sgRNA structures ..... 65
Figure 19. Modifications on all mito-sgRNAs maintain Cas9 cleavage ..... 66
Figure 20. Schematic flow to determine timing for mito-sgRNA transfection ..... 67
Figure 21. Schematic flow for in vivo mito-sgRNA screening and calculation ..... 68
Figure 22. Mito-sgRNA with only linker on 5' end has the highest import efficiency ..... 69
Figure 23. Schematic flow for expression of mito-Cas9 in vivo ..... 70
Figure 24. Impaired cellular physiology after transfection of Cas9-GFP ..... 71



doi:10.6342/NTU201902787

**Figure 25. Physiological anomaly occurs after transfection of mito-Cas9-GFP** ..... 72
**Figure 26. Plasmid map for pSL296** ..... 73
**Figure 27. Plasmid map for pSL307 which has not been cloned yet** ..... 74
**Figure 28. Hypothesized influence of PNPase expression on mitochondrial RNA import** ... 75

## 表 目 錄

**Table 1. Strains, plasmids and primers used in this study** ..... 76
**Table 2. Humanized SpCas9 sequence and mitochondria-targeting sequences** ..... 81
**Table 3. T7 in vitro transcribed RNAs (IVT RNAs) used in this study** ..... 86
**Table 4. PCR condition and program setting for DNA template of IVT RNA** ..... 88
**Table 5. Amount of Lipofectamine 2000 for transfection of different mito-sgRNAs** ..... 93
**Table 6. Raw data for qPCR of mito-sgRNA screening** ..... 94

## 附 錄

**Appendix 1. Setup flow of Urea-PAGE for RNA in vitro transcription** ..... 96
**Appendix 2. Setup for arrangement of RT-qPCR loading** ..... 97



doi:10.6342/NTU201902787

# Introduction

## 1. Significance of mitochondria

Mitochondria serve as the powerhouse of cells. They not only produce energy, but also participate in several essential cellular processes, like calcium regulation, redox potential, cell cycle control, antiviral response and apoptosis[1]. According to endosymbiosis hypothesis, mitochondrion originated from a bacterium which was engulfed into a protoeukaryotic host cell during evolution[2]. Consequently, mitochondria possess a bacterium-like size and contain plasmid-like DNA. Through evolution, mitochondria have kept simplifying its own genome and integrating parts of mitochondrial genome (mtDNA) into the host nuclear genome, creating the so-called nuclear mitochondrial pseudogenes[3]. Human mtDNA is an intronless circular double-stranded DNA that harbors 16,569 base pairs. Each mtDNA encodes 37 essential genes, including 13 protein subunits, 22 tRNAs and 2 rRNAs[4]. Due to its crucial biological roles and concise genetic organization, mutations to mtDNA have high probability of disrupting the genetic information and affecting mitochondrial functionality. Single-nucleotide variations and deletions are the top two genomic changes within mtDNA that commonly result in mitochondrial diseases. For years, scientists have attempted to manipulate mtDNA by creating double-strand breaks (DSB) and introducing sequence changes via DNA repair process. Methods including mtDNA-targeting restriction enzymes, zinc-finger nucleases (ZFNs), and transcription activator-like effector nucleases (TALENs) have been applied to trigger DSB on mtDNA for depletion of pathogenic mtDNA[5-7]. Nevertheless, all the methods mentioned above have their own shortcomings. On the contrary, the utilization of CRISPR-Cas9 on mtDNA has yet been fully explored. The goal of this thesis is to engineer mitochondria-targeting CRISPR-Cas9 system (mito-CRISPR) to trigger site-specific mtDNA cleavage.



doi:10.6342/NTU201902787

## 2. Diseases caused by pathogenic mtDNA mutations

Several mitochondrial diseases are caused by single-nucleotide mutations. The disease symptom varies depending on the cell type in which the mtDNA is mutated. In general, high energy-demanding organs, like brain, heart, and muscle, are usually the first ones to show defective mitochondrial phenotypes. Since mitochondrial phenotypic defects determined by mtDNA are highly correlated with each other, a certain disease symptom can be caused by more than one type of mutation. For instance, Leber hereditary optic neuropathy (LHON) is a common cause of inherited blindness in young males. Point mutations like m.3460G>A, m.11778G>A and m.14484T>C are three sites commonly associated with this syndrome[8]. On the contrary, point mutations such as m.8344A>G and m.8993T>G/C may lead to Leigh syndrome, a progressive neurodegenerative disorder with early-onset occurrence in infancy and childhood[9,10].

However, not every individual who possesses mtDNA mutations succumbs to metabolic abnormality. A single human cell contains on average 1,000 copies of mtDNA[11]. Wild-type and mutated mtDNA usually co-exist within the same cell, a phenomenon known as mtDNA heteroplasmy[12]. Thus, it requires elevated ratio of pathogenic mtDNA mutation over the wild-type mtDNA to disrupt mitochondrial functions. Different tissues and diseases may have various thresholds, but the threshold for common mitochondrial defects falls around 80%[13]. Since human mitochondria lack efficient DSB repair, one strategy to shift the wild-type-to-mutant ratio is to target the mutant mtDNA for degradation and allow repopulation of wild-type mtDNA. Upon linearization, mtDNA is reported to be degraded spontaneously due to the lack of an efficient repair mechanism and undergoes a heteroplasmic shift[5,14]. A reduction in mutant mtDNA was



doi:10.6342/NTU201902787

observed, followed by an increase in wild-type mtDNA[15-17]. Furthermore, instead of repairing the damaged mtDNA, cells also tend to induce mitophagy to destroy malfunctioning organelles[18].

## 3. Current status in mitochondrial genome manipulation

In order to specifically trigger DSB on mutant mtDNA, methods including restriction enzyme (RE), zinc-finger nuclease (ZFN), and transcription activator-like effector nuclease (TALEN) have been developed[5-7,19]. Mitochondria-targeting SmaI and XmaI recognize and degrade m.8399T>G mutation, which is the cause of NARP (neuropathy, ataxia, and retinitis pigmentosa) and Leigh syndromes, to allow restoration of intracellular ATP level[15,16,20]. Mitochondria-targeting ApaLI induces heteroplasmic shift on well-characterized mouse model possessing two polymorphic mtDNA variants, NZB and BALB/c[5,14]. In general, mitochondria-targeting REs provide dramatic heteroplasmic shift and show no off-target effect on both mouse model and human culture cell lines[20,21].[5,15]. However, among ~200 pathogenic mutation sites on mtDNA, only two can be targeted by the existing restriction enzymes[17].

To overcome the target restriction of REs, programmable DNA endonucleases such as ZFN and TALEN technologies, have been engineered to target and cleave a broader range of mutant mtDNA. Both technologies utilize programmable DNA binding domains, either zinc finger DNA binding modules or transcription activator-like effector (TALE) DNA binding domains, to direct the dimerization of a non-specific nuclease FokI and trigger DNA breaks at the targeted mutation sites[7,22-24]. Some zinc finger DNA binding modules can recognize three nucleotides which makes up a codon and are possible to target all combinations of 64 codons[25]. For instance, mitochondria-targeting ZFNs (mito-ZFNs) have been reported to target a 12-nucleotide sequence and specifically remove mutant mtDNA which possesses only one single nucleotide variation



doi:10.6342/NTU201902787

from the wild-type mtDNA[26]. Mito-ZFNs also demonstrate profound reduction of mtDNA and a heteroplasmic shift toward wild-type mtDNA in human cells by targeting m.8993T>G mutation associated with NARP and Leigh syndromes[7]. In comparison, one TALE DNA binding domain recognizes one single nucleotide, offering a higher flexibility on DNA targeting by rearranging four different TALE domains. In mouse model, mitochondria-targeting TALENs (mito-TALENs) can reduce successful alteration on mtDNA heteroplasmy ratio on NZB and BALB/c[17]. Mito-TALENs also demonstrate permanent elimination of both mtDNA harboring single nucleotide variation or common deletion in patient-derived cells[6,27].

Nevertheless, DNA targeting by mito-ZFNs and mito-TALENs requires combinations and rearrangements of their DNA-binding domains. It is therefore more laborious to design a new pair of ZFN or TALEN. A more flexible and user-friendly programmable gene-editing tool for mtDNA manipulation is still highly desirable.

## 4. CRISPR-Cas9 gene editing technology and its application on mtDNA

The clustered regularly interspaced short palindromic repeats (CRISPR)-Cas (CRISPR-associated proteins) systems are adaptive immune systems found in most archaea and many bacteria. Directed by a CRISPR RNA molecule (crRNA), CRISPR-Cas nucleases are capable of sequence-specific recognition and cleavage of target DNA. This simple defense immunity is effective against invading foreign nucleic acids, such as DNA viruses and conjugative elements.

Currently, there are six types of CRISPR-Cas systems[28]. Types I, III and IV systems involve multiple protein subunits to perform functional cleavage of target nucleic acid. In contrast, in type II, V and VI systems, a single nuclease protein is responsible for the same purpose. Among all the systems, type II CRISPR-Cas9 is the best-characterized system. In CRISPR-Cas9 system,



doi:10.6342/NTU201902787

Cas9 is the effector protein that is activated upon binding to two-RNA molecules: crRNA and a trans-activating crRNA (tracrRNA). These two RNA molecules can also be fused by a GAAA tetraloop to form a chimeric single guide RNA (sgRNA). Once Cas9 binds sgRNA, it undergoes conformational change and is able to recognize NGG PAM (protospacer adjacent motif) nearby the target DNA region. Using the sequence information provided by the sgRNA, Cas9 can be loaded onto the target DNA by RNA:DNA basepairing interactions and activate its two endonuclease domains, RuvC and HNH domains, to produce a blunt-ended double-strand break. Since the establishment of this technique in 2012[29], CRISPR-Cas9 has emerged as a predominant genetic tool for manipulation of nuclear DNA in a wide variety of organisms. Since the DNA targeting activity is solely defined by the sgRNA sequence, Cas9 can be reprogramed to cleave nearly any sequence possible. Yet, despite of its extensive applications on nuclear genome, the usage of CRISPR-Cas9 on organellar DNA, such as mitochondrial or chloroplast, has not been fully explored.

To date, three published research articles have mentioned mtDNA editing by CRISPR-Cas9 system. In 2015, Jo and colleagues first reported CRISPR-Cas9-mediated mtDNA editing[30]. Unfortunately, their data was recently under debate in a review paper due to its lack of proof of the mechanism how the Cas9 with nucleus-leading sequence (NLS) and the sgRNA without any modification can localize into mitochondria spontaneously[31]. In addition, even though in the later part of their paper they engineered a modified Cas9 by adding a specific mitochondria-targeting sequence (MTS), we could not reproduce their results with the same Cas9 construct, suggesting that mitochondria-targeting Cas9 (mito-Cas9) might need a different MTS in order to enter mitochondria efficiently. In 2018, Loutre *et al.* introduced mitochondria-targeting Cas9 and mitochondria-targeting sgRNA to edit mtDNA in human culture cell line HepG2. However, their



doi:10.6342/NTU201902787

results did not provide any evidence regarding the localization of the sgRNA within mitochondria[32]. Recently, Bian and his team also published their work using CRISPR-Cas9 technology to edit mtDNA both in human cell line and zebrafish embryo. Similarly, they did not provide solid proof for the mitochondrial localization of their sgRNA[33]. Therefore, my goal is to establish a more robust CRISPR-Cas9 platform for mtDNA manipulation by providing a measurable efficiency for transport of both Cas9 and sgRNA into mitochondrial matrix.

## 5. DNA double-strand break repair mechanism in mammalian mitochondria

After a successful colocalization of Cas9 and sgRNA within mitochondrial matrix, a targeted DNA double-strand break (DSB) is expected to occur. Following the DSB, whether the damaged mtDNA undergoes a repair process, like homology-directed repair (HDR) or nonhomologous end joining (NHEJ), is a crucial question. For mtDNA gene editing to occur, DSB repair pathway is needed. For instance, through electroporation of an active Cas9:sgRNA ribonucleoprotein complex (Cas9 RNP), scientists can generate a specific knock-out through introducing random insertion/deletion (indels) by NHEJ repair or a specific knock-in with an exogenous single-stranded DNA oligonucleotide template by HDR in nuclear genome[34].

For eukaryotes, studies in yeast and *Chlamydomonas reinhardtii* confirm functional HDR pathways[35,36]. In contrast, recombination-mediated DNA repair seems to be an infrequent event in mammalian mitochondria[37-39]. Although *in vitro* joining of blunt-end DNA fragments was detected in the protein extract made from mammalian mitochondria[40], DSBs by mitochondria-targeting restriction endonucleases generally led to large deletions or reduction in mtDNA copy-number[39,41]. These experiments suggest that mammalian mitochondria lack an efficient DSB repair mechanism and degradation of the damaged mtDNA seems a simpler solution due to high



doi:10.6342/NTU201902787

abundance of mtDNA[42,43]. While nuclear genome faces a "repair or die" constraint after DSBs occur, mtDNA exists in hundreds to thousands of copies. Under normal cell physiology, a few copies of damaged mtDNA can undergo degradation without detrimental impact on mitochondrial functions. It may be more efficient to maintain mtDNA level by DNA replication than by importing and maintaining a complete set of the DNA repair machineries in mitochondria. With this in mind, it is more realistic to first focus on DSB-mediated elimination of targeted mtDNA through CRISPR-Cas9 DNA cleavage activity.

## 6. Mitochondrial protein import machinery

For a successful cleavage of target mtDNA to happen, an active Cas9 protein needs to be translocated into the mitochondrial matrix, where mtDNA locates. Although several essential mitochondrial proteins are encoded by mtDNA, the vast majority of the human mitochondrial proteins (about 1,500) are encoded by nuclear genome and translated as precursor proteins in the cytosol. These precursor proteins enter mitochondria through a series of mitochondrial protein import machineries. Generally, proteins are directed to their intramitochondrial destinations through four principle pathways: the β-barrel pathway into the outer membrane, the redox-regulated import pathway into the intermembrane space, the carrier protein pathway to the inner membrane, and the presequence pathway to the matrix and inner membrane[44].

For all four pathways, the translocase of the outer membrane (TOM) serves as the common entrance for precursor proteins. To send Cas9 into mitochondrial matrix, we decided to explore the presequence pathway. Most of the precursor proteins possess mitochondria-targeting sequence (MTS) at their N-termini, which is recognized by TOM. MTSs are a group of peptides which usually consist of 15 to 50 amino acids and can form positively charged amphipathic α



doi:10.6342/NTU201902787

helix. The hydrophobic and positively charged surfaces of the amphipathic α helix are recognized by TOM20 and TOM22, respectively[45-47]. The precursor proteins cross the outer membrane under the assistance of TOM20 and TOM22. In the intermembrane space, the precursor proteins are further recognized by the translocase of inner membrane 23 (TIM23). Utilizing two different energy sources, the membrane potential generated through the electron-transfer chain and the adenosine triphosphate (ATP), TIM23 allows the transportation of the precursor proteins across the inner membrane and into the matrix[47,48]. Once the precursor proteins enter the mitochondrial matrix, their MTS is proteolytically cleaved by the mitochondrial processing peptidase (MPP) and folded into functional mature protein with the help of mitochondrial chaperons[44]. When constructing mitochondrial-targeting Cas9 (mito-Cas9), we need to take the proteolytic processing of MTS into consideration to avoid clipping off the RuvC nuclease domain at the N-terminal end of Cas9.

## 7. Mitochondrial RNA import machinery

Several nuclear-encoded non-coding RNAs are imported in human mitochondria[49]. These non-coding RNAs include 5S ribosomal RNA (5S rRNA), RNase P RNA, RNase MRP RNA, the RNA component of human telomerase (hTERC), a lncRNA called SAMMSON, and various microRNAs. It is also reported that several yeast tRNAs can be imported into human mitochondria[50,51]. The exact functions of these RNAs in mitochondria and the pathways through which these RNAs are imported from cytosol into mitochondria are still unclear[49].

A putative mechanism of RNA translocation involves a multifunctional protein called polynucleotide phosphorylase (PNPase). Encoded by human *PNPT1* gene, PNPase was originally recognized as an evolutionarily conserved 3’ to 5’ exonuclease from bacteria to



doi:10.6342/NTU201902787

human[52,53]. Its function as poly(A) polymerase was also found in *E. coli* and plant chloroplast[54,55]. Human PNPase is a homotrimeric complex and locates mainly in the intermembrane space and partially in the matrix[56]. Besides its exonuclease activity, which may play an important role in the maintenance of mitochondrial RNA decay, PNPase was recently postulated to be a mitochondrial RNA transporter. Researchers found that the stem-loop structures on 5S rRNA, RNase P RNA and RNase MRP RNA might be recognized by PNPase and facilitate their import into mitochondrial matrix from the cytosol[52]. However, there are still many questions on how these nucleus-encoded RNAs cross the outer membrane and enter intermembrane space and how PNPase helps these RNAs cross the inner membrane and finally reach matrix[52]. I aim to explore the PNPase pathway and engineer mitochondria-targeting sgRNA (mito-sgRNA) by carrying the mitochondrial importing stem-loop structures.

## 8. Specific aim of this study

The overarching goal of this thesis is to repurpose CRISPR-Cas9 genome editing technology for mtDNA targeting. To achieve this, I seek to utilize the current knowledge of mitochondrial protein and RNA import to develop strategies to transport Cas9 protein and sgRNA into mitochondrial matrix where mtDNA is located. My specific aims are to: (**1**) identify mitochondria-targeting sequence capable of efficient localization of Cas9 into mitochondria; (**2**) engineer and test sgRNA carrying mitochondria-importing RNA stem-loops to enable import into mitochondrial matrix; (**3**) determine target mtDNA cleavage efficiency upon co-introduction of mito-Cas9 and mito-sgRNA. The methods and findings of this thesis will provide a foundation for CRISPR-Cas9-based mitochondrial genome editing in the future.



doi:10.6342/NTU201902787

# Results

## 1. Folded protein cannot be transported into mitochondria

Electroporation of preassembled Cas9:sgRNA ribonucleoprotein (Cas9 RNP) into cells is a well-established protocol in our lab[34]. It has advantages, like shorter half-life time, lower toxicity, higher expression, and lower possibility of genome-integrating, when compared to vector-based methods. However, since a pure Cas9 protein is as large as about 150 kDa, we need to verify whether a mitochondria-targeting sequence (MTS) is able to import such a huge protein into mitochondria. To make the condition much simpler, we firstly used enhanced green fluorescence protein (EGFP) with double repeats of COX8A MTS (termed mito-EGFP; plasmid was kindly provided by Dr. Wei-Yuan Yang) to test if a folded small protein with MTS can get into mitochondria. If even a folded mito-EGFP cannot enter mitochondria, not to mention a folded Cas9 or Cas9 RNP. (Figure 2)

We expressed the plasmid in *E. coli* and purified mito-EGFP protein. We transfected either the plasmid or the purified protein forms of mito-EGFP into HeLa cells through nucleofection. We observed a clear concentration effect of mito-EGFP within mitochondria in plasmid group (Figure 3A-C). The green fluorescent signal of mito-EGFP neatly overlaps the red signal of mitochondria, showing yellow signal in merged figure. By contrast, protein form of mito-EGFP showed no such phenomenon but spread all over the cell, even in the nucleus (Figure 3D-F). This data suggests that electroporation may produce temporary diffusion of desired particles within the whole cells, so both plasmids and proteins can localize into the nucleus. The plasmid can undergo transcription and produce mRNA which is further exported to the cytosol. During translation, the polypeptide generated from the mRNA can enter mitochondria with the help of



doi:10.6342/NTU201902787

MTS. On the contrary, once electroporation finishes, purified proteins stuck *in situ* and cannot cross the organellar membranes.

Our results were consistent with other scientists' findings that the translocation of proteins with MTS is coupled with translation (Figure 4)[57]. Namely, these nuclear-encoded mitochondrial proteins are co-translationally recognized by protein receptors on the mitochondrial outer membrane, like TOM20 and TOM22, and enter mitochondria as polypeptide chains[58]. The imported polypeptide may undergo different pathways and localize into the correct intramitochondrial site where it is folded into its mature form and perform normal function. Consequently, a folded protein, such as purified mito-EGFP in this case, can no longer enter mitochondria. This result suggests that a preassembled Cas9:sgRNA RNP cannot be used for mitochondrial genome editing, but a plasmid-based method is needed. Furthermore, according to the mitochondrial protein import mechanisms, Cas9 needs to enter mitochondria as polypeptide through the assistance of mitochondria-targeting sequence. In that condition, unfolded Cas9 polypeptide can no longer hold its single guide RNA (sgRNA). As a result, we need to import Cas9 and sgRNA separately.

## 2. A novel MTS is able to import mito-Cas9 into mitochondria

Firstly, we established a series of plasmids (pSL127 series, see Figure 5 and Table 1) to express Cas9 (without or with different MTSs) through electroporation (Figure 6). Since a pure Cas9 cannot localize into mitochondria (Figure 7B), in order to send Cas9 into mitochondrial matrix through transfection of plasmid, we need to seek a suitable mitochondria-targeting sequence (MTS). Although COX8A MTS is a well-known MTS to deliver small proteins, like EGFP (38 kDa), into mitochondria, it may be less efficient to carry a large protein, like Cas9



doi:10.6342/NTU201902787

(~150 kDa)[59]. Controversially, a study from Jo and colleagues demonstrated that mito-Cas9 (mitochondria-targeting Cas9) bearing a COX8A MTS (1-21 amino acids of cytochrome c oxidase subunit 8A) can localize into mitochondria[30]. In contrast, according to our result, Cas9 with double repeats of COX8A MTS does not perform such localization within mitochondria (Figure 7C). Another well-studied MTS is from *S. cerevisiae* COX4P[60] (1-24 amino acids of cytochrome c oxidase subunit 4 in *Saccharomyces cerevisiae*. see Table 2). Nevertheless, fusion of COX4P MTS does not help Cas9 enter mitochondria either (Figure 7D).

In order to find a more suitable MTS for directing mito-Cas9 into mitochondria, we searched on UniProt website for large mitochondrial proteins which are encoded by nucleus and later transported into mitochondria during translation (Figure 8). I chose the four largest mitochondrial proteins which are over 100 kDa on molecular mass and have been reported to be translocated into mitochondria after their mRNA transcribed from nuclear genome. Four candidate MTSs were chosen either by reported studies, by prediction of UniProt online software, or randomly from their N termini. Their lengths range from the first 25 to 40 nucleotides of their sequences (Table 2).

The largest protein I chose is acetyl-CoA carboxylase 2 (UniProt entry: O00763), which is almost 280 kDa and has been reported to localized into mitochondria after translation[61]. Its MTS which encodes the first 40 amino acids of acetyl-CoA carboxylase 2 was cloned into pSL127D and marked as ACACB MTS. The second protein is mitochondrial glycine dehydrogenase (UniProt entry: P23378), which is 113 kDa and has been reported to localized into mitochondria[62]. The first 35 amino acids of mitochondrial glycine dehydrogenase sequence were analyzed by manual assertion as an MTS, so I cloned their presequence into pSL127E and marked it as GLDC MTS. Next protein I chose is mitochondrial DNA polymerase subunit



doi:10.6342/NTU201902787

gamma-1 (UniProt entry: P54098), which is 140 kDa and has been reported to be localized into mitochondria[63]. The presequence which encodes the first 38 amino acids of mitochondrial DNA polymerase subunit gamma-1 was cloned into pSL127F and marked as POLG MTS. Finally, the last protein is mitochondrial monofunctional C1-tetrahydrofolate synthase (UniProt entry: Q6UB35), which is 106 kDa and has been reported to be localized into mitochondria[64]. The first 31 amino acids of mitochondrial monofunctional C1-tetrahydrofolate synthase have been confirmed to be its MTS by experiments[65], and thus its presequence was cloned into pSL127G and marked as MTHFD1L MTS. After human codon optimization, *Streptococcus pyogenes* Cas9 sequence following aforementioned MTSs were cloned into plasmids (Table 1 and 2) and transfected into HeLa cells through nucleofection (Figure 5 and 6).

However, three out of the four MTSs do not have the ability to transport Cas9 across the mitochondrial double membrane (Figure 9). Fortunately, we found that the MTS from mitochondrial monofunctional C1-tetrahydrofolate synthase (MTHFD1L MTS) provided the best transport efficiency among all the six MTSs (Figure 10).

### 3. Putative RNA transporter and its counterpart RNAs exist in HeLa mitochondria

However, ApoCas9 (protein alone) does not have DNA cleavage activity. It must be activated by binding to single guide RNA (sgRNA) in order to edit targeted DNA sequence. After confirmation of mitochondrial localization of mito-Cas9 with MTHFD1L MTS, I further investigated a possible mitochondrial RNA import pathway for sgRNA. In contrast to the well-established study of mitochondrial protein import mechanisms, the mechanisms by which cells import nuclear-encoded RNAs into mitochondria are still under debate, leading to skepticism of applying CRIPSR technology onto mitochondrial genome[31].



doi:10.6342/NTU201902787

Despite the lack of research articles on mitochondrial RNA import mechanisms, there are still several groups who mentioned possible pathways nuclear-encoded RNAs may utilize to enter mitochondria[50,66-68]. In brief, a multifunctional protein called polynucleotide phosphorylase (PNPase) which mainly localizes in the mitochondrial intermembrane space and partially in the matrix was reported to be involved in the mitochondrial import of several nuclear-encoded non-coding RNAs, like 5S rRNA, RNase P RNA and RNase MRP RNA (Figure 11)[66,67]. When the gene encoding PNPase (*PNPT1*) was knocked out, these RNA transcripts lost the ability to enter mitochondria[52]. Although how this protein which mainly localizes in the intermembrane space can recognize RNAs in cytosol and which protein is also involved in this pathway are still unknown, PNPase seems to be the most possible candidate as a putative mediator for mitochondrial RNA pathway[52,68].

From our data, we confirmed that PNPase indeed localizes at mitochondria, in spite of the fact that we cannot determine its actual intramitochondrial localization due to the limited resolution of confocal microscope (Figure 12). Furthermore, we conducted mitochondria purification with RNase treatment to collect only the RNAs within mitochondria (Figure 13). Through RT-qPCR, we confirmed that 5S rRNA, RNase P RNA and RNase MRP RNA all exist in the mitochondria of our cultured HeLa cell line (Figure 15).

## 4. Structures from nucleus-encoded mitochondrial RNAs maintain Cas9 cleavage

With the perspective of utilizing PNPase as an RNA transporter for our sgRNAs, we cloned the secondary structures of 5S rRNA (5S), RNase P RNA (RP) and RNase MRP RNA (MRP) in front of our sgRNAs (see Figure 16 and Table 3 and 4). We also collected another two RNA hairpin structures, F1D1 and HD, which originate from $tRNA^{Lys}$ of yeast and had been reported



doi:10.6342/NTU201902787

to have the ability to import RNA into human mitochondria (Table 3 and 4) [69,70]. Finally, since the 3' untranslated region (3' UTR) of the mRNA of human mitochondria ribosomal protein S12 (MRPS12) had been studied to confer localization to mitochondrial outer membrane[71], I added MRPS12 3' UTR sequence at the 3' end of several sgRNAs (Table 3 and 4). In total, 15 sgRNAs were synthesized through T7 *in vitro* transcription (Figure 18). Before we tested the mitochondrial localization efficiency of these modified sgRNAs, we wondered if the attached motifs may influence the DNA cleavage performance of Cas9. Thus, we conducted *in vitro* cleavage assay to determine Cas9 activity along with each sgRNAs (Figure 19). According to our result, compared to the original sgRNA36 and sgRNA51 which only possesses 10-nucleotide long linker, sgRNAs with modifications on either 5' end only or both ends had impeded Cas9 performance (Figure 19C). On the other hand, modifications on the internal scaffold of sgRNA did not hinder Cas9 editing efficiency.

## 5. Mito-sgRNA with only linker on 5' end performs the best import

We utilized commercial Lipofectamine 2000 reagent (Thermo Fisher Scientific) to transfect mito-sgRNAs. Each mito-sgRNA was firstly surrounded by Lipofectamine 2000 to form lipid micelles and crosses plasma membrane through either fusion of endocytosis (Figure 20). Within the cytosol, each mito-sgRNA enters mitochondria according to its modification. Before we screened the *in vivo* mitochondrial translocation efficiency of all the synthesized mito-sgRNAs, the first step is to determine the timing when the most amount of mito-sgRNA can accumulate within the cytosol through Lipofectamine 2000-mediated transfection. In this part, we used mito-sgRNA51 to serve as a representative for all the mito-sgRNAs generated in this study. After transfection with the indicated time period, total RNA was lysed by TRIzol reagent, purified



doi:10.6342/NTU201902787

through commercial Direct-zol RNA recovery kit and finally analyzed by RT-qPCR targeting mito-sgRNA with primers listed in Table 1. As we expanded the transfection period from 3 hours to 9 hours, the amount of mito-sgRNA51 increased and peaked at 9 hours (Figure 20B). Afterwards, the amount decreased as the transfection was expanded to 12 hours, suggesting cellular degradation of exogenous RNAs.

Afterwards, I conducted 9-hour transfections of all mito-sgRNAs generated throughout this study by Lipofectamine 2000 reagent to test whether modifications on sgRNA can enhance mitochondrial import. After transfection, a small portion of cells were collected and underwent TRIzol lysis to extract total RNA. The rest of transfected cells firstly went through mitochondrial purification using anti-TOM22-antibody coated nanoparticles and then RNase A/T1 treatment for 20 minutes before mitochondrial RNA recovery by TRIzol. The relative amount of each mito-sgRNA was compared to the endogenous mitochondrial 5S rRNA by the indicated formula (see Figure 21B). According to our data, compared to 5S rRNA, the abundance of mito-sgRNA51 is the highest among all the sgRNAs synthesized in this study (Figure 22 and Table 6).

## 6. Cellular abnormality observed after sorting of mito-Cas9-GFP-positive cells

After identifying that mito-Cas9 possessing MTHFD1L MTS can efficiently localize to mitochondria and that mito-sgRNA51 has the best mitochondrial import rate, we aimed to co-transfect the two cargos through Lipofectamine reagents to determine whether our mito-Cas9 and mito-sgRNA can work together within mitochondria and trigger *in vivo ND4* cleavage. However, since the expression level of mito-Cas9 was low by electroporation of pSL127G (Figure 10), we decided to enhance it by utilizing Lipofectamine-3000-mediated transfection of either pSL294, which expresses Cas9 fused with turboGFP, or pSL295, which expresses mito-Cas9 following



doi:10.6342/NTU201902787

MTHFD1L MTS as well as turboGFP. 2 days after transfection, the turboGFP-positive cells were sorted out and seeded onto cultured dishes for another day. By immunofluorescence assay, we determined the localization of Cas9 or mito-Cas9 by anti-FLAG antibody (Figure 24).

According to our results, several Cas9 proteins without MTS were located at the cytosol. On the other hand, mito-Cas9 with MTHFD1L MTS showed localization within mitochondria as expected. However, when we observed with a broader field, we found that the cellular morphology in both groups appeared unhealthy and may undergo apoptosis at the timing (Figure 25).



doi:10.6342/NTU201902787

# Discussion

## 1. Previous research on mtDNA editing by CRISPR-Cas9 system

CRISPR-Cas9 genome editing technology is a robust system which has been widely used to manipulate nuclear DNA. However, not much attention has been drawn to mitochondrial or chloroplast DNA. So far, only three papers claimed a success by using CRISPR-Cas9 gene editing technology to cleave targeted mtDNA[31,33,34].

In Jo's report, the authors constructed lentiviral vectors which expressed either Cas9 with nuclear localization sequence (NLS) or mitochondria-targeting Cas9 (mito-Cas9) with COX8A MTS, and sgRNA. According to their immunofluorescence and Western blot results, Cas9 with NLS and mito-Cas9 can be partially or specifically localized into mitochondria, respectively. What made their results less unconvincing was that their sgRNA was cloned onto the viral vector following U6 promoter. Since U6 promoter is coupled with RNA polymerase III system and is responsible for generation of short RNAs (usually between 20 and 30 nt) like short hairpin RNAs (shRNAs) and small interfering RNAs (siRNAs)[72]. After transcription by RNA polymerase III, unlike mRNA, these RNAs do not undergo nuclear export pathway and can only accumulate within the nucleus. Therefore, the authors' claim for a successful mtDNA reduction by U6 promoter-generated sgRNA was unsolid without any proof of mitochondrial localization of these sgRNA.

In the report by Loutre *et al*., they used human HepG2 cells expressing Cas9 with COX8A MTS on the N terminus. For guide RNA, they generated various sgRNA fused with different hairpin structures to serve as import determinants by T7 *in vitro* transcription. Their sgRNAs were *in vitro* transcribed and transfected into HepG2 cells. Even though they provided Northern blot result to confirm the mitochondrial localization of their sgRNAs, they did not further offer



doi:10.6342/NTU201902787

any detail about the purity of their mitochondrial fraction, leaving the quality of their subcellular fraction questionable.

Finally, Bian *et al.* used vectors to express mito-Cas9 which was flanked with 2 COX8A MTSs, one from human and one from zebrafish. On the same vector, mtDNA-targeting sgRNA can be synthesized *in vivo* through U6 promoter. Their microscopy results were too unclear to claim a colocalization of mito-Cas9 within mitochondria. Secondly, U6-generated sgRNA, as mentioned before, cannot be exported out of nucleus, thereby rendering its transport into mitochondria improbable. Finally, mitochondria do not possess a well-studied DNA import pathway, how the authors claimed a successful import of HEX-tagged ssDNA into mitochondria is controversial.

To sum up, these reports do not validify the localization of their single guide RNAs (sgRNAs). Without an MTS to transport sgRNAs from cytosol to mitochondria and any mean to prove its localization, the authors failed to prove that their sgRNA can truly localize into mitochondria and trigger the activity of Cas9. Consequently, their declaration of successful gRNA-mediated editing on mtDNA by Cas9 did not hold solidly. We were motivated to establish a novel system to co-localize both Cas9 and sgRNA into mitochondria and cleave the targeted mtDNA sequence.

**2. Cas9 can only enter mitochondria with the assistance of a novel MTS**

In this thesis, we tried to use electroporation to transfect both plasmid and purified EGFP protein with 2xCOX8A MTS, which is the same as the Korean group[30], and saw if we can directly send folded protein into mitochondria through electroporation. Unfortunately, the answer was negative. Although cells transfected with plasmid can express EGFP signals in their



doi:10.6342/NTU201902787

mitochondria, cells transfected with purified proteins express EGFP signals all over the cell, indicating that the MTS on EGFP cannot translocate folded protein into mitochondria. Since EGFP is much smaller than Cas9, we believe that transfection of purified Cas9 protein through electroporation would be harder and impracticable. Consequently, we tested several other MTSs collected from other known nucleus-encoded large mitochondrial proteins and saw if these MTSs have better ability to send our mito-Cas9 into mitochondria.

Among the six candidate sequences, the MTS from MTHFD1L (UniProt: Q6UB35) has shown the best localization ability. By mean of confocal images, we observed a clear concentration effect of this MTHFD1L MTS-Cas9 within mitochondria. However, the expression level of MTHFD1L MTS-Cas9 was too low through electroporation or lipofection of plasmids. Consequently, we decided to use lentivirus system to establish a HeLa cell line which is able to express higher level of MTHFD1L MTS-Cas9 within mitochondria. Again, through confocal imaging, we proved that virus-expressed MTHFD1L MTS-Cas9 as well has a concentration effect within mitochondria and the expression level is higher than its plasmid-expressed counterpart. Nevertheless, subcellular fractionation and Western blotting are needed to further prove that MTHFD1L MTS-Cas9 is able to specifically localize into mitochondria and not exist in nucleus, where lots of mitochondrial pseudogenes exist and may trigger off-target effect.

### 3. All modifications on guide RNA show no complete impediment on Cas9 cleavage ability

On the other hand, concerning the activation of Cas9 after binding with sgRNA, we transfected artificially synthesized sgRNAs into Cas9-expressing HeLa cell lines. All the sgRNAs generated in this study have been designed to target a specific sequence site within *ND4*



doi:10.6342/NTU201902787

gene on mtDNA. ND4 gene encodes the subunit 4 of NADH dehydrogenase which plays a crucial role on oxidative phosphorylation (OXPHOS). We designed a reverse transcription- (RT-) qPCR system to test both the mitochondrial internal control, mitochondrial 16S (M16S) rRNA, and our *in vitro* transcribed sgRNAs. The efficiency of all primer pairs for both internal control and for guide RNAs surpass 90% with R square around 0.95. In order to transport gRNAs into mitochondria, several MTSs for RNA were collected from reported studies (Figure 16). We transfected these modified sgRNAs with various combinations of 5' or internal MTSs. Total RNA and RNA from mitochondrial subcellular fraction were extracted to monitor the increase/decrease of sgRNA expression through RT-qPCR.

**4. Guide RNA with only linker shows unexpectedly high mitochondrial import rate**

From our results, we found the best sg RNA is the one with modifications on both ends. However, in order to further validate this result, other techniques for RNA localization are considered. For example, we hope to utilize three different state-of-the-art fluorescence in situ hybridization technique and confocal imaging to make sure gRNA localized into mitochondria. The first one is DFBHI-induced fluorescence, which express fluorescent signal when chemical DFHBI recognizes and binds specific RNA secondary structure. We are designing four pairs of guide RNAs. Each one has different secondary structure for DFHBI recognition. Our preliminary data showed that guide RNA with BoBs sequence within the 1$^{st}$ hairpin area is able to express the greatest fluorescent signal. The second technique is branched DNA (from ACD), which can enlarge the gRNA signal through a series of annealing of complementary sequence. The last technique is rolling amplification, which is able to amplify the guide RNA signal through rolling



doi:10.6342/NTU201902787

extension of targeted sequence. All in all, three of them will prove whether or not our sgRNA can specifically localize into mitochondria.

**5. Low expression level of mito-Cas9 may hinder downstream experiments**

Ultimately, we still wander the activity of mitoCas9 within mitochondria after its binding with sgRNA. As mentioned above, we have designed a sgRNA to target *ND4* gene. Once Cas9 is combined with this sgRNA and thus activated, it should be capable of making a double-strand break within that specific region. As a result, the cleavage will induce the linearization of mitochondrial genome and potentially lead to a natural degradation of this linearized DNA. Hypothetically, once the linearized mitochondrial genome is degraded, it exhibits a decrease in DNA level through qPCR. After we transfect *in vitro* transcribed sgRNAs through electroporation into cell lines which express mito-Cas9 within mitochondria, we extract DNA from whole cell lysate and conduct qPCR with mitochondria-specific primers. Expectantly, we anticipate to observe a decrease of expression level of targeted mitochondrial sequence. Furthermore, in the future, we hope to use Seahorse machine to detect mitochondrial activity after transfection of sgRNA into Cas9-expressing cell lines. Since NADH dehydrogenase play a crucial role in electron transfer chain, once the *ND4* gene is cleaved by activated Cas9, NADH dehydrogenase activity will drop and an impeded mitochondrial activity should be observed.

**6. Recommendation for future research**

Nevertheless, detailed mechanisms of translocation of mito-Cas9 and mito-sgRNA from cytosol into mitochondria are still largely unknown. A better understanding of these mechanisms may help to optimize the mitochondria-targeting sequences and enhance the translocation



doi:10.6342/NTU201902787

efficiency. On the other hand, many single nucleotide mutations on mitochondrial genome can lead to different diseases. It is an urgent need to have a reprogrammable genome editing technique which is user-friendly and changeable to detect even a single nucleotide variable and cleave the targeted sequence. Also, precision and lower rate of off-target influence come from concentrating both Cas9 and guide RNA into mitochondria rather than nucleus. Through our data we have shown the best combination of mitochondria-targeting sequence for both Cas9 and guide RNA delivery into mitochondria.



doi:10.6342/NTU201902787

# Materials and Methods

## 1. Bacterial strains, primers and plasmids

All the *E. coli* strains used in this study are listed in Table 1. The *E. coli* strains 93 and 189 was a gift from Dr. Jennifer Doudna (UC Berkeley, USA). Homemade *E. coli* TOP10 and Stable3 chemically competent cells were prepared from these two strains as described in the following text. All *E. coli* strains were stored in 40% (v/v) glycerol as stocks at -80°C.

All the primers (Table 1) used in this study were synthesized by Integrated DNA Technologies (IDT, Singapore). After arrival, dried primer molecules were dissolved in 20 mM Tris-HCl (pH8.0) and stored in -20°C.

All the plasmids used in this study are listed in Table 1. The plasmid mito-EGFP was a gift from Dr. Wei-Yuan Yang (Academia Sinica, Taiwan). The plasmids pET28a and pAW006 were gifts from Dr. Jennifer Doudna (UC Berkeley, USA). All the plasmids generated in this work were extracted from the corresponding *E. coli* strains through ZR Plasmid Miniprep™ Classic kit (Zymo Research) according to the manufacturer's instructions.

## 2. Competent cell preparation

Homemade TOP10 and Stable3 chemically competent *E. coli* strains (Table 1) were used as hosts for plasmid construction. To store stock competent cells, TSS buffer was prepared as follows: For 50 mL TSS buffer, 5 g PEG3350, 0.3 g $MgCl_2 \cdot 6H_2O$, 2.5 mL DMSO and 1.25 g LB powder were mixed up with $ddH_2O$ until the final volume reaches 50 mL. Small amount of HCl was added in TSS buffer to adjust pH value to about 6.5. The TSS buffer was filtered through Millipore Steriflip® (50 mL) and stored at 4°C before usage.



doi:10.6342/NTU201902787

Strain 93 or 189 (for TOP10 and Stable3, respectively) was inoculated in 50 mL Terrific Broth (TB) and shaken at 30°C overnight. 500 μL cells were subcultured into 100 mL TB at 37°C until $OD_{600nm}$ reaches 0.5. Cells were transferred into a 50 mL tube and remained on ice for 10 min. Centrifuge the cells at 3,000 x g, 4°C for 10 minutes. Discard the supernatant and resuspend the cell pellet with 10 mL TSS buffer. The cells were distributed as 50 μL aliquots in each 1.5 mL Eppendorf tubes, immediately frozen by liquid nitrogen and finally stored at -80°C.

## 3. Plasmid construction

Plasmids used in this study are listed in Table 1. Restriction enzymes, like BamHI and BbsI, 10X T4 ligation buffer, T4 polynucleotide kinase (PNK), T4 ligase and HiFi DNA Assembly Master Mix for Gibson assembly were all bought from New England Biolabs and were used according to the manufacturer's protocol. The constructed plasmid products were transformed into homemade TOP10 or Stable3 competent cells according to the protocol written below. Plasmid was extracted from subcultured *E. coli* through ZR Plasmid Miniprep Classic (Zymo Research) according to the manufacturer's protocol. The extracted plasmid underwent Sanger sequencing conducted by Academia Sinica Core Facility.

The plasmid pSL122 was constructed through Gibson assembly of two PCR amplicons. One was amplified from pET28a with primers SL410 and SL412. The other amplicon was amplified from plasmid mito-EGFP with primers SL411 and SL413. The Gibson assembly was conducted by mixing 1 μL HiFi DNA Assembly Master Mix and 0.5 μL of each amplicon and heated at 50°C for 1 hour. The product was transformed into homemade Stable3 competent cell.

The plasmid pSL127 was constructed through Gibson assembly of three PCR amplicons. All three of them were amplified from plasmid pAW006 with primers either SL434 and SL439,



doi:10.6342/NTU201902787

SL435 and SL436, or SL437 and SL438. The Gibson assembly was conducted by mixing 1 μL HiFi DNA Assembly Master Mix and 0.33 μL of each amplicon and heated at 50°C for 1 hour. The product was transformed into homemade Stable3 competent cell. The ligation was conducted by

The plasmids pSL127B to pSL127G were all constructed through Gibson assembly of two PCR amplicons. One of the two amplicons is the same for all the six plasmids and was amplified from pSL127 with primers SL448 and SL449. The other amplicons are different but were all amplified from a commercially synthesized gBlock gene fragment SL533 from IDT with various primer pairs. For pSL127B, primers SL456 and SL457 were used to amplify DNA segment of double repeats of COX8A MTS. For pSL127C, primers SL460 and SL461 were used to amplify DNA segment of *S. cerevisiae* COX4P MTS. For pSL127D, primers SL450 and SL451 were used to amplify DNA segment of ACACB optimized MTS. For pSL127E, primers SL454 and SL455 were used to amplify DNA segment of GLDC optimized MTS. For pSL127F, primers SL452 and SL453 were used to amplify DNA segment of POLG optimized MTS. For pSL127g, primers SL458 and SL459 were used to amplify DNA segment of MTHFD1L optimized MTS. The Gibson assembly was conducted by mixing 1 μL HiFi DNA Assembly Master Mix and 0.5 μL of each amplicon and heated at 50°C for 1 hour. The product was transformed into homemade Stable3 competent cell.

The plasmids pSL127Ga, pSL127Gb and pSL127Ge were generated through "round-the-horn" technique. Firstly, pSL127G was amplified with primer pairs SL510 and SL509, SL512 and SL511, or SL601 and SL600, respectively. Next, the PCR amplicons were ligated to form the final product. The ligation mixture included 2.5 μL linear PCR product, 0.5 μL molecular dd$H_2O$, 0.5 μL 1 mM ATP, 10x T4 ligation buffer, T4 PNK and T4 ligase. The mixture was



doi:10.6342/NTU201902787

incubated at 37°C for 1 hour. The product was transformed into homemade Stable3 competent cell.

The plasmids pSL127Gc, pSL127Gd and pSL127Gf were generated through Gibson assembly from pSL127Ga, pSL127Gb and pSL127Ge, respectively. In general, pSL127Ga, pSL127Gb and pSL127Ge were all amplified with primer pairs SL563 and SL562 as backbones. On the other hand, the insert sequence for the three constructs was the same one which was amplified from SL533 gBlock (IDT) with primer pairs SL551 and SL552. Finally, the Gibson assembly was conducted by mixing 1 μL HiFi DNA Assembly Master Mix, 0.5 μL backbone PCR product and 0.5 μL insert PCR product and heated at 50°C for 1 hour. The product was transformed into homemade Stable3 competent cell.

The plasmids pSL146, pSL147, pSL148, pSL149, pSL187 and pSL188 were generated through ligation of BbsI-digesed pSL127Ga, pSL127Gb, pSL127Gc, pSL127Gd, pSL127Ge and pSL127Gf, respectively, with annealed oligos. For pSL146 and pSL148, the annealed oligos was SL584 and SL585. For pSL147 and pSL149, the annealed oligos was SL586 and SL587. For pSL187 and pSL188, the annealed oligos was MF3 and MF4.

The plasmids pSL245 was generated through "round-the-horn" technique by amplifying pSL146 with primers MF44 and MF45. After mixing 2.5 μL linear PCR product, 0.5 μL molecular dd$H_2O$, 0.5 μL 1 mM ATP, 0.5 μL 10x T4 ligation buffer, 0.5 μL T4 PNK and 0.5 μL T4 ligase, the mixture was incubated at 37°C for 1 hour. The product was transformed into homemade TOP10 competent cell. Similarly, the plasmid pSL297 was also generated through "round-the-horn" technique by amplifying pSL245 with primers MF94 and MF95. The ligated product was transformed into homemade TOP10 competent cell as well.



doi:10.6342/NTU201902787

The plasmids pSL246 to pSL249 and pSL298 were generated through "round-the-horn" technique by amplifying pSL179 with various primer pairs. For pSL246, primers MF47 and MF48 were used. For pSL247, primers MF49 and MF50 were used. For pSL248, primers MF51 and MF52 were used. For pSL249, primers MF53 and MF54 were used. For pSL298, primers MF96 and MF97 were used. After mixing 2.5 μL linear PCR product, 0.5 μL molecular dd$H_2O$, 0.5 μL 1 mM ATP, 0.5 μL 10x T4 ligation buffer, 0.5 μL T4 PNK and 0.5 μL T4 ligase, the mixture was incubated at 37°C for 1 hour. The product was transformed into homemade TOP10 competent cell.

## 4. Cell culture

HeLa cells were grown in Dulbecco's Modified Eagle Medium (DMEM) supplemented with 10% heated fetal bovine serum (FBS, 56°C for 30 minutes), 1X Antibiotic-Antimycotic (Thermo Fisher Scientific) and 1% HEPES (v/v) and incubated at 37°C in a humidified atmosphere of 5% CO2/95% air. For each time cells were passaged, take a 10-cm dish for instance, cells reached about 80% confluency, were added 1 mL 0.25% trypsin and incubated at 37°C for 3 minutes. After incubation, 9 mL DMEM was added to quench trypsin activity. Cells were then centrifuged at 300 x g for 3 minutes under room temperature and washed with Dulbecco's Phosphate Buffer Saline (DPBS) once. Cell amount was assessed by 0.2% trypan blue staining and Countess™ II automated cell counter (Thermo Fisher Scientific).



doi:10.6342/NTU201902787

## 5. Nucleofection

To efficiently transfect plasmids or proteins, cells were nucleofected by 4D Nucleofector™ X Unit (Lonza) according the manufacturer's instructions with modification written in the following.

For small scale nucleofection, $2x10^5$ HeLa cells were mixed with 20 μL DPBS and indicated cargos (1 μg mito-EGFP plasmid or 500 μM purified mito-EGFP protein). The cells were transferred into 16-well 20 μL Nucleocuvette™ Strip and nucleofected with program CN-114. After nucleofection, 130 μL DMEM was added into each well to resuspend the cells before the cells were transferred into the 35-mm glass bottom dish (#81158, ibidi) with 700 μL prewarmed DMEM at 37°C. The nucleofection well was washed again with 150 μL DMEM, which would be combined into the glass bottom dish.

After nucleofection, in order to reuse the Nucleocuvette Strip, it was firstly washed with a substantial amount of tap water to remove cells, and then was immersed in 20% ethanol. A day before the usage, the strip would be naturally dried out in a biosafety cabinet.

## 6. Immunofluorescence

$2x10^5$ HeLa cells were seeded on 35-mm glass bottom dishes (#81158, ibidi) in 1 mL DMEM. After 24 hours, the cells were washed once with 1 mL DPBS before incubated with 200 nM MitoTracker Deep Red (Invitrogen) in DPBS for 30 minutes at 37°C. After MitoTracker labeling, the cells were washed again with 1 mL DPBS and immersed in 1 mL DMEM. 8 hours after mitochondrial labeling, cells were taken out of the cell culture room. On bench, medium was removed and the cells were fixed with 1 mL 4% (v/v) paraformaldehyde (PFA)/PBS (pH 7.4) for 15 minutes before being washed for three times with 1 mL PBS. Next, cells were penetrated



doi:10.6342/NTU201902787

for 15 minutes by 1 mL 0.1% (v/v) Triton X-100/PBS under room temperature, after which the cells were washed three times with 1 mL PBS.

After penetration, the cells were incubated with either rabbit anti-FLAG antibody (Protintech; 1:2,000 dilution in PBS) to locate Cas9 or rabbit anti-PNPT1 antibody (#ab96176, Abcam; 1:500 dilution in PBS) to locate PNPase at 4°C overnight with aluminum foil covering. After incubation, the cells were firstly washed with 1 mL PBST (PBS containing 0.1% Tween 20) for three times and finally once with 1 mL PBS before being incubated with goat-anti-rabbit IgG antibody which is conjugated with fluorochrome DyLight® 488 (#ab96899, Abcam; 1:250 dilution in PBS) or goat-anti-rabbit IgG antibody with Alexa Fluor 546 (#A-11035, Thermo Fisher Scientific; 1:500 dilution in PBS) for 30 minutes under room temperature with aluminum foil covering. After removing the secondary antibody, the cells underwent nuclear staining by 300 nM DAPI (#D1306, Invitrogen) in PBS for 5 minutes under room temperature with aluminum foil covering. The samples were washed with three times of 1 mL PBST and finally immersed in 1 mL PBS. Images were obtained using confocal microscopy (Olympus FV1000 or Leica SP5 X inverted)

## 7. Synthesis of RNA by T7 *in vitro* transcription

The T7 *in vitro* transcribed RNAs (IVT RNAs) used in this study are listed in Table 2 and their secondary structures are schematically illustrated in Table 3. The DNA templates, including a T7 promoter, a 20-nucleotide target sequence and an optimized sgRNA scaffold[73], were either assembled from synthetic oligonucleotides (IDT, Singapore) by overlapping PCR, or directly amplified through PCR of respective plasmids, using KAPA HiFi PCR kit (Kapa Biosystems,



doi:10.6342/NTU201902787

USA) according to the manufacturer's protocol. PCR conditions and program settings for each DNA template of sgRNA are listed in Table 4.

A day before IVT, 10% polyacrylamide gel containing 6 M urea (Urea-PAGE) should be prepared as following. The front and rear glasses are firstly cleaned by tap water supplemented with Aquet detergent (Scienceware) and Nuclease/EtBr terminator (Protech). After being wiped dry, the two glasses were separated by two plastic strips (0.3 cm thickness) on both sides and fixed with low adhesive yellow tape on the three edges (see Appendix 1A and B). To strengthen the fixation, a shorter piece of tape was used to adhere on the bottom edge (Appendix 1C).

A 500 mL Urea-PAGE premix solution was prepared ahead by mixing 210 g urea, 125 mL acrylamide/bis 29:1 (40%), 50 mL 5X TBE buffer and 165 mL $ddH_2O$, and was stored at 4°C. To prepare a slide of Urea-PAGE with 0.3-cm thickness, 80 mL Urea-PAGE premix solution is prewarmed in 37°C water bath before being mixed with 160 μL 20% ammonium sulfate (APS) and 80 μL TEMED. The mixture was immediately added into the mold by 25 mL autopipette. Notice that when adding the mixture, the mold should be tilted to avoid bubbles (Appendix 1D). Finally, the comb was carefully set onto the mold without forming any bubble. After about 2 hours under room temperature, Urea-PAGE was solidified and stored at 4°C. Before usage, the tapes were torn off from the glasses and the gel mold was set onto the Owl™ Dual-Gel Vertical Electrophoresis System (Thermo Fisher Scientific) (Appendix 1E). The wells were washed for several times by pipette P1000 to ensure the absence of remained gel debris within.

A 300 μL total volume of T7 *in vitro* transcription (IVT) reaction consists of 60 μL of 25 mM ribonucleotide triphosphate (rNTP) mixture, 30 μL of 10X IVT buffer (30 mM Tris–HCl [pH 8], 20 mM $MgCl_2$, 0.01% Triton X-100, 2 mM spermidine), 30 μL of 50% (w/v) polyethylene glycol 3000 (PEG3000), 6 μL of 1 M dithiothreitol (DTT), 30 μL of 100 μg/mL



doi:10.6342/NTU201902787

homemade T7 polymerase and 144 μL of PCR product as DNA template. The reaction was incubated at 37°C with shaking for 2 hours. Next, 1 μL of RQ1 RNase-free DNaseI (Promega, Madison, WI) was added to digest the DNA template at 37°C with shaking for 1 hour. The reaction was quenched with 150 μL 2X STOP solution (95% deionized formamide, 0.05% [w/v] bromophenol blue, 0.05% [w/v] xylene cyanol FF, and 20 mM EDTA, pH 8) at 50°C water bath for 10 minutes.

The RNA product underwent electrophoresis in 10% Urea-PAGE aforementioned with EC300XL power supply (Thermo Fisher Scientific) under 300 voltage, 250 mA for 4 hours. For two slides of 0.3-cm thick Urea-PAGE each of which has 3 major wells and one small for marker, each major well is sufficient for 1800 μL solution, that consists of 1200 μL volume of T7 IVT reaction and 600 μL 2X STOP solution (see Appendix 1E). The RNA band was excised from the gel with surgical blade (Feather, #10), grinded up in a 50 mL tube with 15 mL serological pipette (Jet Biofil), eluted with 30 mL DEPC dd$H_2O$ and 5 mL 3M sodium acetate (pH 5), and rotated on RotoFlex tube rotator (Argos Technologies) overnight at 4°C.

Gel debris were pulled down by centrifugation using Allegra X-30R (Beckman Coulter) at 3,500 rpm, 4°C for 15 minutes. The supernatant containing RNA was transferred to another 50 mL tube before being mixed with 40 μL 1 mg/mL glycerol and 25 mL isopropanol. After inverting for several times, the mixture was stored at -20°C overnight to precipitate RNA.

The RNA mixture underwent centrifugation using Allegra X-30R (Beckman Coulter) at 4,000 rpm, 4°C for 15 minutes. White RNA pellet could be observed at the bottom after centrifugation. The supernatant was removed until about 1 mL was left. The RNA pellet was resuspended and transferred to a 1.5 mL Eppendorf tube. Next, the RNA pellet was collected by centrifugation using Centrifuge 5424R (Eppendorf) at 16,000 x g, 4°C for 1 minute. After



doi:10.6342/NTU201902787

removing supernatant, the RNA pellet was washed three times with 70% ethanol, once with 100% ethanol, and dried by vacuum under room temperature for 10 minutes. The RNA pellet was dissolved in 80 μL RNA dissolving buffer (20 mM HEPES [pH 7.5], 150 mM KCl, 10% glycerol, 10 mM $MgCl_2$ and 1 mM 2-mercaptoethanol). Usually, at this step, some gel debris could still be found in the RNA solution. These debris were spinned down and the supernatant was transferred to another 1.5 mL Eppendorf tube. After measurement of concentration by Nanodrop, RNA was immediately frozen by liquid nitrogen and stored at −80°C.

## 8. Calf intestinal alkaline phosphatase (CIP) treatment

The T7 *in vitro* transcribed RNAs (IVT RNAs) used in this study underwent CIP treatment to remove triphosphate group on their 5' end to reduce possible cellular immune response[74]. For one reaction, 600 pmol of respective IVT RNA was mixed with 2 μL CIP (New England Biolabs) and RNA dissolving buffer to make a final volume of 30 μL in a 1.5 mL Eppendorf tube. The mixture was incubated in 37°C water bath for 1 hour. Next, 370 μL 20 mM sodium acetate (pH 5) was added to expand the volume before mixing thoroughly on a vortex with 400 μL phenol:chloroform (low pH) to extract RNA. The mixture was centrifuged using Centrifuge 5424R (Eppendorf) at 21,130 x g for 15 minutes at 4°C. The upper layer was transferred into a new 1.5 mL Eppendorf tube and added 400 μL chloroform. Mixed thoroughly on a vortex, the mixture was again centrifuged at 21,130 x g for 15 minutes at 4°C. The upper layer was again transferred into a new 1.5 mL Eppendorf tube, but this time was added 10 μL 1 mg/mL glycogen, 100 μL 3 M sodium acetate (pH 5) and 1 mL isopropanol before vortex and storage in -20°C overnight to precipitate RNA. The RNA pellet could be observed after a centrifugation of 16,000 x g for 10 minutes at 4°C. The pellet was washed with 1 mL 70% ethanol for 3 times and finally



doi:10.6342/NTU201902787

once with 100% ethanol. After the ethanol wash, the pellet was dried in the vacuum (EYELA) with the lid opened under room temperature for 10 minutes. The dehumidified RNA pellet was dissolved in 20 μL RNA dissolving buffer and frozen by liquid nitrogen before being stored in -80°C. To refold the RNA, the RNA was heated to 65°C for 1 min and naturally cooled to room temperature before usage.

## 9. *In vitro* cleavage assay

To determine the activity of purified Cas9 proteins or the validity of sgRNA, *in vitro* cleavage assay was conducted by mixing Cas9, sgRNA and DNA subtract all together in an Eppendorf tube and its result was checked by DNA agarose gel electrophoresis written as following. For all the sgRNAs used in this study, their target site is located on the *ND4* gene of mtDNA. The DNA subtract was amplified through PCR by mixing 195 μL molecular dd$H_2O$, 60 μL 5X KAPA HiFi Fidelity buffer, 10 μL 100 ng/μL HeLa genomic DNA, 20 μL 10 μM MF78/SL470 primer premix, 9 μL KAPA dNTP Mix and 6 μL KAPA HiFi DNA polymerase. The mixture was distributed as 50 μL aliquot into six PCR tubes and underwent PCR in thermal cycler 6325 Mastercycler Pro S (Eppendorf) with 98°C for 30 seconds, 30 cycles of amplification, 72°C for 2 minutes and 12°C for 5 minutes, in which each cycle of amplification consists 10 seconds of 98°C denaturation, 20 seconds of 59°C annealing and 1 minute of 72°C elongation.

To start the *in vitro* cleavage assay, firstly, all the CIP-treated refolded sgRNAs were diluted into 3 μL 1.2 μM with RNA dissolving buffer and distributed into PCR tubes. After incubation at 65°C for 1 minute, the RNAs were maintained in room temperature for 10 minutes for refolding. Next, 3 μL 1 μM homemade purified Cas9 was added into each RNA tubes. Finally, 3 μL 1 μM



doi:10.6342/NTU201902787

DNA subtract supplemented with 1 μL RNA dissolving buffer was added into the Cas9/sgRNA mixture. Later, the mixture was incubated at 37°C for 30 minutes. The reaction was firstly stopped by adding 1 μL RNase A/T1 and incubated at 37°C for 5 minutes to digest all the sgRNAs. The reaction was completely turned off by adding 10 μL STOP solution (0.5% SDS, 0.5 mg/mL protease K and 3X DNA loading dye in molecular dd$H_2O$ prepared freshly) and incubated at 50°C for 20 minutes. The final product was stored in 4°C before gel electrophoresis.

## 10. RNA transfection

We used Lipofectamine 2000 (Thermo Fisher Scientific) to transfect mito-sgRNAs into cells according to the manufacturer's protocol with slight modifications written below. $3x10^6$ HeLa cells were seeded onto 10-cm culture dish with 10 mL DMEM two days before transfection.

20 μL of each 10 μM CIP-treated mito-sgRNAs were firstly heated at 65°C for 1 minute in a thermal cycler and awaited to cool down to refold under room temperature for 10 minutes. For each mito-sgRNA, two Eppendorf tubes were prepared in the biosafety cabinet. One tube contained 750 μL Opti-MEM (Thermo Fisher Scientific) and respective volume of Lipofectamine 2000 directly proportional to the molecular weight of its corresponding RNA (see Table 5). For instance, for sgRNA51 which has a molecular weight of 38166.5, it needed 17 μL Lipofectamine 2000; for sgRNA54 which has a molecular weight of 94546.9, it needed 41 μL Lipofectamine 2000. The other tube contained 750 μL Opti-MEM and respective 20 μL 10 μM refolded CIP-treated sgRNA. The latter was evenly mixed into the former tube by pipetman P1000 and incubated for 15 minutes under room temperature. The whole mixture was dispensed into the culture cells and incubated for 9 hours at 37°C. The medium was finally removed and the cells were washed once with 1 mL DPBS to terminate the reaction.



doi:10.6342/NTU201902787

## 11. Dynabead mitochondrial extraction

Conjugation

Dynabeads® Co-immunoprecipitation kit was purchased from Thermo Fisher Scientific. To co-precipitate mitochondria, 5 mg Dynabeads were coupled with 100 μg anti-TOMM22 mouse monoclonal antibody (#ST1704, Merck Millipore) according to the manufacturer's protocol.

Prewash

Before usage, anti-TOMM22-antibody-coupled Dynabeads were prewashed as following. To extract mitochondria from $1x10^7$ HeLa cells, 30*X μL Dynabeads (X = sample number) were resuspended and transferred to another 1.5 mL Eppendorf tube. 900 μL Blocking buffer (1X PBS and 0.01% BSA) was added and the tube was rotated for 5 minutes under room temperature. Notice that soft rotation is required and bubble formation should be avoided. After spinning down, the tube was set onto the magnetic separator DynaMag™-2 (Thermo Fisher Scientific) for 1 minute. The supernatant was discarded and 900 μL new MSH buffer (210 mM mannitol, 70 mM sucrose, 10 mM Tris HCl [pH 8.0], 50 mM NaCl, 1 mM EDTA [pH 8.0], 1 mM EGTA, 1 mM TCEP-HCl and 1X Protease Inhibitor Cocktail [Roche]) was added before the tube was rotated for another 5 minutes under room temperature. After spinning down, the tube was set onto the magnetic separator for 1 minute. The supernatant was discarded. The washing step of new MSH buffer was repeated for another two times. 30*X μL new MSH buffer was added and the washed beads can be stored at 4°C before usage.

Mitochondrial extraction

For $1x10^7$ HeLa cells grown in a 10-cm dish, cells were detached with 1 mL 0.25% trypsin at 37°C for 3 minutes and quenched with 9 mL DMEM. After centrifuge at 300 x g for 3 minutes under room temperature, the cells were washed with 5 mL DPBS twice. The supernatant was



doi:10.6342/NTU201902787

discarded and 1 mL new MSH buffer supplemented with 50 μL 10% Tween 20 was added to resuspend the cell pellet. Next, the cells were sonicated with Microtip (Q700, Qsonica) on ice for 9 pulses, with 1-second on and 20-second off intervals.

For RNA recovery, 30 μL of the lysed cells was collected and labelled as "Total" (total RNA) before mixing with 300 μL TRIzol (Thermo Fisher Scientific). All "Total" tubes remained on ice.

The rest of the cells underwent centrifuge at 500 x g for 5 minutes at 4°C to discard contact cells, nuclei and cell debris. The supernatant was added 30 μL washed anti-TOMM20-antibody-coupled Dynabeads and shacked on RotoFlex tube rotator (Argos Technologies) for 1 hour at 4°C. After rotation, the tube was set onto the magnetic separator for 1 minute. After removing the supernatant, the pellet underwent 3 times of washing with 1 mL new MSH buffer.

For RNA recovery, the pellet was resuspended by 30 μL Storage buffer (MACS kit, see below) and added 1 μL RNase A/T1 (Thermo Fisher Scientific). Then, the tube was incubated under room temperature for 20 minutes to removed RNA outside of mitochondria before adding 300 μL TRIzol and labeling as "Mito" (mitochondrial RNA).

Finally, all "Total" and "Mito" tubes were immediately frozen by liquid nitrogen and stored at -80°C overnight before RNA extraction.

## 12. MACS mitochondrial extraction

Mitochondria Isolation kit for human cell was purchased from MACS® Technology (Miltenyi Biotec) and was applied according to the manufacturer's protocol with modifications written as following. For $1x10^7$ HeLa cells grown in a 10-cm dish, cells were detached with 1 mL 0.25% trypsin at 37°C for 3 minutes and quenched with 9 mL DMEM. After centrifuge at 300 x g for 3 minutes under room temperature, the cells were washed with 5 mL DPBS twice.



doi:10.6342/NTU201902787

The cell pellet was resuspended by 1 mL Lysis buffer before being sonicated with Microtip (Q700, Qsonica) on ice for 9 pulses, with 1-second on and 20-second off intervals.

For RNA recovery, 30 μL of the lysed cells was collected and labelled as "Total" (total RNA) before mixing with 300 μL TRIzol (Thermo Fisher Scientific). All "Total" tubes remained on ice.

The rest of the cells underwent centrifuge at 500 x g for 5 minutes at 4°C to discard contact cells, nuclei and cell debris. The supernatant was added into 9 mL 1X Separation buffer supplemented with 50 μL anti-TOMM22 MicroBeads and shacked on rotator for 1 hour at 4°C.

The LS column was set onto the homemade Neodymium magnet cylinder and was rinsed with 3 mL 1X Separation buffer before usage. After 1-hour shaking, the cells were transferred into the LS column. The column was washed with 9 mL 1X Separation buffer before the magnet cylinder was removed. After 750 μL 1X Separation buffer was added into the column, the plunger was immediately settled onto the column and pressed to elute purified mitochondria. Before the bubbles went out the column, the plunger was removed and another 750 μL 1X Separation buffer was added into the column. Again, the plunger was used to elute mitochondria and was removed before bubbles came out of the column. The elutes were centrifuged at 21,130 x g for 5 minutes at 4°C to form mitochondria pellet.

For RNA recovery, the pellet was resuspended by 30 μL Storage buffer and added 1 μL RNase A/T1 (Thermo Fisher Scientific). Then, the tube was incubated under room temperature for 20 minutes to removed RNA outside of mitochondria before adding 300 μL TRIzol and labeling as "Mito" (mitochondrial RNA).

Finally, all "Total" and "Mito" tubes were immediately frozen by liquid nitrogen and stored at -80°C overnight before RNA extraction.



doi:10.6342/NTU201902787

## 13. RNA extraction

We used Direct-zol™ RNA MiniPrep kit (Zymo Research, #R2052) to extract RNA from TRIzol-treated samples after mitochondrial extraction according to the manufacturer's protocol with slight modifications. The TRIzol-treat sample, usually 30 μL sample with 300 μL TRIzol, was added 330 μL 100% ethanol and transferred into the Zymo-Spin™ IC Column in a Collection Tube. Following the manufacturer's protocol, the DNaseI treatment was conducted in column on a 37°C dry bath for 15 minutes. Finally, RNA was eluted with 20 μL DEPC-treat deionized water and stored at -80°C. For $1x10^7$ HeLa cells extracted by MACS, the average concentration for total RNA was 300 ng/μL and that of mitochondria fraction was about 30 ng/μL. For $1x10^7$ HeLa cells extracted by Dynabeads, the average concentration for total RNA was 200 ng/μL and that of mitochondria fraction was about 20 ng/μL.

## 14. Reverse transcription-quantitative polymerase chain reaction (RT-qPCR)

After RNA extraction, 50 ng RNA was mixed in DEPC $ddH_2O$ to reach a total volume of 6 μL and added with 1 μL 10 mM dNTP and 6 μL 2 μM reverse primer mixture containing MF17, MF19, MF85, MF87, MF89 and MF91 dissolved in DEPC $ddH_2O$. To anneal the primers, the RNA mixture underwent 65°C heating using thermocycler for 5 minutes before being cooled down on ice for 2 minutes. Next, reverse transcription (RT) reaction mixture which consists 4 μL 5X SSIV buffer, 1 μL 0.1 M DTT, 1 μL RNase OUT and 1 μL SuperScript IV Reverse Transcriptase (#18090050, Thermo Fisher Scientific) was premixed and added into the RNA mixture, making a total volume of 20 μL. RT reaction was conducted on Mastercycler 6325 Pro S (Eppendorf) at 60°C for 50 minutes and 80°C for 10 minutes to obtain cDNA.



doi:10.6342/NTU201902787

After RT, cDNA was diluted from 2500 to 10 ng/μL by molecular dd$H_2O$. Primers used for RT-qPCR are listed in Table 1. To quantify RNA levels of the indicated transcripts in whole cell extract or purified mitochondria, qPCR was conducted in triplicate for all samples by using Power SYBR Green Master Mix (#4367659, Thermo Fisher Scientific) on the StepOnePlus™ Real-Time PCR System (Applied Biosystems) as following.

Firstly, SYBR Green/primer mixture was premixed on ice according to the number of samples. Take the relative abundance of sgRNA over endogenous 5S rRNA in 10 samples for instance, a total volume of 399 μL SYBR Green/primer mixture was prepared in one 1.5 mL Eppendorf tube before being distributed as 37.5 μL aliquot for ten 1.5 mL Eppendorf tubes (samples) and as 13.5 μL aliquot for one 1.5 mL Eppendorf tube (no template control, NTC) (see Appendix 2). Next, 12.5 μL of 10 ng/μL indicated cDNA samples or 4.5 μL molecular water (for NTC) were loaded into individual tubes, respectively. The mixture was thoroughly vortexed at the lowest amplitude for three times (~1 second each) and spinned down. This vortex process was repeated for another two times before the mixture was aliquoted as 15 μL into optical tubes or 96-well for qPCR using low retention tips. After being loaded, sample was centrifuged at 300 x g under room temperature for 1 minute and put onto the StepOnePlus™ Real-Time machine for qPCR.



doi:10.6342/NTU201902787

# Figures and Tables

| Non-programmable | Programmable | Programmable |
|---|---|---|
| Protein:DNA pairing | Protein:DNA pairing | RNA:DNA pairing |
| restriction enzyme | ZFN & TALEN | CRISPR-Cas9 |
| 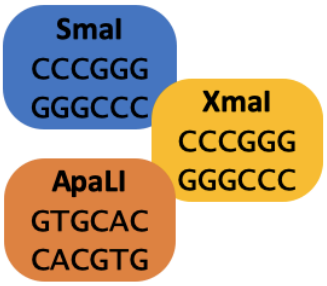  | 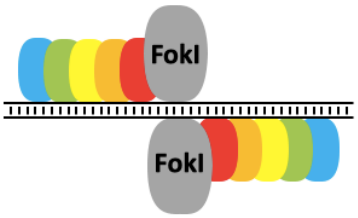  | 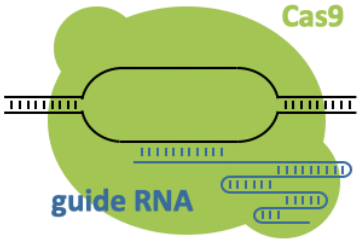  |
| limited target sites | slowly target switch | one protein for multi-targets |

**Figure 1. Comparison between current methods for mtDNA manipulation**

Restriction enzymes were firstly introduced into the field of mtDNA manipulation. Despite its high efficiency on targeted mtDNA cleavage, restriction enzyme is hard to use due to its limitation on target selection. One the other hand, artificial DNA endonucleases, like ZFN and TALEN, involve a nonspecific restriction enzyme FokI and different combinations of DNA binding domains to enable specific cleavage on targeted mtDNA region. Despite the high specificity on DNA targeting, ZFN and TALEN take time to rearrange and recombine various domains when switching onto a different target. Compared to the other two methods, CRISPR-Cas9 gene editing technology is user-friendly because it depends on one single protein Cas9 and is able to cleave different mtDNA by simply changing its guide RNA.



doi:10.6342/NTU201902787

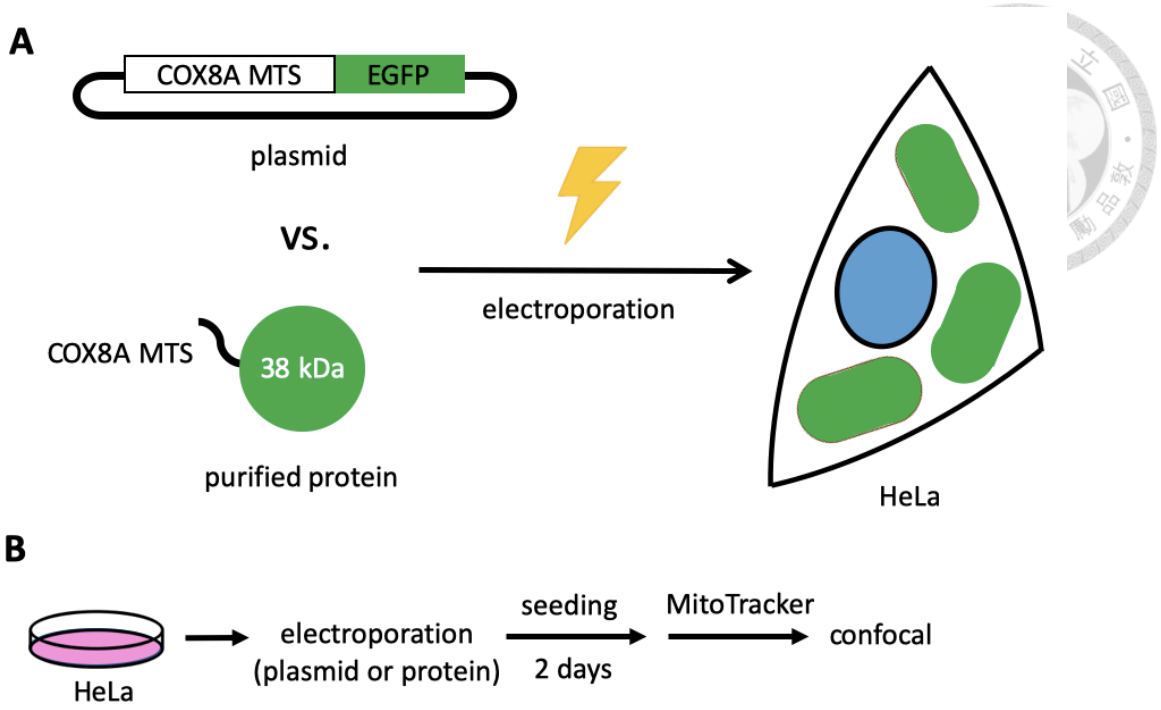


**Figure 2. Schematic design for mito-EGFP transfection**

(A) To test our hypothesis whether we could send an MTS-tagged Cas9 RNP into mitochondria through electroporation, we used a relatively smaller MTS-tagged EGFP to simplify the condition. By electroporating either a plasmid form or a purified protein form of COX8A MTS-EGFP, we wanted to see which form of EGFP can localize to mitochondria after the transfection. (B) Schematic flow: mito-EGFP is transiently expressed in HeLa cells 2 days after transfection with 1 μg plasmid or 500 μM purified protein through electroporation. MitoTracker Deep Red is used to stain mitochondria one day ahead of confocal microscopy imaging.



doi:10.6342/NTU201902787

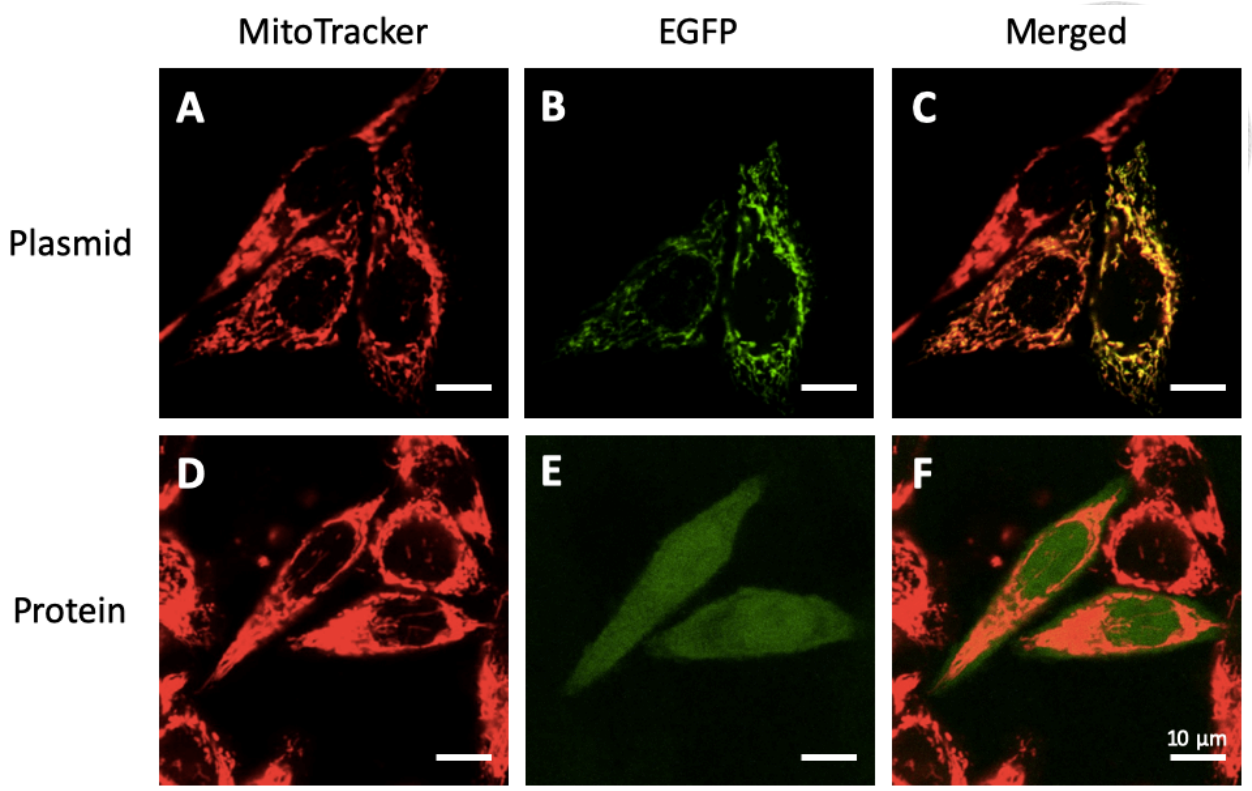


**Figure 3. The intracellular localization of mito-EGFP**

Mito-EGFP (COX8A MTS-EGFP) is transiently expressed in HeLa cells 2 days after nucleofection with 1 μg plasmid (upper row) or 500 μM purified protein (lower row) through electroporation. Mitochondria were marked by MitoTracker Deep Red (red, see panels A and D). (B) The well-folded purified EGFP in the protein group spreads all over the cells at the indicated timing, showing no concentration effect even with the help of COX8A MTS. (C) Merged image shows protein form EGFP even localize into nucleus, where mitochondrial pseudogenes exist and may cause gene instability if a folded MTS-tagged Cas9 RNP directly enter nucleus. (E) The plasmid form of EGFP, after transcription and translation, can generate concentrated EGFP signal only within mitochondria. (F) Co-localization appears yellow on digitally merged image.



doi:10.6342/NTU201902787

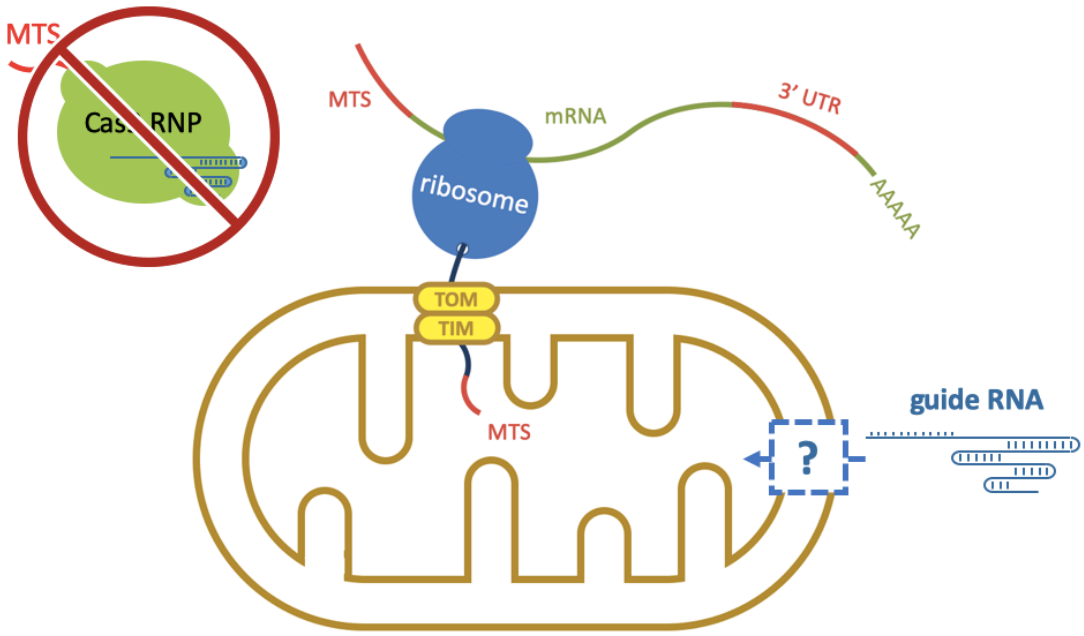


**Figure 4. Co-translational mechanism for mitochondrial protein import**

According to our data along with studies from other scientists, mitochondrial protein import mechanism is largely coupled with translation. Firstly, mRNA approaches the outer membrane of mitochondria through the help of its 3' UTR, which would be recognized by proteins in charge of this process. Furthermore, once the ribosome is combined with the mRNA and starts translation, the polypeptide generated would be identified by TOM through the MTS signal on the N terminal of the polypeptide. The polypeptide is transported through TOM-TIM channel and finally undergoes refolding to form functional protein within the mitochondrial matrix. Referring this theory, a well-folded Cas9 RNP cannot be used in this study. Cas9 must be transfected in either plasmid, viral vector, or mRNA form, and later transported to mitochondria coupling with translation. To be noticed, since polypeptide form of Cas9 can no longer bind guide RNA, we postulate that guide RNA needs to enter mitochondria separately through a different pathway.



doi:10.6342/NTU201902787

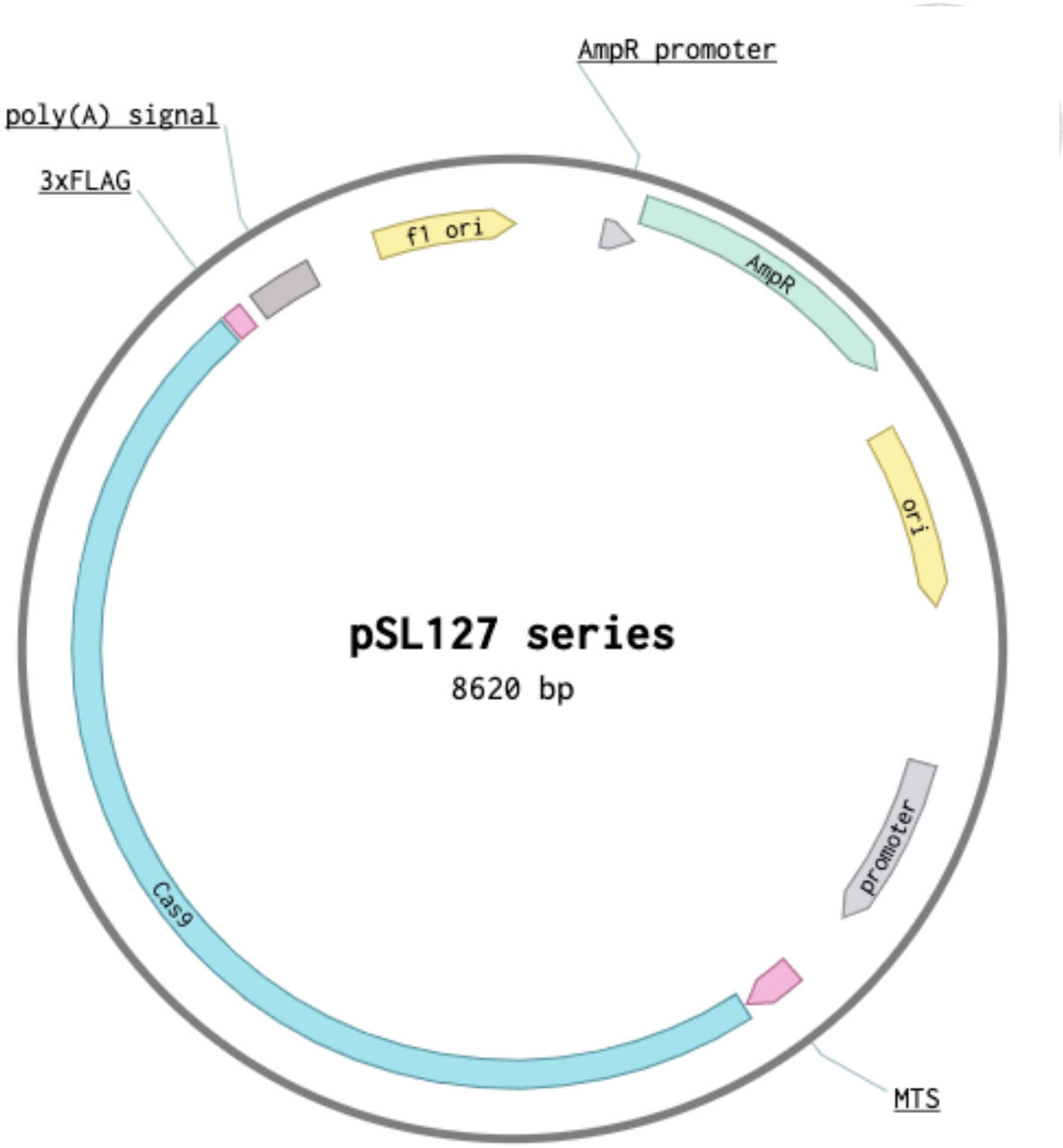


**Figure 5. Plasmid map for pSL127 series**

A series of Cas9 harboring either without or with an MTS was generated through this study. Triple repeats of FLAG motifs were cloned following the Cas9 sequence to enhance FLAG signal.



doi:10.6342/NTU201902787

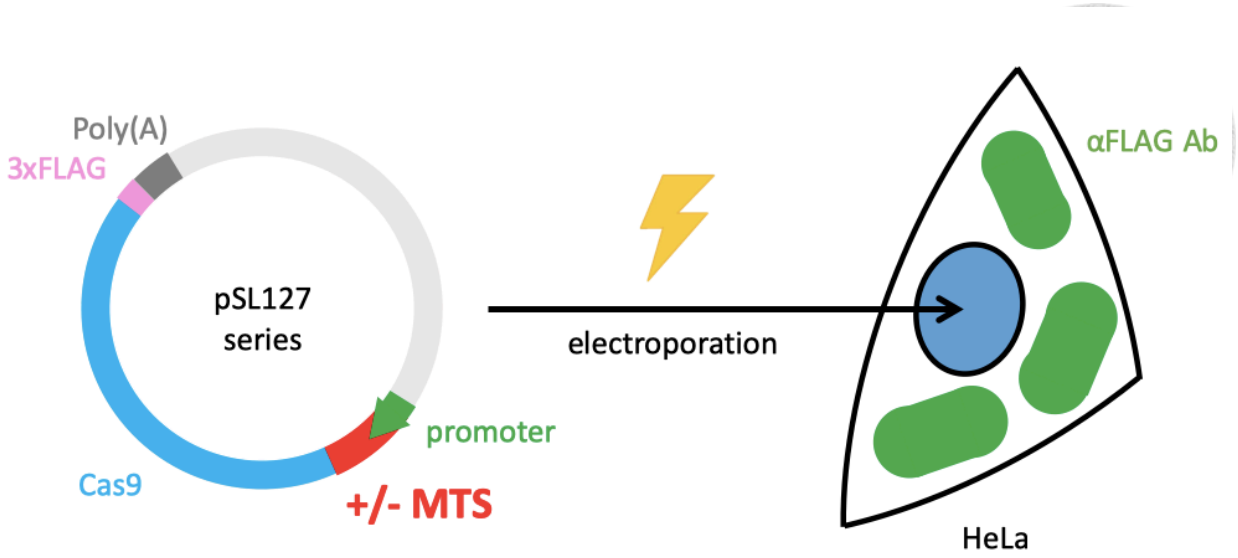


**Figure 6. Schematic flow to determine localization of mito-Cas9s**

After electroporation of the different versions of pSL127 series, we hope to see that Cas9 cannot enter mitochondria but Cas9 with MTS can show a concentration effect within mitochondria.



doi:10.6342/NTU201902787

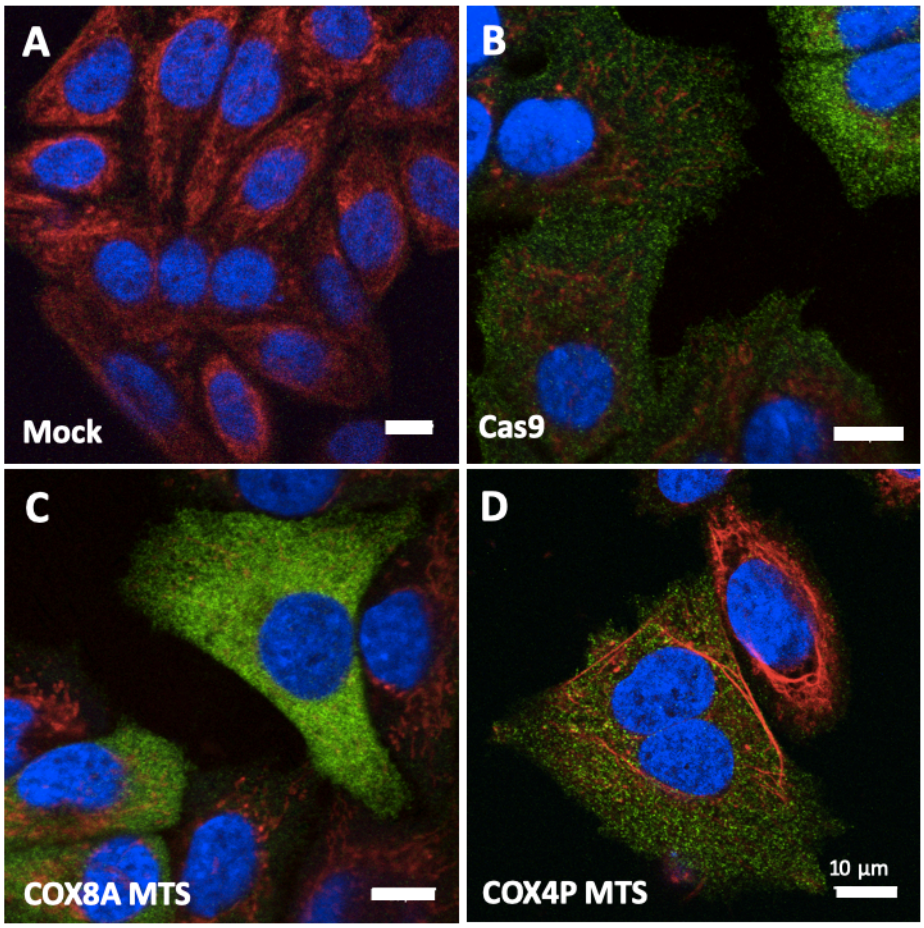


**Figure 7. Common MTSs are not enough for mito-Cas9 to enter mitochondria**

(A) Untreated HeLa cells serve as negative control. (B) Cas9 without or with different MTSs in HeLa cells 2 days after transfection was detected by anti-FLAG antibody (see panels B-H). (B) Pure Cas9 spreads all over the cytosol and cannot enter mitochondria. (C) Cas9 with double-repeats of reported MTS from COX8A, 1-21 aa, shows no concentration effect within mitochondria, suggesting that COX8A MTS is not sufficient for Cas9. (D) Cas9 fused with a reported MTS from *S. cerevisiae* COX4P, 1-24 aa, cannot enter mitochondria, indicating this MTS is not suitable for Cas9. Blue signal, nuclei stained by DAPI. Red signal, mitochondria stained by MitoTracker Deep Red. Green signal, Cas9 determined by anti-FLAG antibody.



doi:10.6342/NTU201902787


| Size (kDa) | Protein name | MTS |
|---|---|---|
| 277 | Acetyl-CoA carboxylase 2 | ACACB MTS (1-40 aa) |
| 140 | Mitochondrial DNA polymerase γ subunit 1 | POLG MTS (1-25 aa) |
| 113 | Mitochondrial glycine dehydrogenase | GLDC MTS (1-35 aa) |
| 106 | Mitochondrial monofunctional C1-tetrahydrofolate synthase | MTHFD1L MTS (1-31 aa) |

**Figure 8. Candidate MTSs from large nuclear-encoded mitochondrial proteins on UniProt**

To search a suitable MTS for mitochondrial import of such a large Cas9, which is about 160 kDa, we found all the nuclear-encoded mitochondrial proteins on online protein database UniProt and prioritize them by their size. We chose four candidate MTS from the first four largest proteins with reported or predicted MTS. Each MTS was named by the gene its corresponding protein is encoded. To be noticed, each MTS is composed of various length of amino acids.



doi:10.6342/NTU201902787

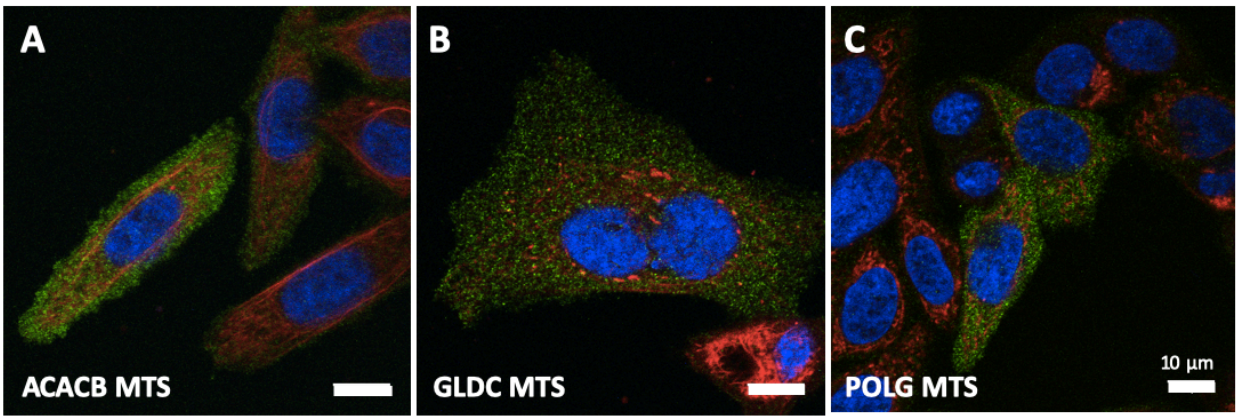


**Figure 9. Most candidate MTSs from UniProt are not suitable for mito-Cas9**

(A) Cas9 with an MTS from Acetyl-CoA carboxylase 2 (UniProt ID: O00763), 1-40 aa, shows no concentration effect within mitochondria, suggesting that this MTS is not sufficient for Cas9. (B) Cas9 fused with a predicted MTS from mitochondrial glycine dehydrogenase (UniProt ID: P23378), 1-35 aa, cannot enter mitochondria, indicating this MTS is not suitable for Cas9 as well. (C) Cas9 fused with an MTS from DNA polymerase subunit gamma-1 (UniProt ID: O00763), 1-38 aa, can neither enter mitochondria, showing this MTS is inappropriate for Cas9. Blue signal, nuclei stained by DAPI. Red signal, mitochondria stained by MitoTracker Deep Red. Green signal, Cas9 determined by anti-FLAG antibody.



doi:10.6342/NTU201902787

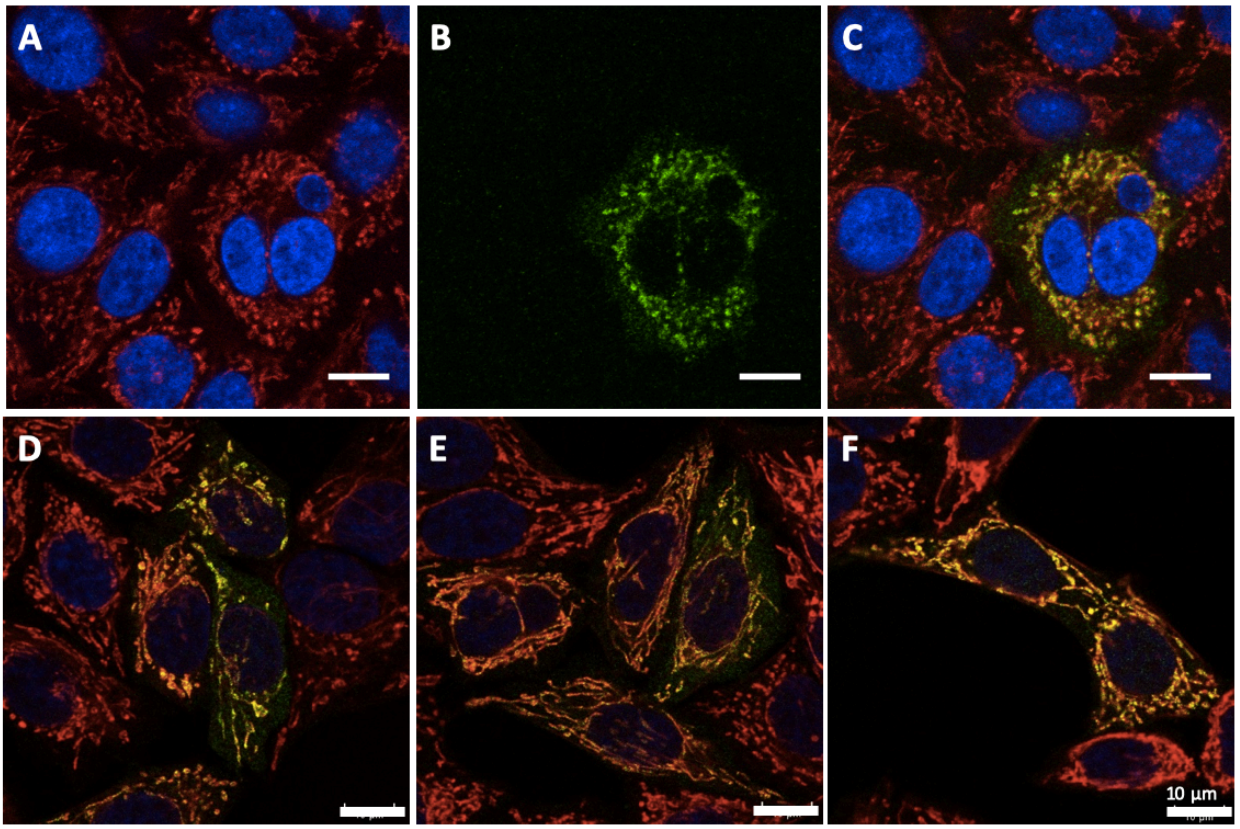


**Figure 10. MTHFD1L MTS is suitable for mito-Cas9**

Cas9 fused with an MTS from mitochondrial monofunctional C1-tetrahydrofolate synthase (UniProt ID: Q6UB35), 1-38 aa, can localize into mitochondria, suggesting this MTS is able to bring a protein as large as Cas9 into mitochondria. (A) After transfection for 2 days, the nuclei were stained by DAPI, showing blue signal, and the mitochondria were stained by MitoTracker Deep Red, showing red signal. (B) mito-Cas9 was firstly located by primary anti-FLAG antibody and an Alexa Flour 488-conjugated secondary antibody, thereby showing green signal. (C-F) Merged images from different samples all indicate co-localization of mito-Cas9 and mitochondria, showing yellow signals.



doi:10.6342/NTU201902787

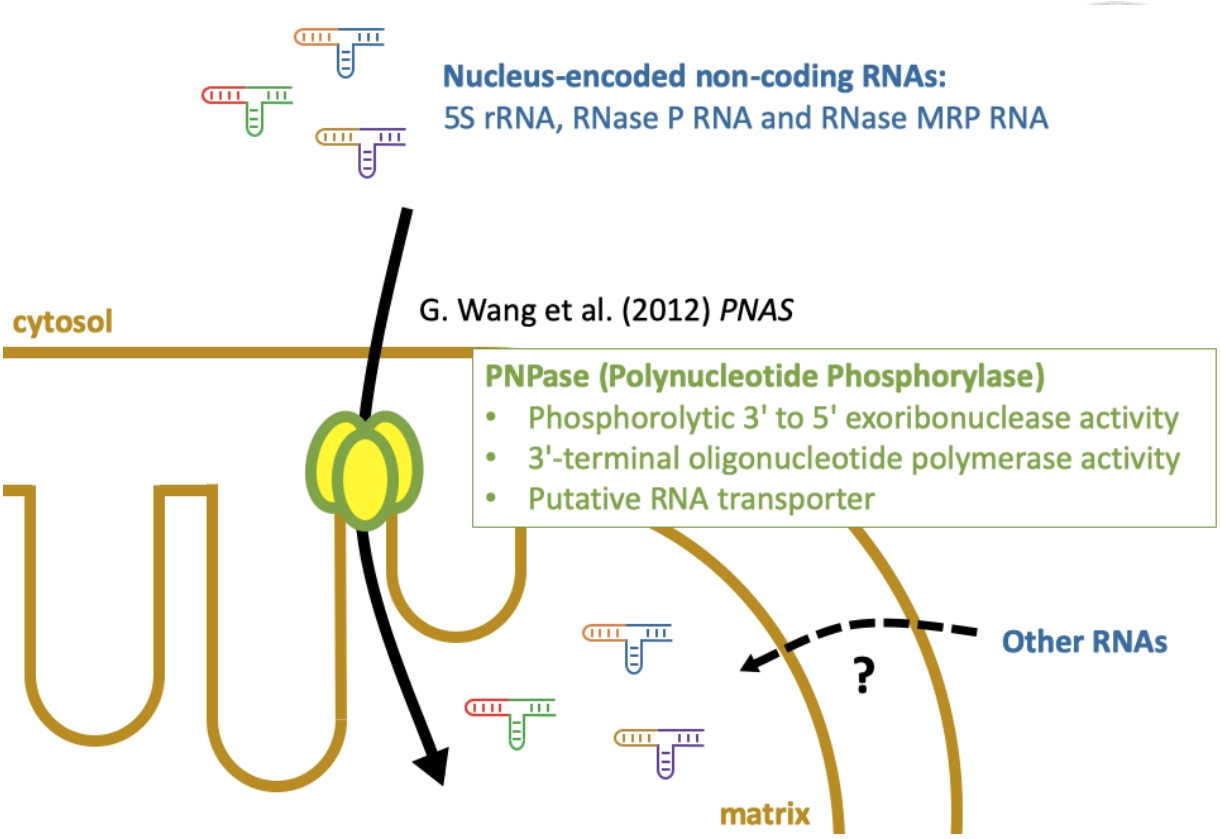


**Figure 11. PNPase as a putative RNA transporter**

Polynucleotide phosphorylase (PNPase) was previously published to function as a RNA exonuclease and polymerase in both bacteria and plants. This multifunctional protein which had been found over 60 years ago was recently uncovered a new function to import several nuclear-encoded non-coding RNAs, including 5S rRNA, RNase P RNA, and RNase MRP RNA, into mitochondria. These non-coding RNAs are postulated to involve numeral crucial mitochondrial metabolisms like transcription and translation. Nevetheless, questions like how PNPase, which is mainly located at the mitochondrial intermembrane space, can facilitate RNA import from cytosol and whether there are other mitochondrial RNA import mechanisms existing are still under debate.



doi:10.6342/NTU201902787

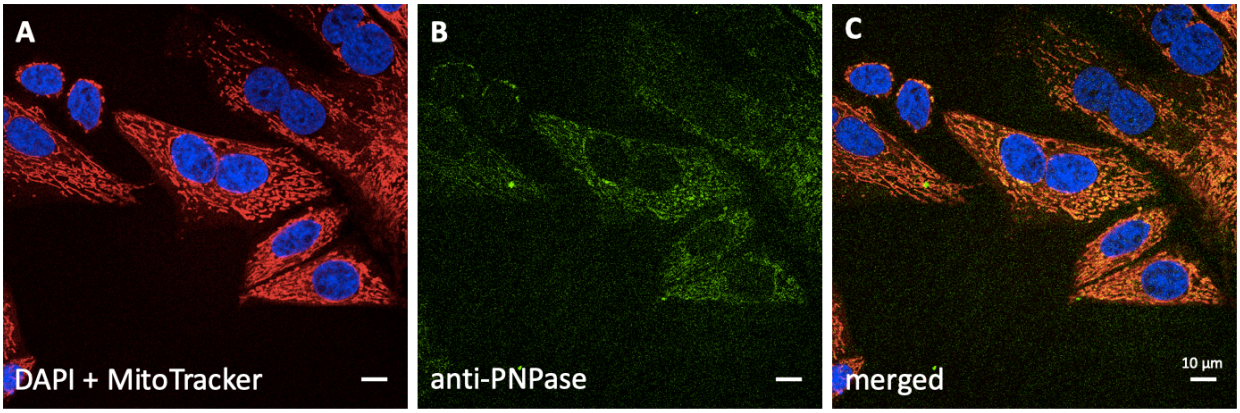


**Figure 12. PNPase exists in HeLa mitochondria**

Untreated HeLa cells were observed under confocal microscope with immunofluorescent signals to determine the localization of PNPase (A-C). (A) DAPI and MitoTracker Deep Red locate nuclei and mitochondria, respectively. (B) PNPase was firstly located by primary anti-PNPase antibody and emits fluorescent signal using Alexa Fluor 488-conjugated secondary antibody. (C) Merged image illustrates co-localization of PNPase with mitochondria, thus showing yellow signal.



doi:10.6342/NTU201902787

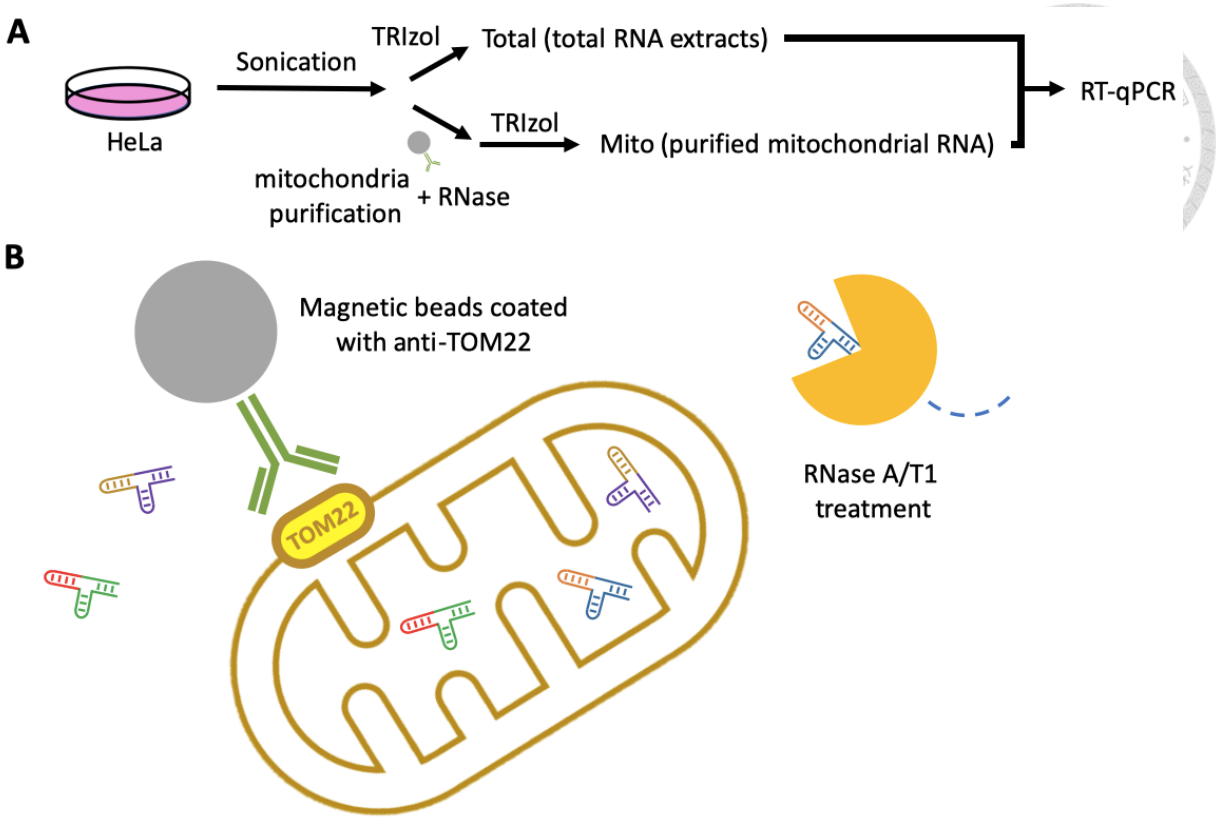


**Figure 13. Schematic flow for mitochondrial RNA extraction**

(A) Simplified work flow demonstrates how total RNA and mitochondrial RNA were extracted from one HeLa sample. After sonication, a portion of whole cell lysate was collected and underwent TRIzol-mediated RNA recovery to generate total RNA. The rest of the cell lysate went through mitochondrial purification and RNase A/T1 treatment before adding TRIzol to ensure RNA purity. Both total RNA and mitochondrial RNA underwent RT-qPCR to analyze mitochondrial import rates of the three PNPase-related nuclear-encoded non-coding RNAs. (B) Cartoon illustration simplifies the process for mitochondrial purification. After sonication, the mitochondria were released and pulled down by anti-TOM22-antibody-conjugated magnetic beads. After discarding supernatant which contains cell debris and intact cells, the mitochondrial pellet was resuspended by storage buffer and treated with RNase A/T1 under room temperature for 20 minutes to degrade all the RNA contamination outside of purified mitochondria



doi:10.6342/NTU201902787

**Concept**

$$\text{Translocation ratio} = \frac{[\text{target RNA}]_{\text{Mito}}}{[\text{target RNA}]_{\text{Total}}}$$

**Formula**

$$\Delta\Delta Ct = \Delta Ct_{Mito}(\text{target-M16S}) - \Delta Ct_{Total}(\text{target-M16S})$$

$$\text{Ratio} = 2^{-\Delta\Delta Ct}$$

**Example**

| Sample | Target | CT | ΔCT | ΔΔCT | Ratio |
|---|---|---|---|---|---|
| Mito | 5.8S | 30.0 | =30-24.2=5.8 | =5.8-(-4.2) | =2^(-10) |
| Mito | M16S | 24.2 | | =10 | =0.1% |
| Total | 5.8S | 16.7 | =16.7-20.9=-4.2 | | |
| Total | M16S | 20.9 | | | |

Mito = purified mitochondrial RNA
Total = total RNA extracts
5.8S = 5.8S rRNA (cytosolic)
M16S = M16S rRNA (mitochondrial)

**Figure 14. Calculation for mitochondrial translocation rates of PNPase-related RNAs**

To calculate the mitochondrial translocation ratio of endogenous nuclear-encoded RNAs, we adopted the concept that the ratio equals to the amount of a specific RNA within the purified mitochondria over its total amount within cells. To calculate the real value from qPCR results, the Ct value of target RNA was firstly normalized to its corresponding M16S rRNA Ct value in both total RNA and mitochondrial RNA fractions. Then, the delta-delta Ct value equals to the delta Ct of mitochondrial RNA group taken away the delta Ct of total RNA group. Finally, the translocation ratio equals to 2 to the power of minus delta-delta Ct value. For example, a real data set was written above to calculate the translocation ration of negative control 5.8S rRNA. The result shows its ratio is 0.1%, indicating no import as expected.



doi:10.6342/NTU201902787

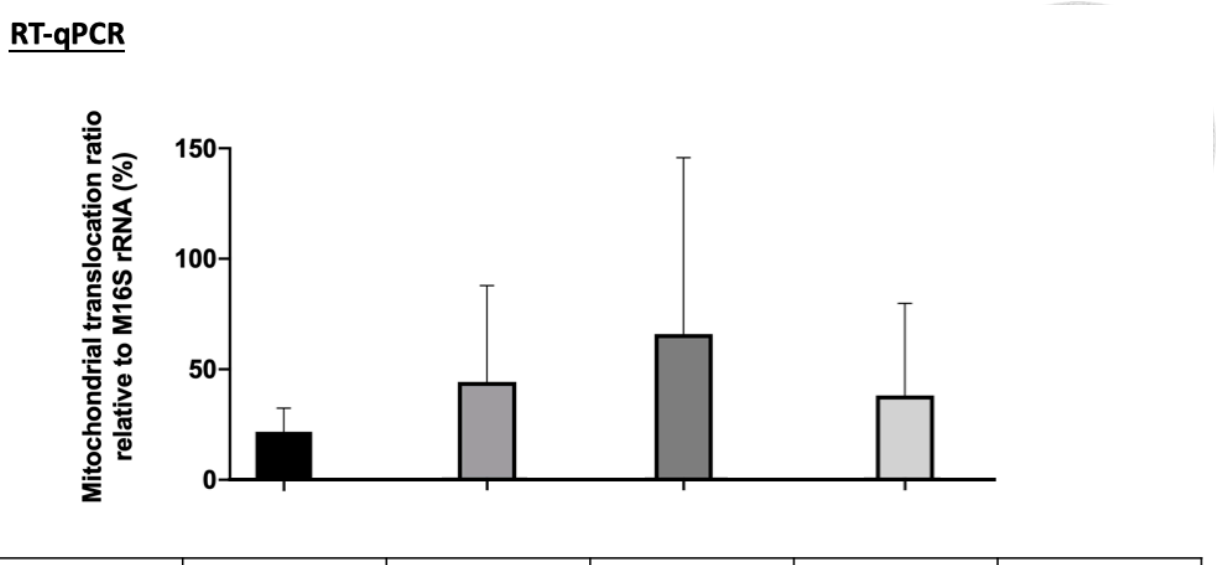


| M16S rRNA | 5.8S rRNA | 5S rRNA | RNase P RNA | RNase MRP RNA | **Name** |
|---|---|---|---|---|---|
| mtDNA | nuclear DNA | nuclear DNA | nuclear DNA | nuclear DNA | **Encoded by** |
| mitochondria | cytosol | cytosol (mainly) & mitochondria | cytosol (mainly) & mitochondria | cytosol (mainly) & mitochondria | **Localizaion** |

**Figure 15. PNPase-related nuclear-encoded RNAs exist in HeLa mitochondria**

Total RNA and mitochondrial RNA were extracted from untreated HeLa cells according to the methods aforementioned. After reverse transcription with a mixture of specific reverse primers for M16S rRNA, 5.8S rRNA, 5S rRNA, RNase P RNA and RNase MRP RNA (see Table 1), qPCR was conducted to evaluate the translocation ratio of each RNA. According to our data, 5.8S rRNA, a nuclear-encode cytosolic ribosomal RNA, expresses the lowest import rate as expected, showing our RNase treatment was adequate to eliminate RNA contamination outside of purified mitochondria. All the three PNPase-related nuclear-encoded RNAs exist in our HeLa mitochondria.



doi:10.6342/NTU201902787

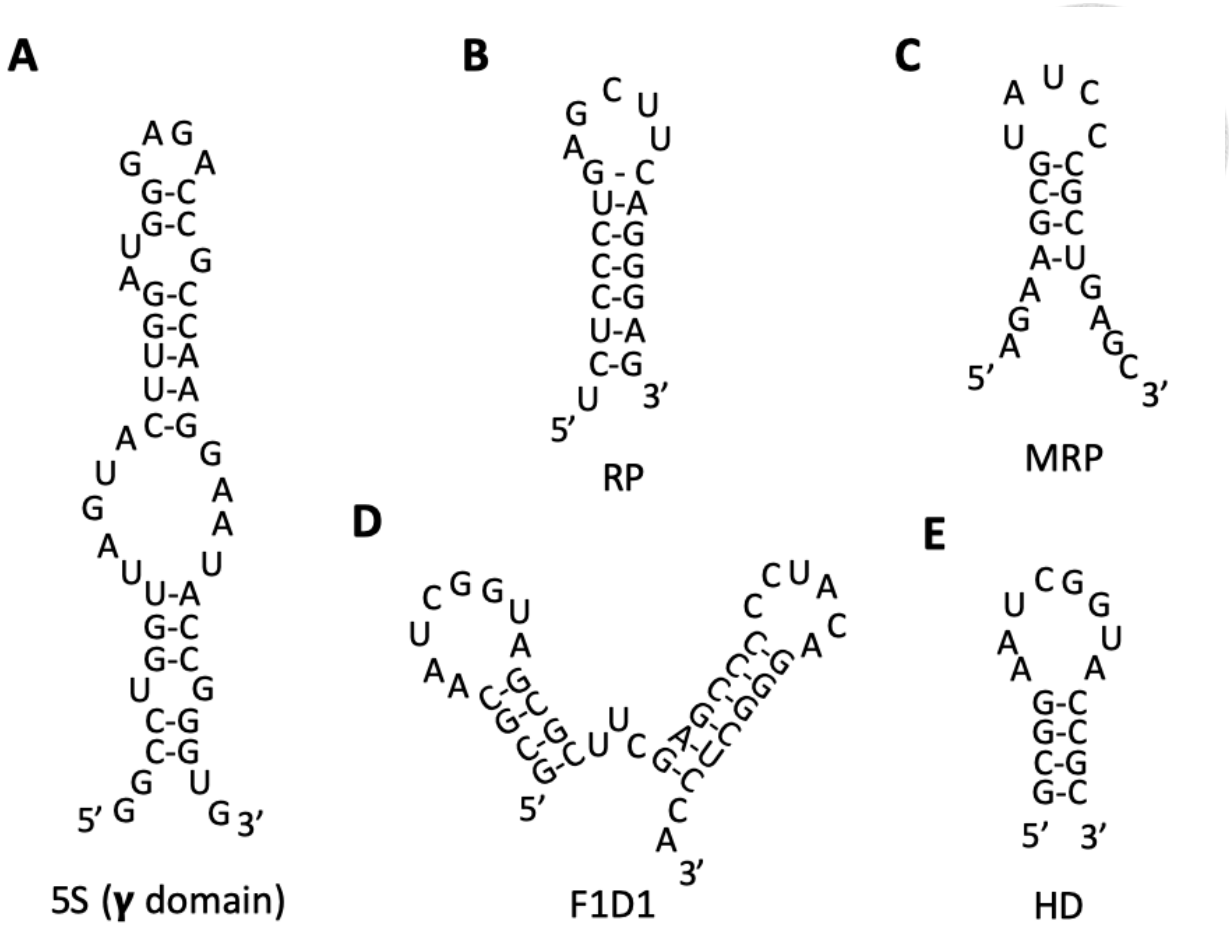


**Figure 16. Reported hairpin-shaped motifs for mitochondrial RNA transportation**

All the hairpin-shaped RNA motifs used in this study have been experimentally proven that they have the ability to import RNA fragments into human mitochondria (A-E). (A) The hairpin structure from the gamma domain of 5S rRNA, 65-110 nt. (B) The hairpin structure form RNase P RNA, 1-20 nt. (C) The hairpin structure form RNase MRP RNA, 150-169 nt. (D) The double hairpin structure from F-form of yeast $tRNA^{Lys}$. (E) The single hairpin structure from F-form of yeast $tRNA^{Lys}$.



doi:10.6342/NTU201902787

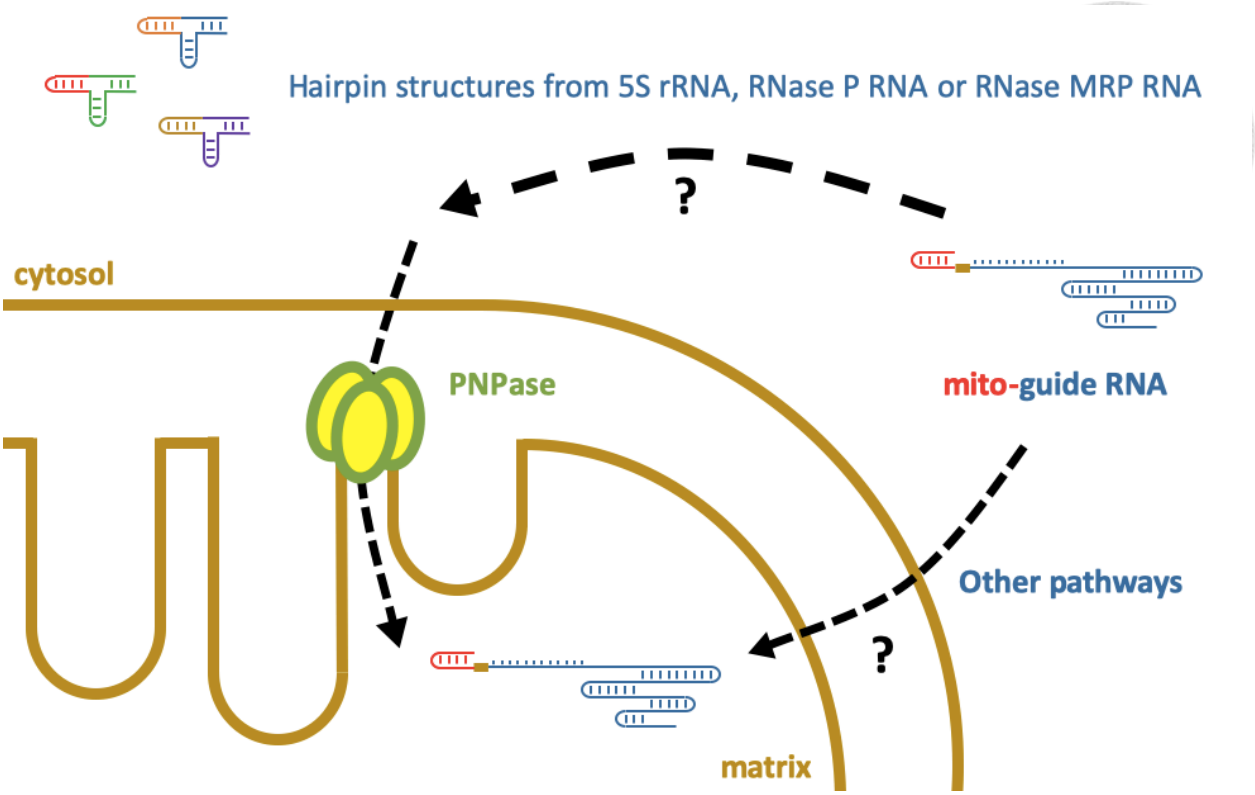


**Figure 17. Hypothesis for PNPase-mediated mitochondrial import of mito-sgRNA**

Studies have revealed that the hairpin-shaped motifs on PNPase-related non-coding RNAs, like 5S rRNA, RNase P RNA and RNase MRP RNA may be involved in the recognition of PNPase and their import into mitochondrial matrix. Without the motifs, studies have shown loss of expression of these RNAs within mitochondria. Hence, we collected all these hairpin-shaped RNA motifs and fused them onto our single guide RNAs to form a series of 15 mito-sgRNAs. Theoretically, we hope that, with the help of these RNA motifs, our mito-sgRNAs can enter mitochondria through PNPase-mediated pathway or other unknown pathways.



doi:10.6342/NTU201902787

| | | | | | |
|---|---|---|---|---|---|
| mito-sgRNA36 | 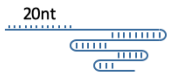 | mito-sgRNA51 | 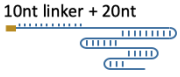 | | |
| mito-sgRNA52 |  | mito-sgRNA69 |  | mito-sgRNA54 |  |
| mito-sgRNA53 |  | mito-sgRNA70 | 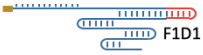 | mito-sgRNA55 |  |
| mito-sgRNA56 | 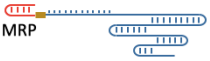 | mito-sgRNA71 | 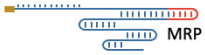 | mito-sgRNA57 |  |
| mito-sgRNA68 |  | mito-sgRNA72 |  | | |
| mito-sgRNA73 |  | mito-sgRNA74 | 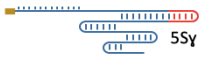 | | |

**Figure 18. Cartoon illustration of predicted mito-sgRNA structures**

15 mito-sgRNAs generated through this study were *in vitro* transcribed and treated with CIP to remove the triphosphate on the 3' end in order to reduce their toxicity toward cells. Mito-sgRNA36 is the original guide RNA targeting *ND4* gene on mtDNA without any modification. Since any modification on guide RNA may change its conformation and further influences its binding affinity with Cas9, we put a 10-nucleotide linker to extend the motif away from the guide RNA scaffold. Mito-sgRNA51 was added a 10-nucleotide linker. Mito-sgRNA52, 53, 56, 68 and 73 were generated by adding different hairpin-like RNA motifs in front of the 10-nucleotide linker of mito-sgRNA51. Mito-sgRNA69, 70, 71, 72 and 74 were generated through adding hairpin motifs onto the internal region of guide RNA scaffold. Mito-sgRNA54, 55 and 57 possess hairpin motifs on the 5' end as well as a 3' UTR sequence from mRNA, which have the ability to recruit cytosolic RNA to proximity of mitochondrial outer membrane.



doi:10.6342/NTU201902787

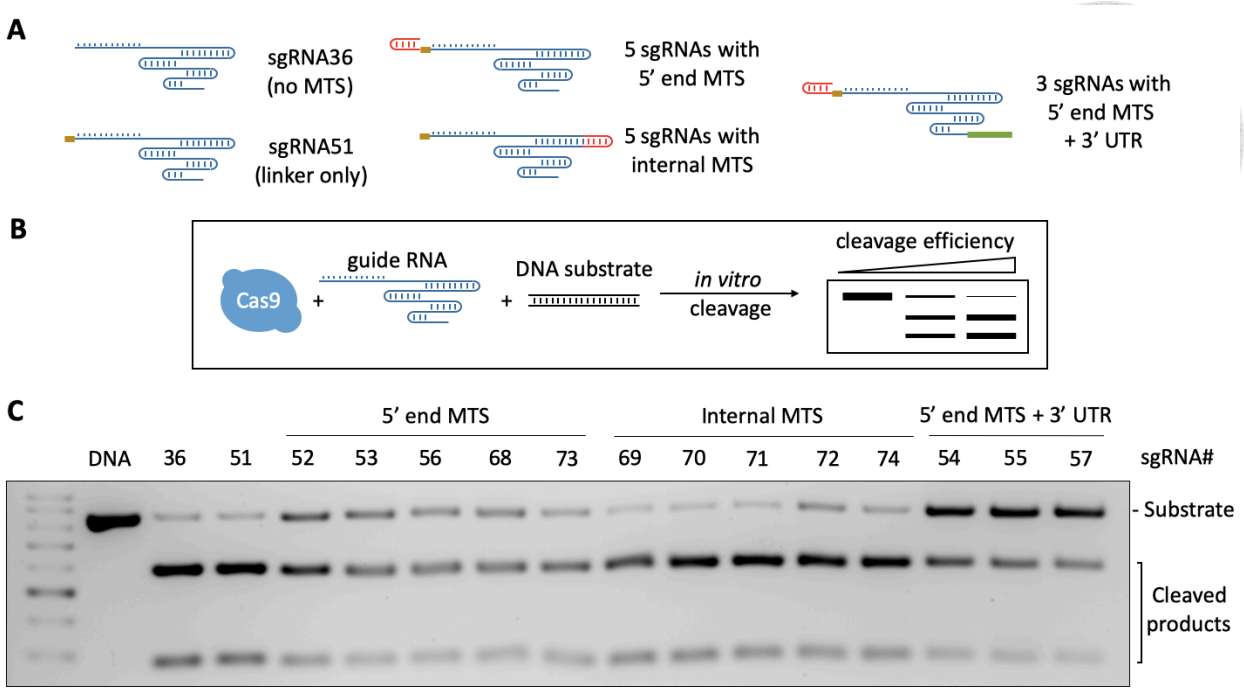


**Figure 19. Modifications on all mito-sgRNAs maintain Cas9 cleavage**

(A) Simplified structures of mito-sgRNAs synthesized in this study. Modifications are marked with different colors. Brown indicates 10-nucleotide linker sequence. Red is putative RNA hairpin structures which assist the import of RNA through PNPase. Green is the 3' untranslated region of mitochondrial ribosomal protein S12, which confer RNA localization to mitochondrial outer membrane. (B) Schematic demonstration of in vitro cleavage assay. The higher the Cas9 cleavage efficiency is, the more cleaved products are shown in the lower bands. (C) *ND4* DNA subtract was incubated with purified Cas9 and respective *in vitro* transcribed mito-sgRNA at 37°C for 30 minutes. The products were separated through agarose electrophoresis. Mito-sgRNAs with modifications on the internal RNA scaffold show the best cleavage efficiency, as good as the nonmodified one and the one with only 10-nucleotide linker motif.



doi:10.6342/NTU201902787

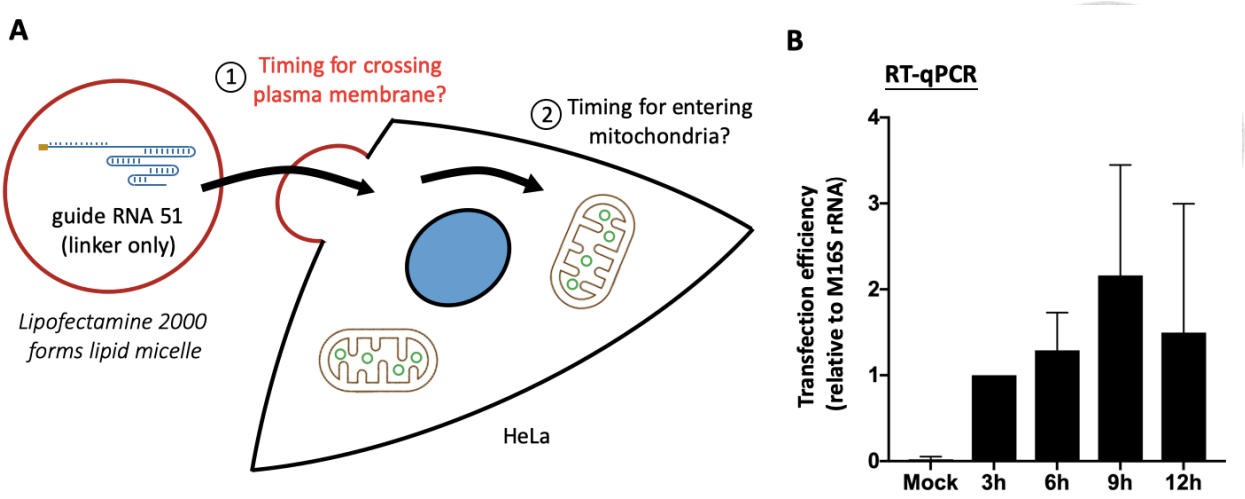


**Figure 20. Schematic flow to determine timing for mito-sgRNA transfection**

(A) mito-sgRNA51 served as representative for all the mito-sgRNA generated through this study and was transfected into cell through Lipofectamine 2000. After mixing mito-sgRNA51 with Lipofectamine 2000, small lipid micelles surrounding the mito-sgRNA form in Opti-MEM reagent. The mixture was added into the cell medium and engulfed by cells through either fusion or endocytosis. Once a mito-sgRNA reached cytosol, it would be further recruited into mitochondria according to the modification on it. (B) To determine the best timing when the most amount of mito-sgRNA accumulates within cytosol, we transfected mito-sgRNA51 with increasing time span from 3 to 12 hours. At the indicated timing, total RNA of each group was extracted through TRIzol-mediated RNA recovery and was analyzed by RT-qPCR. According to our data, the amount of mit-sgRNA51 increased as the transfection time was expanded from 3 to 9 hours, but started to decrease afterwards, indicating that incubation for 9 hours is the best timing for mito-sgRNA transfection.



doi:10.6342/NTU201902787

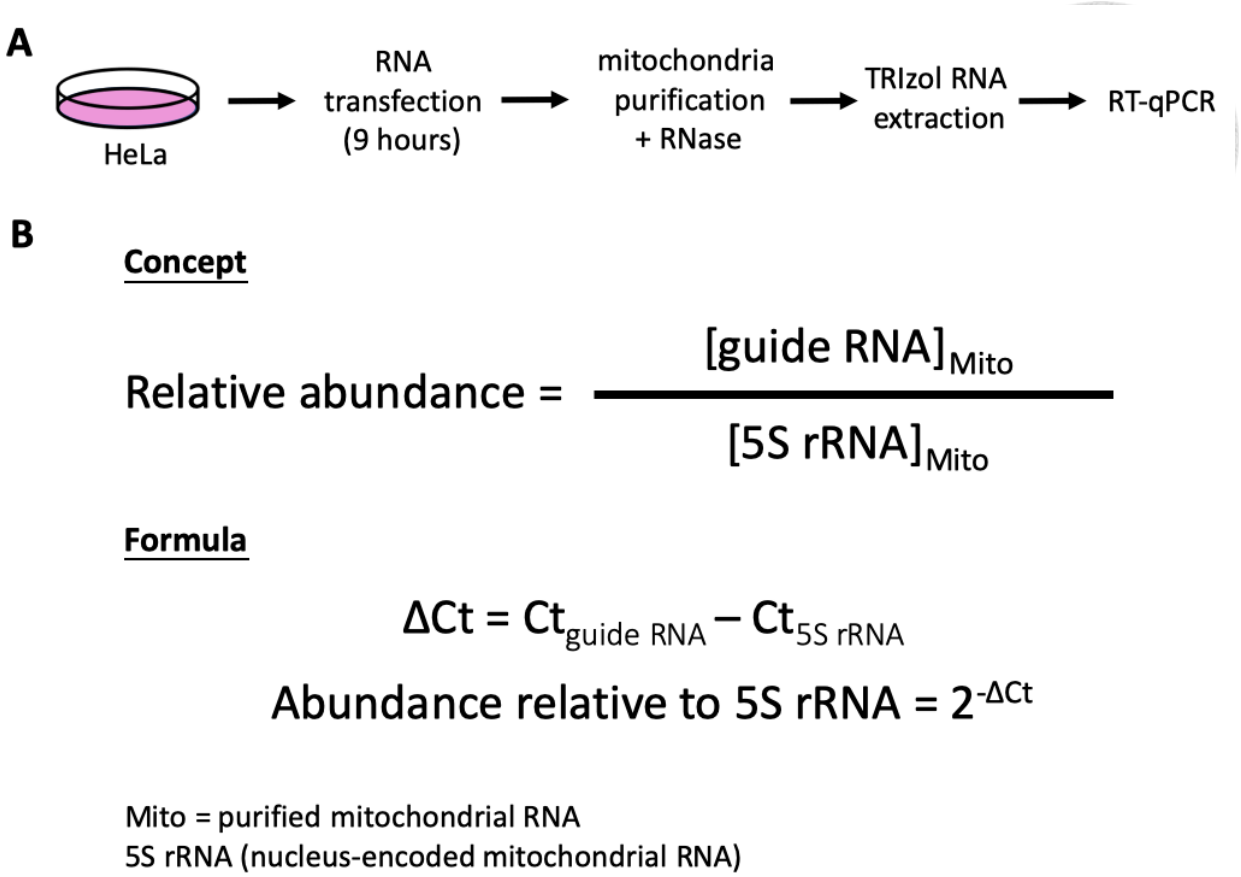


**Figure 21. Schematic flow for *in vivo* mito-sgRNA screening and calculation**

(A) To determine the *in vivo* relative abundance of all the mito-sgRNAs generated throughout this study, we conducted a 9-hour transfection of individual mito-sgRNA before the mitochondrial purification and RNase A/T1 treatment. The RNA was extracted from purified mitochondria by TRIzol-mediated recovery and analyzed by RT-qPCR. (B) The concept for the relative abundance of individual mito-sgRNA is the amount of target mito-sgRNA within mitochondria over the amount of RNase P RNA within mitochondrial fraction. To calculate from the real data, the delta Ct value equals to the Ct value of targeted mito-sgRNA taken away the Ct value of RNase P RNA. The result of 2 to the power of minus delta Ct value will be the relative abundance of targeted mito-sgRNA over RNase P RNA in mitochondria.



doi:10.6342/NTU201902787

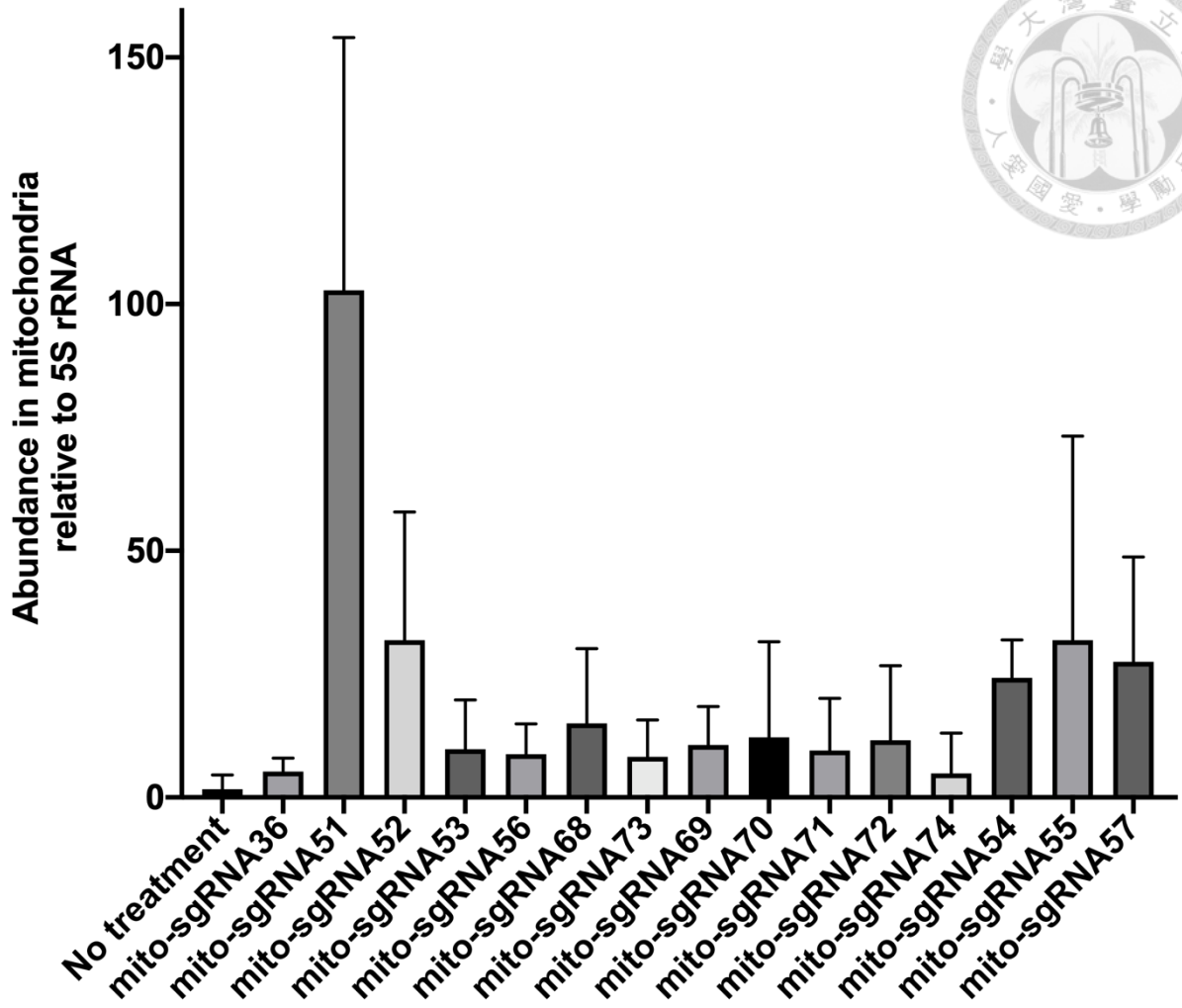


**Figure 22. Mito-sgRNA with only linker on 5' end has the highest import efficiency**

*In vivo* test for mitochondrial abundance of target mito-sgRNAs relative to 5S r RNA by reverse transcription-qPCR of mitochondrial RNA extracts. The abundance of mito-sgRNA51, which has no modification but a short 10-nucleotide linker, is over one hundred times as high as that of endogenous 5S rRNA level within mitochondria. All the other mito-sgRNAs, which possess MTSs either at their 5' ends, internal region, or both ends, is much less than mito-sgRNA51.



doi:10.6342/NTU201902787

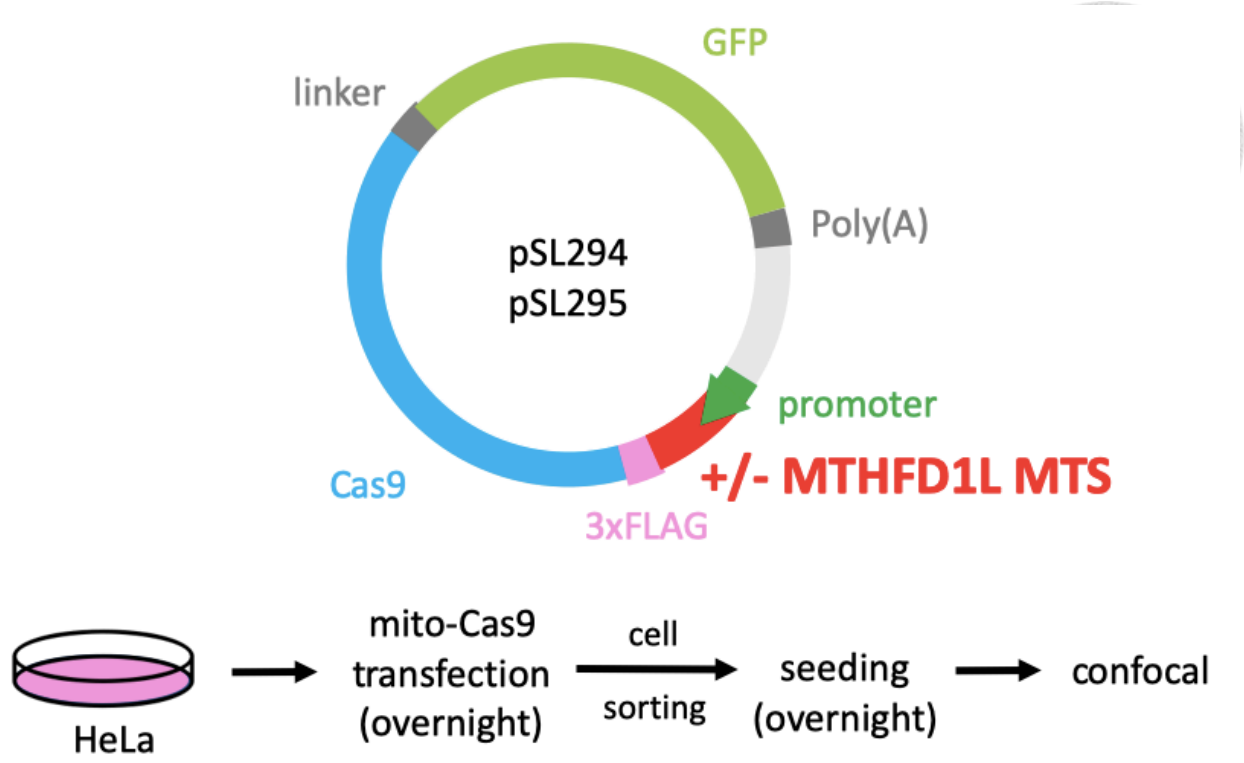


**Figure 23. Schematic flow for expression of mito-Cas9 *in vivo***

Since the expression level of mito-Cas9 (MTHFD1L MTS-Cas9) was low after electroporation of corresponding plasmids, we used Lipofectamine 3000 in hope that we could enhance the transfection efficiency. In this part of experiment, the plasmid not only has MTHFD1L MTS in front of the Cas9 sequence, but was also fused with a signal-enhanced turboGFP sequence (Lonza). In order to test the *in vivo* influence of transfection with mito-Cas9, after 2 days of transfection for mito-Cas9 through Lipofectamine 3000, GFP-positive cells were sorted out and seeded onto culture dish for 1 day. Later, cellular and mitochondrial morphology were determined by confocal microscope imaging.



doi:10.6342/NTU201902787

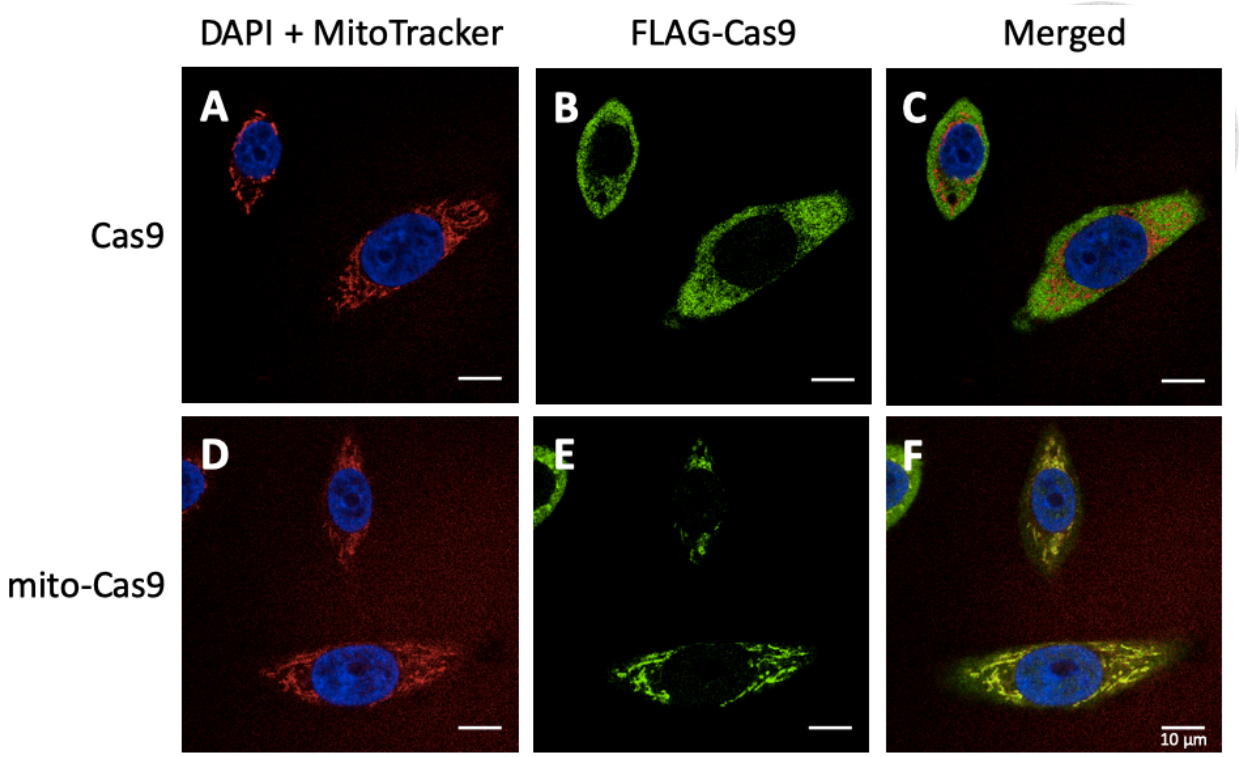


**Figure 24. Impaired cellular physiology after transfection of Cas9-GFP**

Cellular and mitochondrial morphology detected by immunofluorescence and confocal microscopy after transfection of plasmid which expresses either normal Cas9 or mito-Cas9 with MTHFD1L MTS. (A) The cells transfected with normal Cas9 showed typical phenotype of HeLa mitochondria structure. (B) Cas9 without MTS could only localize at the cytosol. (C) Merged image indicates no co-localization between Cas9 and mitochondria. (D) The cells transfected with mito-Cas9 (MTHFD1L MTS-Cas9) showed abnormal mitochondrial phenotype, suggesting that mitophagy was induced by overexpression of mito-Cas9 and GFP. (E) Mito-Cas9 showed no concentration effect within mitochondria, but spread all over the cytosol. (F) Merged image indicates no co-localization between mito-Cas9 and mitochondria.



doi:10.6342/NTU201902787

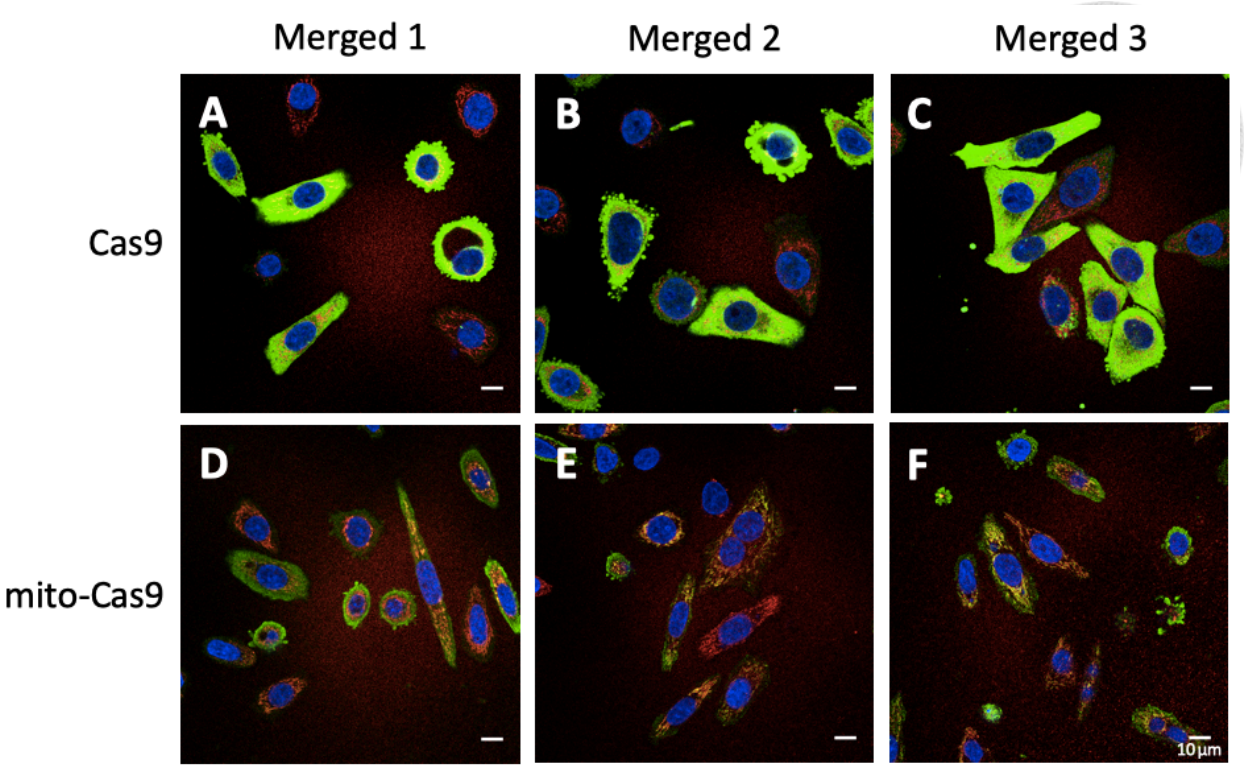


**Figure 25. Physiological anomaly occurs after transfection of mito-Cas9-GFP**

Cellular and mitochondrial morphology detected by immunofluorescence under a larger confocal microscopy field after transfection of plasmid which expresses either normal Cas9 or mito-Cas9 with MTHFD1L MTS. (A-C) The majority of the cells transfected with normal Cas9 (pSL294) showed atypical phenotype of HeLa cells. Cells became smaller and apoptotic bubbles were even observed surrounding the cells. (D-F) Similarly, most of the cells transfected with mito-Cas9 (MTHFD1L MTS-Cas9) showed abnormal cellular phenotype, like spindle- or sphere-shaped outlooks, suggesting that mitophagy was induced by overexpression of mito-Cas9-GFP.



doi:10.6342/NTU201902787

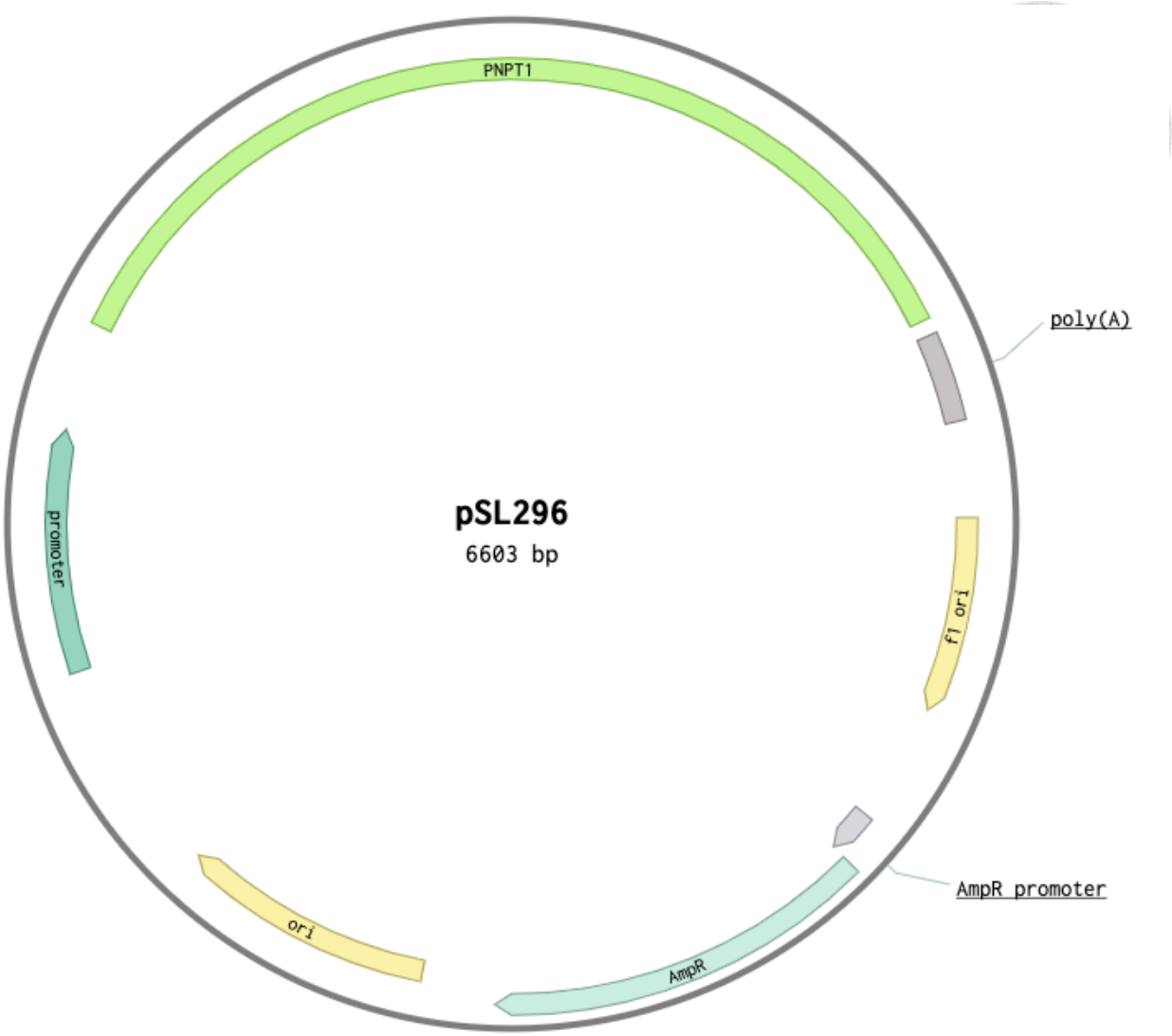


**Figure 26. Plasmid map for pSL296**

A plasmid harboring human PNPase sequence (*PNPT1* gene), following CMV enhancer and chicken β-acting promoter, was generated through this study.



doi:10.6342/NTU201902787

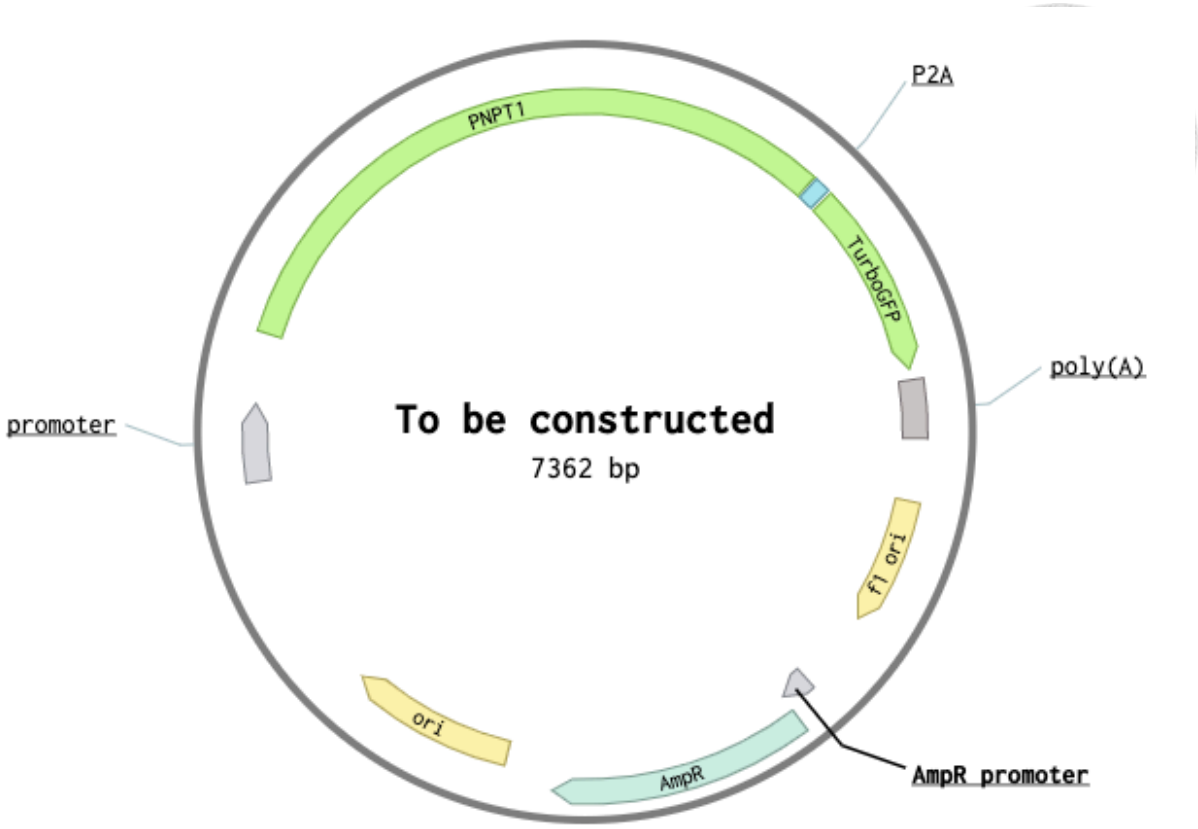


**Figure 27. Plasmid map for pSL307 which has not been cloned yet**

A plasmid harboring human PNPase sequence (*PNPT1* gene), followed by self-cleavable peptide P2A and signal-upgraded turboGFP sequence, will be generated through this study in the future.



doi:10.6342/NTU201902787

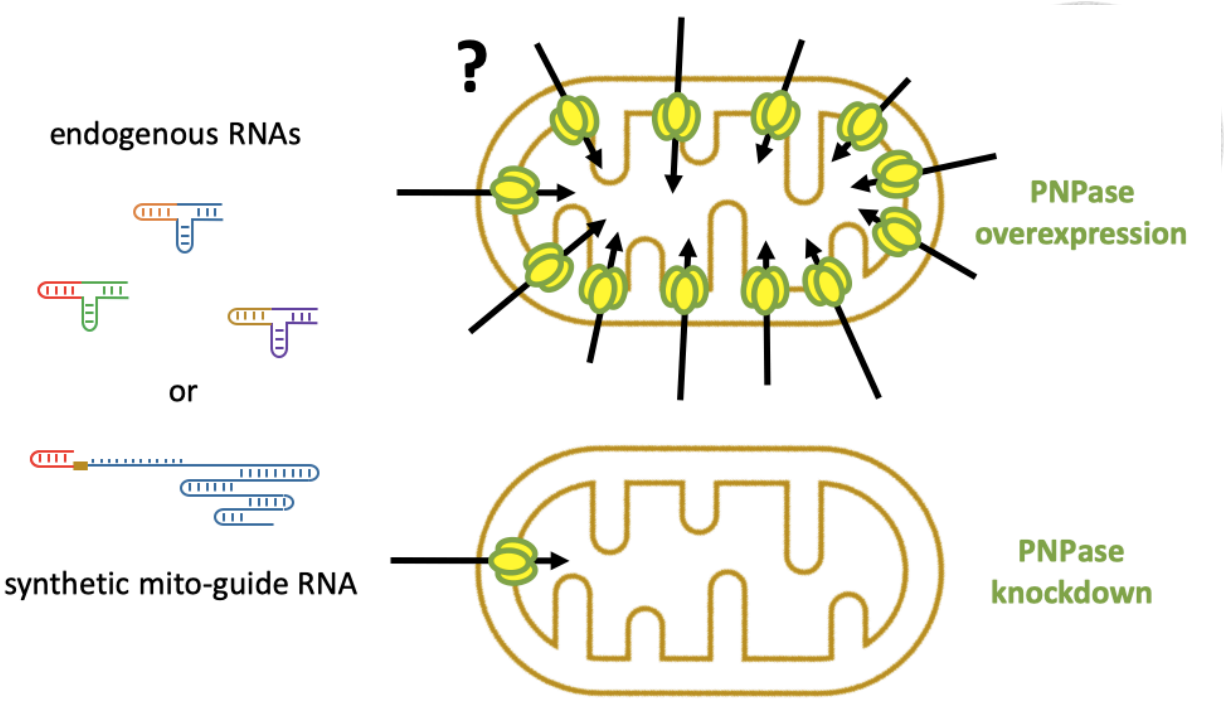


**Figure 28. Hypothesized influence of PNPase expression on mitochondrial RNA import**

In order to determine whether the expression level of PNPase affects the mitochondrial RNA import efficiency of both endogenous RNAs, like 5S rRNA, RNase P RNA and RNase MRP RNA, and exogenous RNAs, like mito-sgRNAs generated through this study, we also intend to overexpress PNPase by transfect pSL296 (see Table 1) or knockdown its expression level by introducing shRNA targeting *PNPT1* gene.



doi:10.6342/NTU201902787

**Table 1. Strains, plasmids and primers used in this study**

| Strain | Characteristics | Source |
|---|---|---|
| 93 | Homemade TOP10 | Our lab |
| 189 | Homemade Stable3 | Our lab |
| 203 | pSL122 | This work |
| 209 | pSL127 | This work |
| 212 | pSL127B | This work |
| 216 | pSL127C | This work |
| 218 | pSL127D | This work |
| 213 | pSL127E | This work |
| 215 | pSL127F | This work |
| 214 | pSL127G | This work |
| 220 | pSL127Ga | This work |
| 221 | pSL127Gb | This work |
| 240 | pSL127Gc | This work |
| 241 | pSL127Gd | This work |
| 280 | pSL127Ge | This work |
| 281 | pSL127Gf | This work |
| 270 | pSL146 | This work |
| 271 | pSL147 | This work |
| 272 | pSL148 | This work |
| 273 | pSL149 | This work |
| 311 | pSL179 | This work |
| 315 | pSL187 | This work |
| 316 | pSL188 | This work |
| 356 | pSL245 | This work |
| 357 | pSL246 | This work |
| 358 | pSL247 | This work |
| 359 | pSL248 | This work |
| 360 | pSL249 | This work |
| 431 | pSL296 | This work |
| 412 | pSL297 | This work |
| 413 | pSL298 | This work |
| | | |
| **Plasmid** | **Characteristics** | **Source** |
| mito-EGFP | 2xCOX8A MTS-EGFP-Kan$^R$ | Our lab |
| pET28a | lacI-lacI promoter-T7 promoter-lac operator-f1 ori-Kan$^R$-ori | Our lab |
| pAW006 | Ori-U6 promoter-2xBbsI-sgRNA scaffold-CMV enhancer-chicken β actin promoter-3xFLAG-NLS-SpCas9-NLS-poly(A)-AAV2 ITR-f1 ori-Amp$^R$ | Our lab |
| pSL122 | pET28a Gibson assembly::(2xCOX8A MTS-EGFP-10xHis tag) | This work |
| pSL127 | pAW006 Gibson assembly::(BamHI-SpCas9-3xFLAG tag-NheI) | This work |
| pSL127B | pSL127 BamHI::(2xCOX8A MTS) | This work |
| pSL127C | pSL127 BamHI::(*S. cerevisiae* COX4P MTS) | This work |



doi:10.6342/NTU201902787

| | | |
|---|---|---|
| pSL127D | pSL127 BamHI::(ACACB MTS) | This work |
| pSL127E | pSL127 BamHI::(GLDC MTS) | This work |
| pSL127F | pSL127 BamHI::(POLG MTS) | This work |
| pSL127G | pSL127 BamHI::(MTHFD1L MTS) | This work |
| pSL127Ga | pSL127G Round-the-horn::(5' RP MTS) | This work |
| pSL127Gb | pSL127G Round-the-horn::(5' F1D1 MTS) | This work |
| pSL127Gc | pSL127Ga Gibson assembly::(MRPS12 3' UTR) | This work |
| pSL127Gd | pSL127Gb Gibson assembly::(MRPS12 3' UTR) | This work |
| pSL127Ge | pSL127G Round-the-horn::(5' MRP MTS) | This work |
| pSL127Gf | pSL127Ge Gibson assembly::(MRPS12 3' UTR) | This work |
| pSL146 | pSL127Ga 2xBbsI::(30 nt ND4 target site 6) | This work |
| pSL147 | pSL127Gb 2xBbsI::(30 nt ND4 target site 6) | This work |
| pSL148 | pSL127Gc 2xBbsI::(30 nt ND4 target site 6) | This work |
| pSL149 | pSL127Gd 2xBbsI::(30 nt ND4 target site 6) | This work |
| pSL179 | pUC (ori-T7 promoter-30 nt ND4 target site 6-sgRNA scaffold-internal BoB Spinach-sgRNA scaffold-Amp$^R$) | Our lab |
| pSL187 | pSL127Ge 2xBbsI::(30 nt ND4 target site 6) | This work |
| pSL188 | pSL127Gf 2xBbsI::(30 nt ND4 target site 6) | This work |
| pSL245 | pSL146 Round-the-horn::(5' HD MTS) | This work |
| pSL246 | pSL179 Round-the-horn::(internal RP MTS) | This work |
| pSL247 | pSL179 Round-the-horn::(internal MRP MTS) | This work |
| pSL248 | pSL179 Round-the-horn::(internal F1D1 MTS) | This work |
| pSL249 | pSL179 Round-the-horn::(internal HD MTS) | This work |
| pSL296 | pAW006 Round-the-horn::(PNPT1) | This work |
| pSL297 | pSL245 Round-the-horn::(5' 5Sγ MTS) | This work |
| pSL298 | pSL179 Round-the-horn::(internal 5Sγ MTS) | This work |
| | | |
| **Primer** | **Sequence (5'-3')** | **Usage** |
| T25G | TAA TAC GAC TCA CTA TAG | IVT sgRNA |
| SLKS2 | GCA CCG ACT CGG TGC CAC TTT TTC AAG | IVT sgRNA |
| SL297 | GCA CCG ACT CGG TGC CAC TTT TTC AAG TTG ATA ACG GAC TAG CCT TAT TTT AAC TTG CTA TGC TGT TTC CAG CAT | IVT sgRNA36 |
| SL410 | CAG GAC GGA CAT GGT ATA TCT CCT TCT TAA AGT TAA ACA AAA TTA TTT CTA GAG GG | Construct pSL122 |
| SL411 | GGA GAT ATA CCA TGT CCG TCC TGA CGC CGC TGC TGC | Construct pSL122 |
| SL412 | GTA CAA GGG GCA TCA TCA TCA TCA CCA CCA CCA CCA CCA CTG AG | Construct pSL122 |
| SL413 | GAT GAT GAT GAT GCC CCT TGT ACA GCT CGT CCA TGC CGA GAG TG | Construct pSL122 |
| SL434 | CAC CTC CGG ATC CCA TCC AAC CTG AAA AAA AGT GAT TTC AGG C | Construct pSL127 |
| SL435 | GTT GGA TGG GAT CCG GAG GTG ACA AGA AGT ACA GCA TCG GCC TG | Construct pSL127 |



doi:10.6342/NTU201902787

| | | |
|---|---|---|
| SL436 | CCT TAT AGT CTC CAG ATC CTC CGT CGC CTC CCA GCT GAG ACA GGT CG | Construct pSL127 |
| SL437 | GAC GGA GGA TCT GGA GAC TAT AAG GAC CAC GAC GGA GAC TAC AAG G | Construct pSL127 |
| SL438 | CTA GGA ATT CTT ATT AGC TAG CCT TAT CGT CAT CGT CTT TGT AAT CAA TAT C | Construct pSL127 |
| SL439 | GAC GAT AAG GCT AGC TAA TAA GAA TTC CTA GAG CTC GCT GAT CAG C | Construct pSL127 |
| SL448 | CAT CCA ACC TGA AAA AAA GTG ATT TCA GGC AGG | Construct pSL127B-G |
| SL449 | GGA TCC GGA GGT GAC AAG AAG TAC AGC | Construct pSL127B-G |
| SL450 | CCT GAA ATC ACT TTT TTT CAG GTT GGA TGG TTC TGC TGC TGT GCT TGA GC | Construct pSL127D |
| SL451 | CTT CTT GTC ACC TCC GGA TCC GTT CGC CTC TGA CTT GCT TTT GG | Construct pSL127D |
| SL452 | CCT GAA ATC ACT TTT TTT CAG GTT GGA TGT CTC GGC TGC TTT GGA GAA AGG | Construct pSL127F |
| SL453 | CTT CTT GTC ACC TCC GGA TCC ATC AGA TGG ATC TGA AGC AGG AAC | Construct pSL127F |
| SL454 | CCT GAA ATC ACT TTT TTT CAG GTT GGA TGC AGT CTT GTG CTA GAG CCT GG | Construct pSL127E |
| SL455 | CTT CTT GTC ACC TCC GGA TCC GCG ACT TCT AGG AGC CCA ACA TGG | Construct pSL127E |
| SL456 | CCT GAA ATC ACT TTT TTT CAG GTT GGA TGA GTG TGC TGA CGC CAC TGC TG | Construct pSL127B |
| SL457 | CTT CTT GTC ACC TCC GGA TCC GTC CCC CAG CGA GTG GAT CTT GG | Construct pSL127B |
| SL458 | CCT GAA ATC ACT TTT TTT CAG GTT GGA TGG GCA CTC GCT TGC CTC TCG TG | Construct pSL127G |
| SL459 | CTT CTT GTC ACC TCC GGA TCC TGC TCG GCA TGG AAC TCG CAA CC | Construct pSL127G |
| SL460 | CCT GAA ATC ACT TTT TTT CAG GTT GGA TGC TCA GCC TCC GGC AAT CTA TCC | Construct pSL127C |
| SL461 | CTT CTT GTC ACC TCC GGA TCC CAA CAG GTA TCT GCT GGA GCA GAG TG | Construct pSL127C |
| SL467 | TAA TAC GAC TCA CTA TAG CAT CAT AAT CCT CTC TCA GTT TTA GAG CTA TGC TGG AAA CAG CAT AGC AAG TTA AA | IVT sgRNA36 |
| SL509 | TCA GGG AGA CTT TCG TCC TTT CCA CAA GAT ATA TAA AGC CAA GAA ATC G | Construct pSL127Ga |
| SL510 | GCT TCA GGG AGG TCT TCG AGA AGA CCT GTT TAA GAG CTA TGC TGG | Construct pSL127Ga |
| SL511 | GAA GCG CTA CCG ATT GCG CTT TCG TCC TTT CCA CAA GAT ATA TAA AGC CAA GAA ATC G | Construct pSL127Gb |
| SL512 | GAG CCC CCT ACA GGG CTC CAG TCT TCG AGA AGA | Construct |



doi:10.6342/NTU201902787

| | | |
|---|---|---|
| | CCT GTT TAA GAG CTA TGC TGG | pSL127Gb |
| SL547 | TTCTCATAATCGCCCACGGG | qPCR for *ND4* gene |
| SL548 | GGTAAGGCGAGGTTAGCGAG | qPCR for *ND4* gene |
| SL551 | GTG GCA CCG AGT CGG TGC CAG AAG | Construct pSL127Gc, d and f |
| SL552 | CTA GCT CTA AAA CAA AAA AGA TGG AAG AGG C | Construct pSL127Gc, d and f |
| SL562 | CTT CTG GCA CCG ACT CGG TGC CAC TTT TTC AAG TTG | Construct pSL127Gc, d and f |
| SL563 | GCC TCT TCC ATC TTT TTT GTT TTA GAG CTA GAA ATA GCA AGT TAA AAT AAG GCT AGT CCG | Construct pSL127Gc, d and f |
| SL584 | AGG GAG CAC TCA CAG TCG CAT CAT AAT CCT CTC TCA | Construct pSL146 and 148 |
| SL585 | AAA CTG AGA GAG GAT TAT GAT GCG ACT GTG AGT GCT | Construct pSL146 and 148 |
| SL586 | GCT CCA CAC TCA CAG TCG CAT CAT AAT CCT CTC TCA | Construct pSL147 and 149 |
| SL587 | AAA CTG AGA GAG GAT TAT GAT GCG ACT GTG AGT GTG | Construct pSL147 and 149 |
| SL600 | ATA CGC TTC TCT TTC GTC CTT TCC ACA AGA TAT ATA AAG CCA AGA AAT CG | Construct pSL127Ge |
| SL601 | CCC GCT GAG CGT CTT CGA GAA GAC CTG TTT AAG AGC TAT GCT GG | Construct pSL127Ge |
| SL613 | TAA TAC GAC TCA CTA TAG CAC TCA CAG TCG CAT CAT AAT CCT C | IVT sgRNA51 |
| SL615 | TAA TAC GAC TCA CTA TAG CGC AAT CGG TAG CGC TTC GAG C | IVT sgRNA53 and 55 |
| SL616 | AGT GGA AGA GGC GGA GCC AGG ACT TGA ATC | IVT sgRNA54 and 55 |
| SL632 | TAA TAC GAC TCA CTA TAG TCT CCC TGA GCT TCA GGG AGC ACT CAC AG | IVT sgRNA52 and 54 |
| MF3 | CTG AGC CAC TCA CAG TCG CAT CAT AAT CCT CTC TCA | Construct pSL187and |



doi:10.6342/NTU201902787

| | | |
|---|---|---|
| | | 188 |
| MF4 | AAA CTG AGA GAG GAT TAT GAT GCG ACT GTG AGT GGC | Construct pSL187and 188 |
| MF8 | TAA TAC GAC TCA CTA TAG AGA AGC GTA TCC CGC TGA GCC AC | IVT sgRNA56 and 57 |
| MF9 | TAA TAC GAC TCA CTA TAG CAC TCA CAG TCG | IVT sgRNA69-72 |
| MF46 | TAA TAC GAC TCA CTA TAG CGC AAT CGG TAG CGC CAC TC | IVT sgRNA68 |
| MF47 | CTT CAG GGA GCA GCA TAG CAA GTT TAA ATA AGG CTA GTC CGT TAT C | Construct pSL246 |
| MF48 | CTC AGG GAG ACA GCA TAG CTC TTA AAC TGA GAG AGG ATT ATG ATG | Construct pSL246 |
| MF49 | GAG CCC CCT ACA GGG CTC CAC AGC ATA GCA AGT TTA AAT AAG GCT AGT CCG TTA TC | Construct pSL247 |
| MF50 | GAA GCG CTA CCG ATT GCG CCA GCA TAG CTC TTA AAC TGA GAG AGG ATT ATG ATG | Construct pSL247 |
| MF51 | CCG CTG AGC CAG CAT AGC AAG TTT AAA TAA GGC TAG TCC GTT ATC | Construct pSL248 |
| MF52 | GAT ACG CTT CTC AGC ATA GCT CTT AAA CTG AGA GAG GAT TAT GAT G | Construct pSL248 |
| MF53 | GGT AGC GCC AGC ATA GCA AGT TTA AAT AAG GCT AGT CCG TTA TC | Construct pSL249 |
| MF54 | GAT TGC GCC AGC ATA GCT CTT AAA CTG AGA GAG GAT TAT GAT G | Construct pSL249 |
| MF94 | GAG ACC GCC AAG GAA TAC CGG GTG CAC TCA CAG TCG CAT CAT AAT CCT CTC TC | Construct pSL297 |
| MF95 | CCA TCC AAG TACT AAC CAG GCC TTT CGT CCT TTC CAC AAG ATA TAT AAA GCC AAG AAA TC | Construct pSL297 |
| MF96 | GAG ACC GCC AAG GAA TAC CGG GTG CAG CAT AGC AAG TTT AAA TAA GGC TAG TCC GTT ATC | Construct pSL298 |
| MF97 | CCA TCC AAG TAC TAA CCA GGC CCA GCA TAG CTC TTA AAC TGA GAG AGG ATT ATG ATG | Construct pSL298 |
| MF110 | TAA TAC GAC TCA CTA TAG GCC TGG TTA GTA CTT GGA TGG GAG | IVT sgRN74 |



doi:10.6342/NTU201902787

**Table 2. Humanized SpCas9 sequence and mitochondria-targeting sequences**

| Name | Sequence (5'-3') |
|---|---|
| Human codon optimized *S. pyogenes* Cas9 | GACAAGAAGTACAGCATCGGCCTGGACATCGGCACCAACTCTGTGGG<br>CTGGGCCGTGATCACCGACGAGTACAAGGTGCCCAGCAAGAAATTCA<br>AGGTGCTGGGCAACACCGACCGGCACAGCATCAAGAAGAACCTGATC<br>GGAGCCCTGCTGTTCGACAGCGGCGAAACAGCCGAGGCCACCCGGCT<br>GAAGAGAACCGCCAGAAGAAGATACACCAGACGGAAGAACCGGATC<br>TGCTATCTGCAAGAGATCTTCAGCAACGAGATGGCCAAGGTGGACGA<br>CAGCTTCTTCCACAGACTGGAAGAGTCCTTCCTGGTGGAAGAGGATAA<br>GAAGCACGAGCGGCACCCCATCTTCGGCAACATCGTGGACGAGGTGG<br>CCTACCACGAGAAGTACCCCACCATCTACCACCTGAGAAAGAAACTG<br>GTGGACAGCACCGACAAGGCCGACCTGCGGCTGATCTATCTGGCCCT<br>GGCCCACATGATCAAGTTCCGGGGCCACTTCCTGATCGAGGGCGACCT<br>GAACCCCGACAACAGCGACGTGGACAAGCTGTTCATCCAGCTGGTGC<br>AGACCTACAACCAGCTGTTCGAGGAAAACCCCATCAACGCCAGCGGC<br>GTGGACGCCAAGGCCATCCTGTCTGCCAGACTGAGCAAGAGCAGACG<br>GCTGGAAAATCTGATCGCCCAGCTGCCCGGCGAGAAGAAGAATGGCC<br>TGTTCGGAAACCTGATTGCCCTGAGCCTGGGCCTGACCCCCAACTTCA<br>AGAGCAACTTCGACCTGGCCGAGGATGCCAAACTGCAGCTGAGCAAG<br>GACACCTACGACGACGACCTGGACAACCTGCTGGCCCAGATCGGCGA<br>CCAGTACGCCGACCTGTTTCTGGCCGCCAAGAACCTGTCCGACGCCAT<br>CCTGCTGAGCGACATCCTGAGAGTGAACACCGAGATCACCAAGGCCC<br>CCCTGAGCGCCTCTATGATCAAGAGATACGACGAGCACCACCAGGAC<br>CTGACCCTGCTGAAAGCTCTCGTGCGGCAGCAGCTGCCTGAGAAGTAC<br>AAAGAGATTTTCTTCGACCAGAGCAAGAACGGCTACGCCGGCTACAT<br>TGACGGCGGAGCCAGCCAGGAAGAGTTCTACAAGTTCATCAAGCCCA<br>TCCTGGAAAAGATGGACGGCACCGAGGAACTGCTCGTGAAGCTGAAC<br>AGAGAGGACCTGCTGCGGAAGCAGCGGACCTTCGACAACGGCAGCAT<br>CCCCCACCAGATCCACCTGGGAGAGCTGCACGCCATTCTGCGGCGGC<br>AGGAAGATTTTTACCCATTCCTGAAGGACAACCGGGAAAAGATCGAG<br>AAGATCCTGACCTTCCGCATCCCCTACTACGTGGGCCCTCTGGCCAGG<br>GGAAACAGCAGATTCGCCTGGATGACCAGAAAGAGCGAGGAAACCAT<br>CACCCCCTGGAACTTCGAGGAAGTGGTGGACAAGGGCGCTTCCGCCC<br>AGAGCTTCATCGAGCGGATGACCAACTTCGATAAGAACCTGCCCAAC<br>GAGAAGGTGCTGCCCAAGCACAGCCTGCTGTACGAGTACTTCACCGT<br>GTATAACGAGCTGACCAAAGTGAAATACGTGACCGAGGGAATGAGAA<br>AGCCCGCCTTCCTGAGCGGCGAGCAGAAAAAGGCCATCGTGGACCTG<br>CTGTTCAAGACCAACCGGAAAGTGACCGTGAAGCAGCTGAAAGAGGA<br>CTACTTCAAGAAAATCGAGTGCTTCGACTCCGTGGAAATCTCCGGCGT<br>GGAAGATCGGTTCAACGCCTCCCTGGGCACATACCACGATCTGCTGAA<br>AATTATCAAGGACAAGGACTTCCTGGACAATGAGGAAAACGAGGACA<br>TTCTGGAAGATATCGTGCTGACCCTGACACTGTTTGAGGACAGAGAGA<br>TGATCGAGGAACGGCTGAAAACCTATGCCCACCTGTTCGACGACAAA<br>GTGATGAAGCAGCTGAAGCGGCGGAGATACACCGGCTGGGGCAGGCT<br>GAGCCGGAAGCTGATCAACGGCATCCGGGACAAGCAGTCCGGCAAGA<br>CAATCCTGGATTTCCTGAAGTCCGACGGCTTCGCCAACAGAAACTTCA |



doi:10.6342/NTU201902787

| | |
|---|---|
| | TGCAGCTGATCCACGACGACAGCCTGACCTTTAAAGAGGACATCCAG<br>AAAGCCCAGGTGTCCGGCCAGGGCGATAGCCTGCACGAGCACATTGC<br>CAATCTGGCCGGCAGCCCCGCCATTAAGAAGGGCATCCTGCAGACAG<br>TGAAGGTGGTGGACGAGCTCGTGAAAGTGATGGGCCGGCACAAGCCC<br>GAGAACATCGTGATCGAAATGGCCAGAGAGAACCAGACCACCCAGAA<br>GGGACAGAAGAACAGCCGCGAGAGAATGAAGCGGATCGAAGAGGGC<br>ATCAAAGAGCTGGGCAGCCAGATCCTGAAAGAACACCCCGTGGAAAA<br>CACCCAGCTGCAGAACGAGAAGCTGTACCTGTACTACCTGCAGAATG<br>GGCGGGATATGTACGTGGACCAGGAACTGGACATCAACCGGCTGTCC<br>GACTACGATGTGGACCATATCGTGCCTCAGAGCTTTCTGAAGGACGAC<br>TCCATCGACAACAAGGTGCTGACCAGAAGCGACAAGAACCGGGGCAA<br>GAGCGACAACGTGCCCTCCGAAGAGGTCGTGAAGAAGATGAAGAACT<br>ACTGGCGGCAGCTGCTGAACGCCAAGCTGATTACCCAGAGAAAGTTC<br>GACAATCTGACCAAGGCCGAGAGAGGCGGCCTGAGCGAACTGGATAA<br>GGCCGGCTTCATCAAGAGACAGCTGGTGGAAACCCGGCAGATCACAA<br>AGCACGTGGCACAGATCCTGGACTCCCGGATGAACACTAAGTACGAC<br>GAGAATGACAAGCTGATCCGGGAAGTGAAAGTGATCACCCTGAAGTC<br>CAAGCTGGTGTCCGATTTCCGGAAGGATTTCCAGTTTTACAAAGTGCG<br>CGAGATCAACAACTACCACCACGCCCACGACGCCTACCTGAACGCCG<br>TCGTGGGAACCGCCCTGATCAAAAAGTACCCTAAGCTGGAAAGCGAG<br>TTCGTGTACGGCGACTACAAGGTGTACGACGTGCGGAAGATGATCGC<br>CAAGAGCGAGCAGGAAATCGGCAAGGCTACCGCCAAGTACTTCTTCT<br>ACAGCAACATCATGAACTTTTTCAAGACCGAGATTACCCTGGCCAACG<br>GCGAGATCCGGAAGCGGCCTCTGATCGAGACAAACGGCGAAACCGGG<br>GAGATCGTGTGGGATAAGGGCCGGGATTTTGCCACCGTGCGGAAAGT<br>GCTGAGCATGCCCCAAGTGAATATCGTGAAAAAGACCGAGGTGCAGA<br>CAGGCGGCTTCAGCAAAGAGTCTATCCTGCCCAAGAGGAACAGCGAT<br>AAGCTGATCGCCAGAAAGAAGGACTGGGACCCTAAGAAGTACGGCGG<br>CTTCGACAGCCCCACCGTGGCCTATTCTGTGCTGGTGGTGGCCAAAGT<br>GGAAAAGGGCAAGTCCAAGAAACTGAAGAGTGTGAAAGAGCTGCTG<br>GGGATCACCATCATGGAAAGAAGCAGCTTCGAGAAGAATCCCATCGA<br>CTTTCTGGAAGCCAAGGGCTACAAAGAAGTGAAAAAGGACCTGATCA<br>TCAAGCTGCCTAAGTACTCCCTGTTCGAGCTGGAAAACGGCCGGAAG<br>AGAATGCTGGCCTCTGCCGGCGAACTGCAGAAGGGAAACGAACTGGC<br>CCTGCCCTCCAAATATGTGAACTTCCTGTACCTGGCCAGCCACTATGA<br>GAAGCTGAAGGGCTCCCCCGAGGATAATGAGCAGAAACAGCTGTTTG<br>TGGAACAGCACAAGCACTACCTGGACGAGATCATCGAGCAGATCAGC<br>GAGTTCTCCAAGAGAGTGATCCTGGCCGACGCTAATCTGGACAAAGT<br>GCTGTCCGCCTACAACAAGCACCGGGATAAGCCCATCAGAGAGCAGG<br>CCGAGAATATCATCCACCTGTTTACCCTGACCAATCTGGGAGCCCCTG<br>CCGCCTTCAAGTACTTTGACACCACCATCGACCGGAAGAGGTACACCA<br>GCACCAAAGAGGTGCTGGACGCCACCCTGATCCACCAGAGCATCACC<br>GGCCTGTACGAGACACGGATCGACCTGTCTCAGCTGGGAGGCGAC<br>Translation:<br>DKKYSIGLDIGTNSVGWAVITDEYKVPSKKFKVLGNTDRHSIKKNLIGAL<br>LFDSGETAEATRLKRTARRRYTRRKNRICYLQEIFSNEMAKVDDSFFHRL |



doi:10.6342/NTU201902787

| | |
|---|---|
| | EESFLVEEDKKHERHPIFGNIVDEVAYHEKYPTIYHLRKKLVDSTDKADL<br>RLIYLALAHMIKFRGHFLIEGDLNPDNSDVDKLFIQLVQTYNQLFEENPIN<br>ASGVDAKAILSARLSKSRRLENLIAQLPGEKKNGLFGNLIALSLGLTPNFK<br>SNFDLAEDAKLQLSKDTYDDDLDNLLAQIGDQYADLFLAAKNLSDAILL<br>SDILRVNTEITKAPLSASMIKRYDEHHQDLTLLKALVRQQLPEKYKEIFFD<br>QSKNGYAGYIDGGASQEEFYKFIKPILEKMDGTEELLVKLNREDLLRKQR<br>TFDNGSIPHQIHLGELHAILRRQEDFYPFLKDNREKIEKILTFRIPYYVGPL<br>ARGNSRFAWMTRKSEETITPWNFEEVVDKGASAQSFIERMTNFDKNLPN<br>EKVLPKHSLLYEYFTVYNELTKVKYVTEGMRKPAFLSGEQKKAIVDLLF<br>KTNRKVTVKQLKEDYFKKIECFDSVEISGVEDRFNASLGTYHDLLKIIKD<br>KDFLDNEENEDILEDIVLTLTLFEDREMIEERLKTYAHLFDDKVMKQLKR<br>RRYTGWGRLSRKLINGIRDKQSGKTILDFLKSDGFANRNFMQLIHDDSLT<br>FKEDIQKAQVSGQGDSLHEHIANLAGSPAIKKGILQTVKVVDELVKVMG<br>RHKPENIVIEMARENQTTQKGQKNSRERMKRIEEGIKELGSQILKEHPVEN<br>TQLQNEKLYLYYLQNGRDMYVDQELDINRLSDYDVDHIVPQSFLKDDSI<br>DNKVLTRSDKNRGKSDNVPSEEVVKKMKNYWRQLLNAKLITQRKFDNL<br>TKAERGGLSELDKAGFIKRQLVETRQITKHVAQILDSRMNTKYDENDKLI<br>REVKVITLKSKLVSDFRKDFQFYKVREINNYHHAHDAYLNAVVGTALIK<br>KYPKLESEFVYGDYKVYDVRKMIAKSEQEIGKATAKYFFYSNIMNFFKTE<br>ITLANGEIRKRPLIETNGETGEIVWDKGRDFATVRKVLSMPQVNIVKKTE<br>VQTGGFSKESILPKRNSDKLIARKKDWDPKKYGGFDSPTVAYSVLVVAK<br>VEKGKSKKLKSVKELLGITIMERSSFEKNPIDFLEAKGYKEVKKDLIIKLP<br>KYSLFELENGRKRMLASAGELQKGNELALPSKYVNFLYLASHYEKLKGS<br>PEDNEQKQLFVEQHKHYLDEIIEQISEFSKRVILADANLDKVLSAYNKHR<br>DKPIREQAENIIHLFTLTNLGAPAAFKYFDTTIDRKRYTSTKEVLDATLIHQ<br>SITGLYETRIDLSQLGGD |
| 2xCOX8A MTS | ATGAGTGTGCTGACGCCACTGCTGCTGAGAGGACTGACAGGCAGTGC<br>TCGGAGACTCCCAGTACCTAGAGCAAAAATTCATTCTCTTGGAGATCT<br>TTCCGTATTGACTCCTTTGTTGTTGAGAGGCTTGACAGGATCGGCTAG<br>ACGGCTCCCAGTGCCGCGCGCCAAGATCCACTCGCTGGGGGAC<br>Translation:<br>MSVLTPLLLRGLTGSARRLPVPRAKIHSLGDLSVLTPLLLRGLTGSARRLP<br>VPRAKIHSLGD |
| *S. cerevisiae* COX4P MTS | CTCAGCCTCCGGCAATCTATCCGCTTCTTCAAGCCGGCGACTCGGACA<br>CTCTGCTCCAGCAGATACCTGTTG<br>Translation:<br>LSLRQSIRFFKPATRTLCSSRYLL |
| ACACB MTS | ATGGTTCTGCTGCTGTGCTTGAGCTGCCTTATTTTCAGTTGCCTTACAT<br>TTTCTTGGCTCAAAATTTGGGGCAAGATGACTGATTCCAAGCCTATTA<br>CCAAAAGCAAGTCAGAGGCGAAC<br>Translation:<br>MVLLLCLSCLIFSCLTFSWLKIWGKMTDSKPITKSKSEAN |
| GLDC MTS | ATGCAGTCTTGTGCTAGAGCCTGGGGGCTGAGATTGGGGAGGGGTGT<br>CGGGGGGGGCAGAAGGTTGGCCGGTGGGAGTGGACCATGTTGGGCTC<br>CTAGAAGTCGC<br>Translation: |



doi:10.6342/NTU201902787

| | |
|---|---|
| | MQSCARAWGLRLGRGVGGGRRLAGGSGPCWAPRSR |
| POLG MTS | ATGTCTCGGCTGCTTTGGAGAAAGGTCGCGGGGGCGACAGTCGGTCCT<br>GGTCCAGTCCCTGCGCCCGGTCGCTGGGTCTCATCCAGTGTTCCTGCTT<br>CAGATCCATCTGATGGA<br>Translation:<br>MSRLLWRKVAGATVGPGPVPAPGRWVSSSVPASDPSDG |
| MTHFD1L MTS | ATGGGCACTCGCTTGCCTCTCGTGTTGCGACAGTTGAGGCGGCCGCCG<br>CAACCTCCCGGTCCCCCCCGAAGGTTGCGAGTTCCATGCCGAGCA<br>Translation:<br>MGTRLPLVLRQLRRPPQPPGPPRRLRVPCRA |
| Human PNPase sequence | ATGGCGGCCTGCAGGTACTGCTGCTCGTGCCTCCGGCTCCGGCCCCTG<br>AGCGATGGTCCTTTCCTTCTGCCACGGCGGGATCGGGCACTCACCCAG<br>TTGCAAGTGCGAGCACTATGGAGTAGCGCAGGGTCTCGAGCTGTGGC<br>CGTGGACTTAGGCAACAGGAAATTAGAAATATCTTCTGGAAAGCTGG<br>CCAGATTTGCAGATGGCTCTGCTGTAGTACAGTCAGGTGACACTGCAG<br>TAATGGTCACAGCGGTCAGTAAAACAAAACCTTCCCCTTCCCAGTTTA<br>TGCCTTTGGTGGTTGACTACAGACAAAAAGCTGCTGCAGCAGGTAGA<br>ATTCCCACAAACTATCTGAGAAGAGAGATTGGTACTTCTGATAAAGA<br>AATTCTAACAAGTCGAATAATAGATCGTTCAATTAGACCGCTCTTTCC<br>AGCTGGCTACTTCTATGATACACAGGTTCTGTGTAATCTGTTAGCAGT<br>AGATGGTGTAAATGAGCCTGATGTCCTAGCAATTAATGGCGCTTCCGT<br>AGCCCTCTCATTATCAGATATTCCTTGGAATGGACCTGTTGGGGCAGT<br>ACGAATAGGAATAATTGATGGAGAATATGTTGTTAACCCAACAAGAA<br>AAGAAATGTCTTCTAGTACTTTAAATTTAGTGGTTGCTGGAGCACCTA<br>AAAGTCAGATTGTCATGTTGGAAGCCTCTGCAGAGAACATTTTACAGC<br>AGGACTTTTGCCATGCTATCAAAGTGGGAGTGAAATATACCCAACAA<br>ATAATTCAGGGCATTCAGCAGTTGGTAAAAGAAACTGGTGTTACCAA<br>GAGGACACCTCAGAAGTTATTTACCCCTTCGCCAGAGATTGTGAAATA<br>TACTCATAAACTTGCTATGGAGAGACTCTATGCAGTTTTTACAGATTA<br>CGAGCATGACAAAGTTTCCAGAGATGAAGCTGTTAACAAAATAAGAT<br>TAGATACGGAGGAACAACTAAAAGAAAAATTTCCAGAAGCCGATCCA<br>TATGAAATAATAGAATCCTTCAATGTTGTTGCAAAGGAAGTTTTTAGA<br>AGTATTGTTTTGAATGAATACAAAAGGTGCGATGGTCGGGATTTGACT<br>TCACTTAGGAATGTAAGTTGTGAGGTAGATATGTTTAAAACCCTTCAT<br>GGATCAGCATTATTTCAAAGAGGACAAACACAGGTGCTTTGTACCGTT<br>ACATTTGATTCATTAGAATCTGGTATTAAGTCAGATCAAGTTATAACA<br>GCTATAAAtGGGATAAAAGATAAAAATTTCATGCTGCACTACGAGTTT<br>CCTCCTTATGCAACTAATGAAATTGGCAAAGTCACTGGTTTAAATAGA<br>AGAGAACTTGGGCATGGTGCTCTTGCTGAGAAAGCTTTGTATCCTGTT<br>ATTCCCCGAGATTTTCCTTTCACCATAAGAGTTACATCTGAAGTCCTA<br>GAGTCAAATGGGTCATCTTCTATGGCATCTGCATGTGGCGGAAGTTTA<br>GCATTAATGGATTCAGGGGTTCCAATTTCATCTGCTGTTGCAGGCGTA<br>GCAATAGGATTGGTCACCAAAACCGATCCTGAGAAGGGTGAAATAGA<br>AGATTATCGTTTGCTGACAGATATTTTGGGAATTGAAGATTACAATGG<br>TGACATGGACTTCAAAATAGCTGGCACTAATAAAGGAATAACTGCAT<br>TACAGGCTGATATTAAATTACCTGGAATACCAATAAAAATTGTGATGG |



doi:10.6342/NTU201902787

| | |
|---|---|
| | AGGCTATTCAACAAGCTTCAGTGGCAAAAAAGGAGATATTACAGATC<br>ATGAACAAAACTATTTCAAAACCTCGAGCATCTAGAAAAGAAAATGG<br>ACCTGTTGTAGAAACTGTTCAGGTTCCATTATCAAAACGAGCAAAATT<br>TGTTGGACCTGGTGGCTATAACTTAAAAAAACTTCAGGCTGAAACAG<br>GTGTAACTATTAGTCAGGTGGATGAAGAAACGTTTTCTGTATTTGCAC<br>CAACACCCAGTGCTATGCATGAGGCAAGAGACTTCATTACTGAAATCT<br>GCAAGGATGATCAGGAGCAGCAATTAGAATTTGGAGCAGTATATACC<br>GCCACAATAACTGAAATCAGAGATACTGGTGTAATGGTAAAATTATA<br>TCCAAATATGACTGCGGTACTGCTTCATAACACACAACTTGATCAACG<br>AAAGATTAAACATCCTACTGCCCTAGGATTAGAAGTTGGCCAAGAAA<br>TTCAGGTGAAATACTTTGGACGTGACCCAGCCGATGGAAGAATGAGG<br>CTTTCTCGAAAAGTGCTTCAGTCGCCAGCTACAACCGTGGTCAGAACT<br>TTGAATGACAGAAGTAGTATTGTAATGGGAGAACCTATTTCACAGTCA<br>TCATCTAATTCTCAG<br>Translation:<br>MAACRYCCSCLRLRPLSDGPFLLPRRDRALTQLQVRALWSSAGSRAVAV<br>DLGNRKLEISSGKLARFADGSAVVQSGDTAVMVTAVSKTKPSPSQFMPL<br>VVDYRQKAAAAGRIPTNYLRREIGTSDKEILTSRIIDRSIRPLFPAGYFYDT<br>QVLCNLLAVDGVNEPDVLAINGASVALSLSDIPWNGPVGAVRIGIIDGEY<br>VVNPTRKEMSSSTLNLVVAGAPKSQIVMLEASAENILQQDFCHAIKVGVK<br>YTQQIIQGIQQLVKETGVTKRTPQKLFTPSPEIVKYTHKLAMERLYAVFTD<br>YEHDKVSRDEAVNKIRLDTEEQLKEKFPEADPYEIIESFNVVAKEVFRSIV<br>LNEYKRCDGRDLTSLRNVSCEVDMFKTLHGSALFQRGQTQVLCTVTFDS<br>LESGIKSDQVITAINGIKDKNFMLHYEFPPYATNEIGKVTGLNRRELGHGA<br>LAEKALYPVIPRDFPFTIRVTSEVLESNGSSSMASACGGSLALMDSGVPISS<br>AVAGVAIGLVTKTDPEKGEIEDYRLLTDILGIEDYNGDMDFKIAGTNKGIT<br>ALQADIKLPGIPIKIVMEAIQQASVAKKEILQIMNKTISKPRASRKENGPVV<br>ETVQVPLSKRAKFVGPGGYNLKKLQAETGVTISQVDEETFSVFAPTPSAM<br>HEARDFITEICKDDQEQQLEFGAVYTATITEIRDTGVMVKLYPNMTAVLL<br>HNTQLDQRKIKHPTALGLEVGQEIQVKYFGRDPADGRMRLSRKVLQSPA<br>TTVVRTLNDRSSIVMGEPISQSSSNSQ |



doi:10.6342/NTU201902787

**Table 3. T7 *in vitro* transcribed RNAs (IVT RNAs) used in this study**

| IVT RNA | Sequence (5'-3') | Description |
|---|---|---|
| gRNA36 | GCATCATAATCCTCTCTCAGTTTTAGAGCTATGCTGGAAACAGCATAGCAAGTTAAAATAAGGCTAGTCCGTTATCAACTTGAAAAAGTGGCACCGAGTCGGTGC | 20nt ND4 target 6 |
| gRNA51 | GCACTCACAGTCGCATCATAATCCTCTCTCAGTTTAAGAGCTATGCTGGAAACAGCATAGCAAGTTTAAATAAGGCTAGTCCGTTATCAACTTGAAAAAGTGGCACCGAGTCGGTGC | 30nt ND4 target 6 |
| gRNA52 | G**TCTCCCTGAGCTTCAGGGAG**CACTCACAGTCGCATCATAATCCTCTCTCAGTTTAAGAGCTATGCTGGAAACAGCATAGCAAGTTTAAATAAGGCTAGTCCGTTATCAACTTGAAAAAGTGGCACCGAGTCGGTGC | RP MTS - 30nt ND4 target 6 |
| gRNA53 | **GCGCAATCGGTAGCGCTTCGAGCCCCCTACAGGGCTCCA**CACTCACAGTCGCATCATAATCCTCTCTCAGTTTAAGAGCTATGCTGGAAACAGCATAGCAAGTTTAAATAAGGCTAGTCCGTTATCAACTTGAAAAAGTGGCACCGAGTCGGTGC | F1D1 MTS - 30nt ND4 target 6 |
| gRNA54 | G**TCTCCCTGAGCTTCAGGGAG**CACTCACAGTCGCATCATAATCCTCTCTCAGTTTAAGAGCTATGCTGGAAACAGCATAGCAAGTTTAAATAAGGCTAGTCCGTTATCAACTTGAAAAAGTGGCACCGAGTCGGTGC**CAGAAGAAGTGACGGCTGGGGGCACAGTGGGCTGGGCGCCCCTGCAGAACATGAACCTTCCGCTCCTGGCTGCCACAGGGTCCTCCGATGCTGGCCTTTGCGCCTCTAGAGGCAGCCACTCATGGATTCAAGTCCTGGCTCCGCCTCTTCCACT** | RP MTS - 30nt ND4 target 6 – MRPS12 3' UTR |
| gRNA55 | **GCGCAATCGGTAGCGCTTCGAGCCCCCTACAGGGCTCCA**CACTCACAGTCGCATCATAATCCTCTCTCAGTTTAAGAGCTATGCTGGAAACAGCATAGCAAGTTTAAATAAGGCTAGTCCGTTATCAACTTGAAAAAGTGGCACCGAGTCGGTGC**CAGAAGAAGTGACGGCTGGGGGCACAGTGGGCTGGGCGCCCCTGCAGAACATGAACCTTCCGCTCCTGGCTGCCACAGGGTCCTCCGATGCTGGCCTTTGCGCCTCTAGAGGCAGCCACTCATGGATTCAAGTCCTGGCTCCGCCTCTTCCACT** | F1D1 MTS - 30nt ND4 target 6 – MRPS12 3' UTR |
| gRNA56 | G**AGAAGCGTATCCCGCTGAGC**CACTCACAGTCGCATCATAATCCTCTCTCAGTTTAAGAGCTATGCTGGAAACAGCATAGCAAGTTTAAATAAGGCTAGTCCGTTATCAACTTGAAAAAGTGGCACCGAGTCGGTGC | MRP MTS - 30nt ND4 target 6 |
| gRNA57 | G**AGAAGCGTATCCCGCTGAGC**CACTCACAGTCGCATCATAATCCTCTCTCAGTTTAAGAGCTATGCTGGAAACAGCATAGCAAGTTTAAATAAGGCTAGTCCGTTATCAACTTGAAAAAGTGGCACCGAGTCGGTGC**CAGAAGAAGTGACGGCTGGGGGCACAGTGGGCTGGGCGCCCCTGCA** | MRP MTS - 30nt ND4 target 6 – MRPS12 3' UTR |



doi:10.6342/NTU201902787

| | | |
|---|---|---|
| | **GAACATGAACCTTCCGCTCCTGGCTGCCACAGGGT CCTCCGATGCTGGCCTTTGCGCCTCTAGAGGCAGC CACTCATGGATTCAAGTCCTGGCTCCGCCTCTTCCA CT** | |
| gRNA68 | **GCGCAATCGGTAGCGC**CACTCACAGTCGCATCATAAT CCTCTCTCAGTTTAAGAGCTATGCTGGAAACAGCATAG CAAGTTTAAATAAGGCTAGTCCGTTATCAACTTGAAAA AGTGGCACCGAGTCGGTGC | HD MTS - 30nt ND4 target 6 |
| gRNA69 | GCACTCACAGTCGCATCATAATCCTCTCTCAGTTTAAG AGCTATGCTG**TCTCCCTGAGCTTCAGGGAG**CAGCAT AGCAAGTTTAAATAAGGCTAGTCCGTTATCAACTTGAA AAAGTGGCACCGAGTCGGTGC | 30nt ND4 target 6 – internal RP MTS |
| gRNA70 | GCACTCACAGTCGCATCATAATCCTCTCTCAGTTTAAG AGCTATGCTG**GCGCAATCGGTAGCGCTTCGAGCCCC CTACAGGGCTCCA**CAGCATAGCAAGTTTAAATAAGGC TAGTCCGTTATCAACTTGAAAAAGTGGCACCGAGTCGG TGC | 30nt ND4 target 6 – internal F1D1 MTS |
| gRNA71 | GCACTCACAGTCGCATCATAATCCTCTCTCAGTTTAAG AGCTATGCTG**AGAAGCGTATCCCGCTGAGC**CAGCAT AGCAAGTTTAAATAAGGCTAGTCCGTTATCAACTTGAA AAAGTGGCACCGAGTCGGTGC | 30nt ND4 target 6 – internal MRP MTS |
| gRNA72 | GCACTCACAGTCGCATCATAATCCTCTCTCAGTTTAAG AGCTATGCTG**GCGCAATCGGTAGCGC**CAGCATAGCA AGTTTAAATAAGGCTAGTCCGTTATCAACTTGAAAAAG TGGCACCGAGTCGGTGC | 30nt ND4 target 6 – internal HD MTS |
| gRNA73 | **GGCCTGGTTAGTACTTGGATGGGAGACCGCCAAGG AATACCGGGTG**CACTCACAGTCGCATCATAATCCTCT CTCAGTTTAAGAGCTATGCTGGAAACAGCATAGCAAGT TTAAATAAGGCTAGTCCGTTATCAACTTGAAAAAGTGG CACCGAGTCGGTGC | 5S γ domain MTS - 30nt ND4 target 6 |
| gRNA74 | GCACTCACAGTCGCATCATAATCCTCTCTCAGTTTAAG AGCTATGCTG**GGCCTGGTTAGTACTTGGATGGGAGA CCGCCAAGGAATACCGGGTG**CAGCATAGCAAGTTTA AATAAGGCTAGTCCGTTATCAACTTGAAAAAGTGGCAC CGAGTCGGTGC | 30nt ND4 target 6 – internal 5S γ domain MTS |

*Underlined letters, target sequence for guide RNAs. **Bold letters**, mitochondria-targeting sequence.



doi:10.6342/NTU201902787

**Table 4. PCR condition and program setting for DNA template of IVT RNA**

| Target IVT RNA and PCR condition | Thermal cycler and setting |
|---|---|
| **sgRNA36** | **Applied Biosystems SimpliAmp** |
| 195 μL molecular $ddH_2O$ | 98°C, 30 seconds |
| 60 μL KAPA HiFi fidelity buffer (5X) | 98°C, 10 seconds \ |
| 10 μL 10 μM T25G/SLKS2 | 62°C, 10 seconds \| 40 cycles |
| 20 μL 1 μM SL467/SL297 | 72°C, 10 seconds / |
| 9 μL KAPA dNTP mix | 72°C, 2 minutes |
| 6 μL KAPA HiFi DNA polymerase | 12°C, 5 minutes |
| (300 μL in total, distributed 50 μL as aliquot into six PCR tubes) | |
| **sgRNA51** | **Eppendorf 6325 Mastercycler Pro S** |
| 27.5 μL molecular $ddH_2O$ | 98°C, 2 minutes |
| 10 μL KAPA HiFi fidelity buffer (5X) | 98°C, 10 seconds \ |
| 5 μL dimethyl sulfoxide | 61°C, 10 seconds \| 40 cycles |
| 3 μL 1 μM SL613/SLKS2 | 72°C, 15 seconds / |
| 2 μL 1 ng/μL pSL146 | 72°C, 2 minutes |
| 1.5 μL KAPA dNTP mix | 12°C, 5 minutes |
| 1 μL KAPA HiFi DNA polymerase | |
| (50 μL in total in a PCR tube) | |
| **sgRNA52** | **Eppendorf 6325 Mastercycler Pro S** |
| 27.5 μL molecular $ddH_2O$ | 98°C, 2 minutes |
| 10 μL KAPA HiFi fidelity buffer (5X) | 98°C, 10 seconds \ |
| 5 μL dimethyl sulfoxide | 61°C, 10 seconds \| 40 cycles |
| 3 μL 1 μM SL632/SLKS2 | 72°C, 15 seconds / |
| 2 μL 1 ng/μL pSL146 | 72°C, 2 minutes |
| 1.5 μL KAPA dNTP mix | 12°C, 5 minutes |



doi:10.6342/NTU201902787

| | |
|---|---|
| 1 μL KAPA HiFi DNA polymerase<br>(50 μL in total in a PCR tube) | |
| **sgRNA53** | **Eppendorf 6325 Mastercycler Pro S** |
| 27.5 μL molecular dd$H_2O$ | 98°C, 2 minutes |
| 10 μL KAPA HiFi fidelity buffer (5X) | 98°C, 10 seconds \ |
| 5 μL dimethyl sulfoxide | 62°C, 10 seconds \| 40 cycles |
| 3 μL 1 μM SL615/SLKS2 | 72°C, 15 seconds / |
| 2 μL 1 ng/μL pSL147 | 72°C, 2 minutes |
| 1.5 μL KAPA dNTP mix | 12°C, 5 minutes |
| 1 μL KAPA HiFi DNA polymerase<br>(50 μL in total in a PCR tube) | |
| **sgRNA54** | **Eppendorf 6325 Mastercycler Pro S** |
| 27.5 μL molecular dd$H_2O$ | 98°C, 2 minutes |
| 10 μL KAPA HiFi fidelity buffer (5X) | 98°C, 10 seconds \ |
| 5 μL dimethyl sulfoxide | 68°C, 10 seconds \| 40 cycles |
| 3 μL 1 μM SL632/SL616 | 72°C, 15 seconds / |
| 2 μL 1 ng/μL pSL148 | 72°C, 2 minutes |
| 1.5 μL KAPA dNTP mix | 12°C, 5 minutes |
| 1 μL KAPA HiFi DNA polymerase<br>(50 μL in total in a PCR tube) | |
| **sgRNA55** | **Eppendorf 6325 Mastercycler Pro S** |
| 27.5 μL molecular dd$H_2O$ | 98°C, 2 minutes |
| 10 μL KAPA HiFi fidelity buffer (5X) | 98°C, 10 seconds \ |
| 5 μL dimethyl sulfoxide | 65°C, 10 seconds \| 40 cycles |
| 3 μL 1 μM SL615/SL616 | 72°C, 15 seconds / |
| 2 μL 1 ng/μL pSL149 | 72°C, 2 minutes |
| 1.5 μL KAPA dNTP mix | 12°C, 5 minutes |



doi:10.6342/NTU201902787

| | |
|---|---|
| 1 μL KAPA HiFi DNA polymerase<br>(50 μL in total in a PCR tube) | |
| **sgRNA56** | **Eppendorf 6325 Mastercycler Pro S** |
| 27.5 μL molecular dd$H_2O$ | 98°C, 2 minutes |
| 10 μL KAPA HiFi fidelity buffer (5X) | 98°C, 10 seconds \ |
| 5 μL dimethyl sulfoxide | 61°C, 10 seconds \| 40 cycles |
| 3 μL 1 μM MF8/SLKS2 | 72°C, 15 seconds / |
| 2 μL 1 ng/μL pSL187 | 72°C, 2 minutes |
| 1.5 μL KAPA dNTP mix | 12°C, 5 minutes |
| 1 μL KAPA HiFi DNA polymerase<br>(50 μL in total in a PCR tube) | |
| **sgRNA57** | **Eppendorf 6325 Mastercycler Pro S** |
| 27.5 μL molecular dd$H_2O$ | 98°C, 2 minutes |
| 10 μL KAPA HiFi fidelity buffer (5X) | 98°C, 10 seconds \ |
| 5 μL dimethyl sulfoxide | 62°C, 10 seconds \| 40 cycles |
| 3 μL 1 μM MF8/SL616 | 72°C, 15 seconds / |
| 2 μL 1 ng/μL pSL188 | 72°C, 2 minutes |
| 1.5 μL KAPA dNTP mix | 12°C, 5 minutes |
| 1 μL KAPA HiFi DNA polymerase<br>(50 μL in total in a PCR tube) | |
| **sgRNA68** | **Eppendorf 6325 Mastercycler Pro S** |
| 32.5 μL molecular dd$H_2O$ | 98°C, 30 seconds |
| 10 μL KAPA HiFi fidelity buffer (5X) | 98°C, 10 seconds \ |
| 3 μL 1 μM MF46/SLKS2 | 61°C, 10 seconds \| 40 cycles |
| 2 μL 1 ng/μL pSL245 | 72°C, 15 seconds / |
| 1.5 μL KAPA dNTP mix | 72°C, 2 minutes |
| 1 μL KAPA HiFi DNA polymerase | 12°C, 5 minutes |



doi:10.6342/NTU201902787

| | |
|---|---|
| (50 μL in total in a PCR tube) | |
| **sgRNA69** | **Eppendorf 6325 Mastercycler Pro S** |
| 32.5 μL molecular dd$H_2O$ | 98°C, 30 seconds |
| 10 μL KAPA HiFi fidelity buffer (5X) | 98°C, 10 seconds \ |
| 3 μL 1 μM MF9/SLKS2 | 61°C, 10 seconds \| 40 cycles |
| 2 μL 1 ng/μL pSL246 | 72°C, 15 seconds / |
| 1.5 μL KAPA dNTP mix | 72°C, 2 minutes |
| 1 μL KAPA HiFi DNA polymerase | 12°C, 5 minutes |
| (50 μL in total in a PCR tube) | |
| **sgRNA70** | **Eppendorf 6325 Mastercycler Pro S** |
| 32.5 μL molecular dd$H_2O$ | 98°C, 30 seconds |
| 10 μL KAPA HiFi fidelity buffer (5X) | 98°C, 10 seconds \ |
| 3 μL 1 μM MF9/SLKS2 | 61°C, 10 seconds \| 40 cycles |
| 2 μL 1 ng/μL pSL247 | 72°C, 15 seconds / |
| 1.5 μL KAPA dNTP mix | 72°C, 2 minutes |
| 1 μL KAPA HiFi DNA polymerase | 12°C, 5 minutes |
| (50 μL in total in a PCR tube) | |
| **sgRNA71** | **Eppendorf 6325 Mastercycler Pro S** |
| 32.5 μL molecular dd$H_2O$ | 98°C, 30 seconds |
| 10 μL KAPA HiFi fidelity buffer (5X) | 98°C, 10 seconds \ |
| 3 μL 1 μM MF9/SLKS2 | 61°C, 10 seconds \| 40 cycles |
| 2 μL 1 ng/μL pSL248 | 72°C, 15 seconds / |
| 1.5 μL KAPA dNTP mix | 72°C, 2 minutes |
| 1 μL KAPA HiFi DNA polymerase | 12°C, 5 minutes |
| (50 μL in total in a PCR tube) | |
| **sgRNA72** | **Eppendorf 6325 Mastercycler Pro S** |



doi:10.6342/NTU201902787

| | |
|---|---|
| 32.5 μL molecular $ddH_2O$ | 98°C, 30 seconds |
| 10 μL KAPA HiFi fidelity buffer (5X) | 98°C, 10 seconds \ |
| 3 μL 1 μM MF9/SLKS2 | 61°C, 10 seconds \| 40 cycles |
| 2 μL 1 ng/μL pSL249 | 72°C, 15 seconds / |
| 1.5 μL KAPA dNTP mix | 72°C, 2 minutes |
| 1 μL KAPA HiFi DNA polymerase | 12°C, 5 minutes |
| (50 μL in total in a PCR tube) | |
| **sgRNA73** | **Eppendorf 6325 Mastercycler Pro S** |
| 32.5 μL molecular $ddH_2O$ | 98°C, 30 seconds |
| 10 μL KAPA HiFi fidelity buffer (5X) | 98°C, 10 seconds \ |
| 3 μL 1 μM MF110/SLKS2 | 63°C, 10 seconds \| 40 cycles |
| 2 μL 1 ng/μL pSL297 | 72°C, 15 seconds / |
| 1.5 μL KAPA dNTP mix | 72°C, 2 minutes |
| 1 μL KAPA HiFi DNA polymerase | 12°C, 5 minutes |
| (50 μL in total in a PCR tube) | |
| **sgRNA74** | **Eppendorf 6325 Mastercycler Pro S** |
| 32.5 μL molecular $ddH_2O$ | 98°C, 30 seconds |
| 10 μL KAPA HiFi fidelity buffer (5X) | 98°C, 10 seconds \ |
| 3 μL 1 μM T25G/SLKS2 | 56°C, 10 seconds \| 40 cycles |
| 2 μL 1 ng/μL pSL298 | 72°C, 15 seconds / |
| 1.5 μL KAPA dNTP mix | 72°C, 2 minutes |
| 1 μL KAPA HiFi DNA polymerase | 12°C, 5 minutes |
| (50 μL in total in a PCR tube) | |



doi:10.6342/NTU201902787

**Table 5. Amount of Lipofectamine 2000 for transfection of different mito-sgRNAs**

| | g36 | g51 | g52 | g53 | g54 | g55 | g56 | g57 | g68 |
|---|---|---|---|---|---|---|---|---|---|
| **Lipo2000 (μL)** | 15 | 17 | 20 | 22 | 41 | 47 | 20 | 41 | 19 |
| | **g69** | **g70** | **g71** | **g72** | **g73** | **g74** | | | |
| **Lipo2000 (μL)** | 20 | 22 | 20 | 20 | 23 | 23 | | | |



doi:10.6342/NTU201902787

**Table 6. Raw data for qPCR of mito-sgRNA screening**

| Repeat | Sample | Target | CT | ΔCT | Fold (2^-ΔCT) |
|---|---|---|---|---|---|
| #1 | NTC | gRNA | 28.343069 | -2.32462 | 5.00932906 |
| #1 | NTC | 5S rRNA | 30.667686 | | |
| #2 | NTC | gRNA | 28.563665 | 4.153988 | 0.05617267 |
| #2 | NTC | 5S rRNA | 24.409678 | | |
| #3 | NTC | gRNA | 30.194529 | 6.391747 | 0.01190947 |
| #3 | NTC | 5S rRNA | 23.802782 | | |
| #1 | g36 | gRNA | 20.829824 | -1.69335 | 3.23405906 |
| #1 | g36 | 5S rRNA | 22.52317 | | |
| #2 | g36 | gRNA | 17.45186 | -3.06067 | 8.3435829 |
| #2 | g36 | 5S rRNA | 20.512527 | | |
| #3 | g36 | gRNA | 17.015562 | -2.04518 | 4.1272349 |
| #3 | g36 | 5S rRNA | 19.060738 | | |
| #1 | g51 | gRNA | 16.834761 | -6.51346 | 91.3581839 |
| #1 | g51 | 5S rRNA | 23.348223 | | |
| #2 | g51 | gRNA | 17.432344 | -5.86284 | 58.1958538 |
| #2 | g51 | 5S rRNA | 23.295189 | | |
| #3 | g51 | gRNA | 16.843206 | -7.3112 | 158.81496 |
| #3 | g51 | 5S rRNA | 24.154409 | | |
| #1 | g52 | gRNA | 20.144522 | -4.41597 | 21.3471246 |
| #1 | g52 | 5S rRNA | 24.560492 | | |
| #2 | g52 | gRNA | 19.141314 | -5.9427 | 61.5080463 |
| #2 | g52 | 5S rRNA | 25.084017 | | |
| #3 | g52 | gRNA | 16.229689 | -3.67841 | 12.8029624 |
| #3 | g52 | 5S rRNA | 19.908094 | | |
| #1 | g53 | gRNA | 20.944941 | -0.18152 | 1.55393612 |
| #1 | g53 | 5S rRNA | 21.126461 | | |
| #2 | g53 | gRNA | 19.571463 | -4.37296 | 20.7201559 |
| #2 | g53 | 5S rRNA | 23.944426 | | |
| #3 | g53 | gRNA | 16.273195 | -2.90323 | 7.4809976 |
| #3 | g53 | 5S rRNA | 19.176426 | | |
| #1 | g56 | gRNA | 20.95256 | -0.83205 | 1.78021592 |
| #1 | g56 | 5S rRNA | 21.784613 | | |
| #2 | g56 | gRNA | 19.86957 | -3.73703 | 13.3339112 |
| #2 | g56 | 5S rRNA | 23.606598 | | |
| #3 | g56 | gRNA | 17.539602 | -3.48377 | 11.1871331 |
| #3 | g56 | 5S rRNA | 21.023371 | | |
| #1 | g68 | gRNA | 20.953659 | -0.63593 | 1.55393612 |
| #1 | g68 | 5S rRNA | 21.589586 | | |
| #2 | g68 | gRNA | 17.045118 | -4.97438 | 31.436757 |
| #2 | g68 | 5S rRNA | 22.019499 | | |
| #3 | g68 | gRNA | 15.163123 | -3.60117 | 12.1355588 |



doi:10.6342/NTU201902787

| | | | | | |
|---|---|---|---|---|---|
| #3 | g68 | 5S rRNA | 18.764292 | | |
| #1 | g73 | gRNA | 27.648338 | 4.805243 | 0.03576662 |
| #1 | g73 | 5S rRNA | 22.843096 | | |
| #2 | g73 | gRNA | 16.273129 | -3.86818 | 14.6028821 |
| #2 | g73 | 5S rRNA | 20.14131 | | |
| #3 | g73 | gRNA | 16.119631 | -3.33375 | 10.0822916 |
| #3 | g73 | 5S rRNA | 19.453382 | | |
| #1 | g54 | gRNA | 19.47365 | -3.95126 | 15.46844 |
| #1 | g54 | 5S rRNA | 23.424906 | | |
| #2 | g54 | gRNA | 20.546682 | -4.78998 | 27.6648432 |
| #2 | g54 | 5S rRNA | 25.336664 | | |
| #3 | g54 | gRNA | 19.117712 | -4.88935 | 29.6373627 |
| #3 | g54 | 5S rRNA | 24.007057 | | |
| #1 | g55 | gRNA | 22.374603 | 0.004837 | 0.99665284 |
| #1 | g55 | 5S rRNA | 22.369766 | | |
| #2 | g55 | gRNA | 17.77256 | -3.97913 | 15.7701872 |
| #2 | g55 | 5S rRNA | 21.751688 | | |
| #3 | g55 | gRNA | 19.424479 | -6.30107 | 78.8517663 |
| #3 | g55 | 5S rRNA | 25.72555 | | |
| #1 | g57 | gRNA | 20.13299 | -1.89799 | 3.72693893 |
| #1 | g57 | 5S rRNA | 22.030981 | | |
| #2 | g57 | gRNA | 15.358197 | -5.09141 | 34.093075 |
| #2 | g57 | 5S rRNA | 20.449604 | | |
| #3 | g57 | gRNA | 18.511482 | -5.48225 | 44.7015834 |
| #3 | g57 | 5S rRNA | 23.993736 | | |



doi:10.6342/NTU201902787

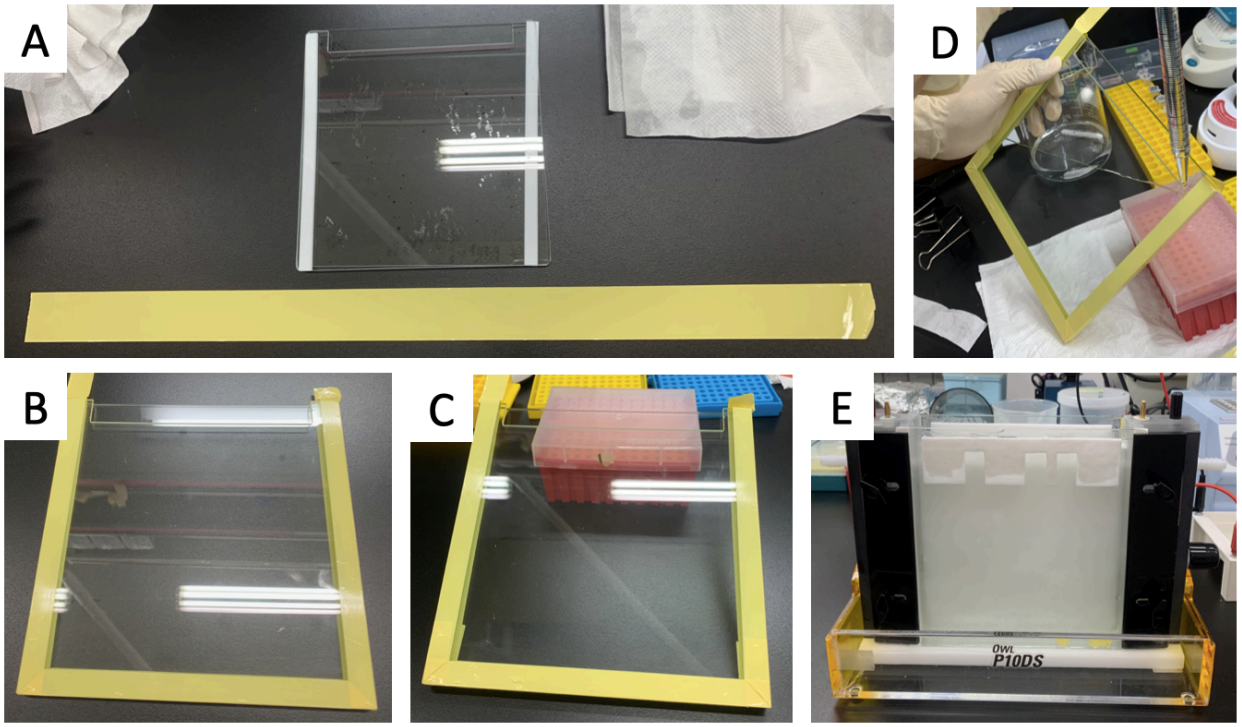


**Appendix 1. Setup flow of Urea-PAGE for RNA in vitro transcription**



doi:10.6342/NTU201902787

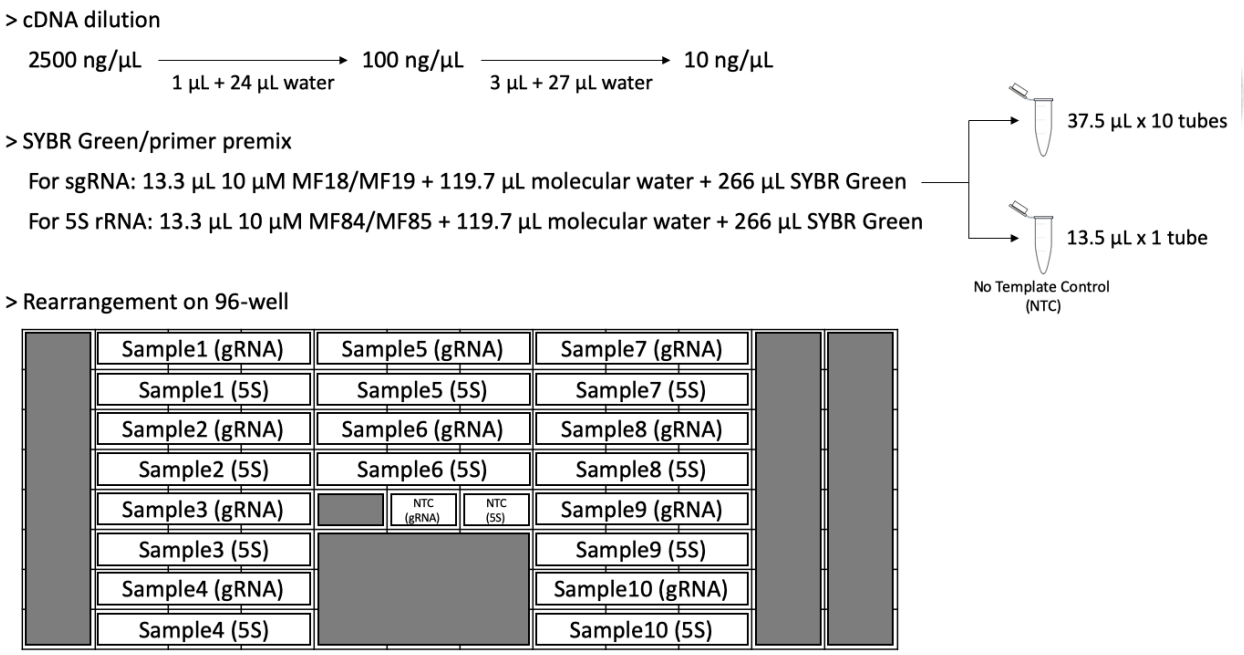


**Appendix 2. Setup for arrangement of RT-qPCR loading**



doi:10.6342/NTU201902787

# Reference


1. McBride, H. M., Neuspiel, M. & Wasiak, S. Mitochondria: more than just a powerhouse. *Curr. Biol.* **16,** R551–60 (2006).
2. Pittis, A. A. & Gabaldón, T. Late acquisition of mitochondria by a host with chimaeric prokaryotic ancestry. *Nature* **531,** 101–104 (2016).
3. Gaziev, A. I. & Shaĭkhaev, G. O. [Nuclear mitochondrial pseudogenes]. *Mol. Biol. (Mosk.)* **44,** 405–417 (2010).
4. Wallace, D. C. Mitochondrial genetic medicine. *Nat. Genet.* **50,** 1642–1649 (2018).
5. Bacman, S. R., Williams, S. L., Duan, D. & Moraes, C. T. Manipulation of mtDNA heteroplasmy in all striated muscles of newborn mice by AAV9-mediated delivery of a mitochondria-targeted restriction endonuclease. *Gene Ther* **19,** 1101–1106 (2011).
6. Bacman, S. R., Williams, S. L., Pinto, M., Peralta, S. & Moraes, C. T. Specific elimination of mutant mitochondrial genomes in patient-derived cells by mitoTALENs. *Nature Medicine 2013 19:9* **19,** 1111–1113 (2013).
7. Gammage, P. A., Rorbach, J., Vincent, A. I., Rebar, E. J. & Minczuk, M. Mitochondrially targeted ZFNs for selective degradation of pathogenic mitochondrial genomes bearing large-scale deletions or point mutations. *EMBO Mol Med* **6,** 458–466 (2014).
8. Man, P. Y. W., Turnbull, D. M. & Chinnery, P. F. Leber hereditary optic neuropathy. *Journal of Medical Genetics* **39,** 162–169 (2002).
9. Rahman, S. *et al.* Leigh syndrome: Clinical features and biochemical and DNA abnormalities. *Ann. Neurol.* **39,** 343–351 (1996).
10. Lake, N. J., Compton, A. G., Rahman, S. & Thorburn, D. R. Leigh syndrome: One disorder, more than 75 monogenic causes. *Ann. Neurol.* **79,** 190–203 (2016).
11. Wallace, D. C. Why Do We Still Have a Maternally Inherited Mitochondrial DNA? Insights from Evolutionary Medicine. *Annual Review of Biochemistry* **76,** 781–821 (2007).
12. Schwartz, M. & Vissing, J. New patterns of inheritance in mitochondrial disease. *Biochem. Biophys. Res. Commun.* **310,** 247–251 (2003).
13. Tuppen, H. A. L., Blakely, E. L., Turnbull, D. M. & Taylor, R. W. Mitochondrial DNA mutations and human disease. *Biochimica et Biophysica Acta (BBA) - Bioenergetics* **1797,** 113–128 (2010).
14. Jenuth, J. P., Peterson, A. C. & Shoubridge, E. A. Tissue-specific selection for different mtDNA genotypes in heteroplasmic mice. *Nat. Genet.* **16,** 93–95 (1997).
15. Alexeyev, M. F. *et al.* Selective elimination of mutant mitochondrial genomes as therapeutic strategy for the treatment of NARP and MILS syndromes. *Gene Ther* **46,** 428–8 (2008).
16. Bacman, S. R., Williams, S. L., Garcia, S. & Moraes, C. T. Organ-specific shifts in mtDNA heteroplasmy following systemic delivery of a mitochondria-targeted restriction endonuclease. *Gene Ther* **17,** 713–720 (2010).
17. Reddy, P. *et al.* Selective Elimination of Mitochondrial Mutations in the Germline by Genome Editing. *Cell* **161,** 459–469 (2015).
18. Van Houten, B., Hunter, S. E. & Meyer, J. N. Mitochondrial DNA damage induced autophagy, cell death, and disease. *Front Biosci (Landmark Ed)* **21,** 42–54 (2016).
19. Patananan, A. N., Wu, T.-H., Chiou, P.-Y. & Teitell, M. A. Modifying the Mitochondrial Genome. *Cell Metabolism* **23,** 785–796 (2016).




doi:10.6342/NTU201902787

20. Tanaka, M. *et al.* Gene therapy for mitochondrial disease by delivering restriction endonuclease SmaI into mitochondria. *J. Biomed. Sci.* **9,** 534–541 (2002).
21. Bayona-Bafaluy, M. P., Blits, B., Battersby, B. J., Shoubridge, E. A. & Moraes, C. T. Rapid directional shift of mitochondrial DNA heteroplasmy in animal tissues by a mitochondrially targeted restriction endonuclease. *Proc. Natl. Acad. Sci. U.S.A.* **102,** 14392–14397 (2005).
22. Smith, J. *et al.* Requirements for double-strand cleavage by chimeric restriction enzymes with zinc finger DNA-recognition domains. *Nucleic Acids Res.* **28,** 3361–3369 (2000).
23. Hockemeyer, D. *et al.* Genetic engineering of human pluripotent cells using TALE nucleases. *Nat. Biotechnol.* **29,** 731–734 (2011).
24. Sung, Y. H. *et al.* Knockout mice created by TALEN-mediated gene targeting. *Nat. Biotechnol.* **31,** 23–24 (2013).
25. Dutta, S., Madan, S. & Sundar, D. Exploiting the recognition code for elucidating the mechanism of zinc finger protein-DNA interactions. *BMC Genomics* **17,** 1037 (2016).
26. Minczuk, M., Papworth, M. A., Miller, J. C., Murphy, M. P. & Klug, A. Development of a single-chain, quasi-dimeric zinc-finger nuclease for the selective degradation of mutated human mitochondrial DNA. *Nucleic Acids Res.* **36,** 3926–3938 (2008).
27. Hashimoto, M. *et al.* MitoTALEN: A General Approach to Reduce Mutant mtDNA Loads and Restore Oxidative Phosphorylation Function in Mitochondrial Diseases. *Mol. Ther.* **23,** 1592–1599 (2015).
28. Wright, A. V., Nuñez, J. K. & Doudna, J. A. Biology and Applications of CRISPR Systems: Harnessing Nature's Toolbox for Genome Engineering. *Cell* **164,** 29–44 (2016).
29. Jinek, M. *et al.* A Programmable Dual-RNA-Guided DNA Endonuclease in Adaptive Bacterial Immunity. *Science* **337,** 816–821 (2012).
30. Jo, A. *et al.* Research Article Efficient Mitochondrial Genome Editing by CRISPR/Cas9. *BioMed Research International* 1–10 (2015). doi:10.1155/2015/305716
31. Gammage, P. A., Moraes, C. T. & Minczuk, M. Mitochondrial Genome Engineering: The Revolution May Not Be CRISPR-Ized. *Trends Genet.* (2017). doi:10.1016/j.tig.2017.11.001
32. Loutre, R., Heckel, A.-M., Smirnova, A., Entelis, N. & Tarassov, I. Can Mitochondrial DNA be CRISPRized: Pro and Contra. *IUBMB Life* **85,** 133 (2018).
33. Bian, W.-P. *et al.* Knock-In Strategy for Editing Human and Zebrafish Mitochondrial DNA Using Mito-CRISPR/Cas9 System. *ACS Synth Biol* **8,** 621–632 (2019).
34. Schumann, K. *et al.* Generation of knock-in primary human T cells using Cas9 ribonucleoproteins. *Proc. Natl. Acad. Sci. U.S.A.* **112,** 10437–10442 (2015).
35. Zhou, J., Liu, L. & Chen, J. Mitochondrial DNA heteroplasmy in Candida glabrata after mitochondrial transformation. *Eukaryotic Cell* **9,** 806–814 (2010).
36. Mileshina, D., Koulintchenko, M., Konstantinov, Y. & Dietrich, A. Transfection of plant mitochondria and in organello gene integration. *Nucleic Acids Res.* **39,** e115–e115 (2011).
37. D'Aurelio, M. *et al.* Heterologous mitochondrial DNA recombination in human cells. *Hum. Mol. Genet.* **13,** 3171–3179 (2004).
38. Gilkerson, R. W., Schon, E. A., Hernandez, E. & Davidson, M. M. Mitochondrial nucleoids maintain genetic autonomy but allow for functional complementation. *J. Cell Biol.* **181,** 1117–1128 (2008).



doi:10.6342/NTU201902787

39. Bacman, S. R., Williams, S. L. & Moraes, C. T. Intra- and inter-molecular recombination of mitochondrial DNA after in vivo induction of multiple double-strand breaks. *Nucleic Acids Res.* **37,** 4218–4226 (2009).
40. Lakshmipathy, U. & Campbell, C. Double strand break rejoining by mammalian mitochondrial extracts. *Nucleic Acids Res.* **27,** 1198–1204 (1999).
41. Srivastava, S. & Moraes, C. T. Double-strand breaks of mouse muscle mtDNA promote large deletions similar to multiple mtDNA deletions in humans. *Hum. Mol. Genet.* **14,** 893–902 (2005).
42. Andreyev, A. Y., Kushnareva, Y. E. & Starkov, A. A. Mitochondrial metabolism of reactive oxygen species. *Biochemistry Mosc.* **70,** 200–214 (2005).
43. Kukat, A. *et al.* Generation of rho0 cells utilizing a mitochondrially targeted restriction endonuclease and comparative analyses. *Nucleic Acids Res.* **36,** e44 (2008).
44. Chacinska, A., Koehler, C. M., Milenkovic, D., Lithgow, T. & Pfanner, N. Importing mitochondrial proteins: machineries and mechanisms. *Cell* **138,** 628–644 (2009).
45. Moberg, P. *et al.* NMR solution structure of the mitochondrial F1beta presequence from Nicotiana plumbaginifolia. *J. Mol. Biol.* **336,** 1129–1140 (2004).
46. Saitoh, T. *et al.* Tom20 recognizes mitochondrial presequences through dynamic equilibrium among multiple bound states. *EMBO J.* **26,** 4777–4787 (2007).
47. Yamano, K. *et al.* Tom20 and Tom22 share the common signal recognition pathway in mitochondrial protein import. *J. Biol. Chem.* **283,** 3799–3807 (2008).
48. Tamura, Y. *et al.* Tim23-Tim50 pair coordinates functions of translocators and motor proteins in mitochondrial protein import. *J. Cell Biol.* **184,** 129–141 (2009).
49. Jeandard, D. *et al.* Import of Non-Coding RNAs into Human Mitochondria: A Critical Review and Emerging Approaches. *Cells* **8,** 286 (2019).
50. Rubio, M. A. T. *et al.* Mammalian mitochondria have the innate ability to import tRNAs by a mechanism distinct from protein import. *Proc. Natl. Acad. Sci. U.S.A.* **105,** 9186–9191 (2008).
51. Mercer, T. R. *et al.* The human mitochondrial transcriptome. *Cell* **146,** 645–658 (2011).
52. Wang, G. *et al.* PNPASE regulates RNA import into mitochondria. *Cell* **142,** 456–467 (2010).
53. Cameron, T. A., Matz, L. M. & De Lay, N. R. Polynucleotide phosphorylase: Not merely an RNase but a pivotal post-transcriptional regulator. *PLoS Genet.* **14,** e1007654 (2018).
54. Mohanty, B. K. & Kushner, S. R. Polynucleotide phosphorylase functions both as a 3‘ right-arrow 5’ exonuclease and a poly(A) polymerase in Escherichia coli. *Proc. Natl. Acad. Sci. U.S.A.* **97,** 11966–11971 (2000).
55. Yehudai-Resheff, S., Hirsh, M. & Schuster, G. Polynucleotide phosphorylase functions as both an exonuclease and a poly(A) polymerase in spinach chloroplasts. *Mol. Cell. Biol.* **21,** 5408–5416 (2001).
56. Golzarroshan, B. *et al.* Crystal structure of dimeric human PNPase reveals why disease-linked mutants suffer from low RNA import and degradation activities. *Nucleic Acids Res.* **46,** 8630–8640 (2018).
57. Fox, T. D. Mitochondrial protein synthesis, import, and assembly. *Genetics* **192,** 1203–1234 (2012).
58. Becker, T., Böttinger, L. & Pfanner, N. Mitochondrial protein import: from transport pathways to an integrated network. *Trends Biochem. Sci.* **37,** 85–91 (2012).



doi:10.6342/NTU201902787

59. Wada, K.-I., Hosokawa, K., Ito, Y. & Maeda, M. Quantitative control of mitochondria transfer between live single cells using a microfluidic device. *Biol Open* **6,** 1960–1965 (2017).
60. Su, X. & Dowhan, W. Translational regulation of nuclear gene COX4 expression by mitochondrial content of phosphatidylglycerol and cardiolipin in Saccharomyces cerevisiae. *Mol. Cell. Biol.* **26,** 743–753 (2006).
61. Abu-Elheiga, L. *et al.* The subcellular localization of acetyl-CoA carboxylase 2. *Proc. Natl. Acad. Sci. U.S.A.* **97,** 1444–1449 (2000).
62. Bravo-Alonso, I. *et al.* Nonketotic hyperglycinemia: Functional assessment of missense variants in GLDC to understand phenotypes of the disease. *Hum. Mutat.* **38,** 678–691 (2017).
63. Bogenhagen, D. F., Rousseau, D. & Burke, S. The layered structure of human mitochondrial DNA nucleoids. *J. Biol. Chem.* **283,** 3665–3675 (2008).
64. Prasannan, P., Pike, S., Peng, K., Shane, B. & Appling, D. R. Human mitochondrial C1-tetrahydrofolate synthase: gene structure, tissue distribution of the mRNA, and immunolocalization in Chinese hamster ovary calls. *J. Biol. Chem.* **278,** 43178–43187 (2003).
65. Walkup, A. S. & Appling, D. R. Enzymatic characterization of human mitochondrial C1-tetrahydrofolate synthase. *Arch. Biochem. Biophys.* **442,** 196–205 (2005).
66. Wang, G., Shimada, E., Koehler, C. M. & Teitell, M. A. PNPASE and RNA trafficking into mitochondria. *Biochim. Biophys. Acta* **1819,** 998–1007 (2012).
67. Wang, G. *et al.* PNPASE Regulates RNA Import into Mitochondria. *Cell* **142,** 456–467 (2010).
68. Smirnov, A., Entelis, N., Martin, R. P. & Tarassov, I. Biological significance of 5S rRNA import into human mitochondria: role of ribosomal protein MRP-L18. *Genes Dev.* **25,** 1289–1305 (2011).
69. Kolesnikova, O. *et al.* Selection of RNA aptamers imported into yeast and human mitochondria. *RNA* **16,** 926–941 (2010).
70. Gowher, A., Smirnov, A., Tarassov, I. & Entelis, N. Induced tRNA import into human mitochondria: implication of a host aminoacyl-tRNA-synthetase. *PLoS ONE* **8,** e66228 (2013).
71. Wang, G. *et al.* Correcting human mitochondrial mutations with targeted RNA import. *Proc. Natl. Acad. Sci. U.S.A.* **109,** 4840–4845 (2012).
72. Lee, N. S. *et al.* Functional and intracellular localization properties of U6 promoter-expressed siRNAs, shRNAs, and chimeric VA1 shRNAs in mammalian cells. *RNA* **14,** 1823–1833 (2008).
73. Chen, B. *et al.* Dynamic Imaging of Genomic Loci in Living Human Cells by an Optimized CRISPR/Cas System. *Cell* **155,** 1479–1491 (2013).
74. Kim, S. *et al.* CRISPR RNAs trigger innate immune responses in human cells. *Genome Res.* **28,** 367–373 (2018).



doi:10.6342/NTU201902787